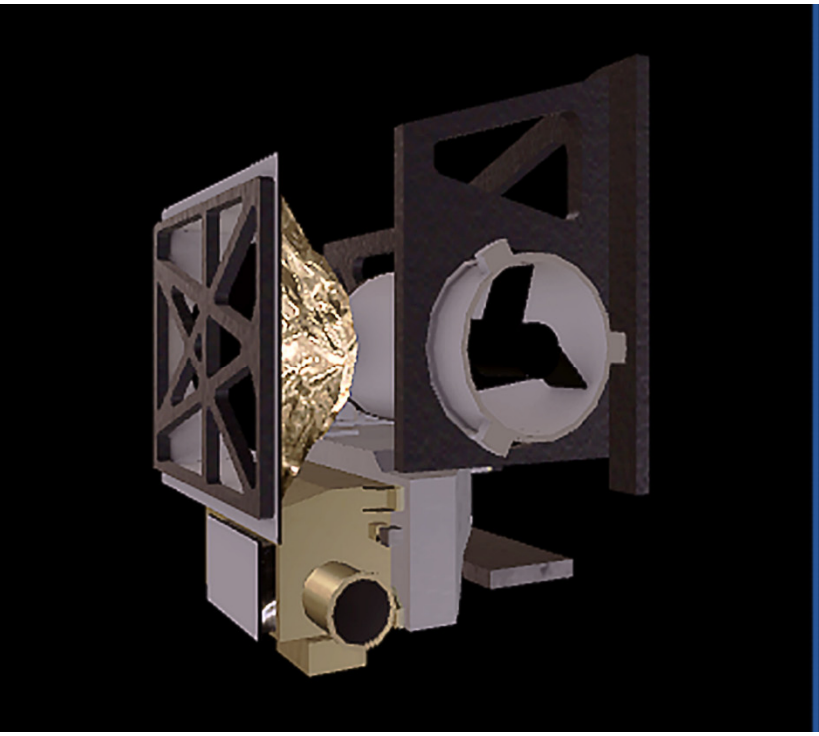

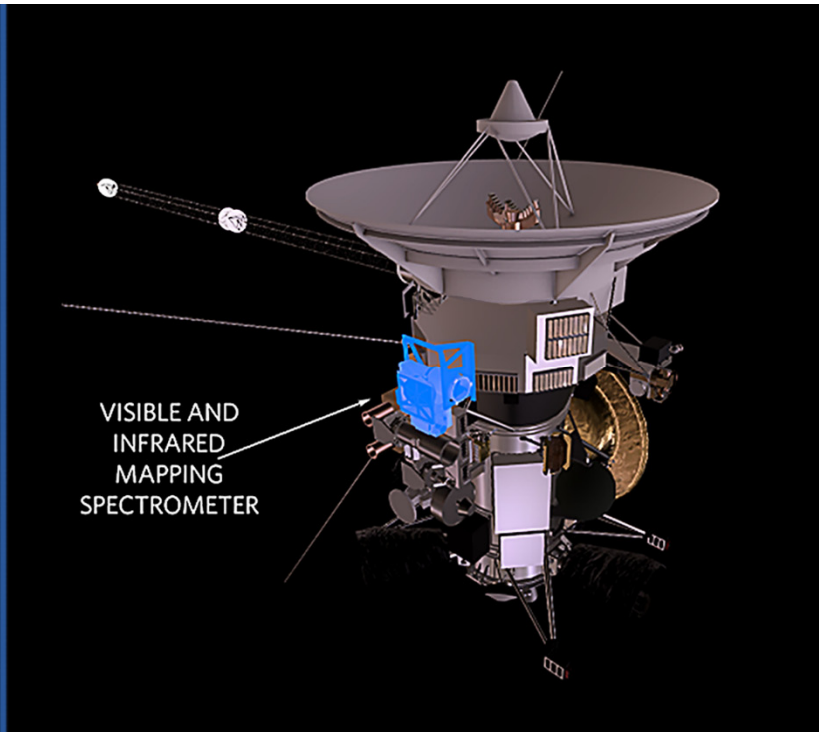

Visible and Infrared Mapping Spectrometer

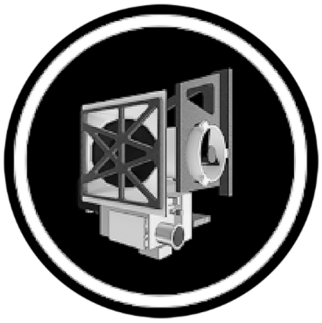

The Visual and Infrared Mapping Spectrometer (VIMS) was a pair of imaging grating spectrometers that were designed to measure reflected and emitted visible and near-infrared light from atmospheres, rings and surfaces over wavelengths from 0.35 to 5.1 microns. The **science objectives** of VIMS were to determine the composition and structure of atmospheres, rings and surfaces in the Saturn system using visual and infrared spectral mapping. Of Cassini's instruments, VIMS was uniquely capable of simultaneously collecting both images and spectra of satellite surfaces, the rings, and the atmospheres of Saturn and Titan without having to scan to make images.

VIMS separated the light into its various wavelengths providing information about the composition of materials from the measured reflected or emitted light. The instrument had the capability to detect 352 different wavelengths of light, many of which are beyond the capability of the human eye to detect. Images could be created from light collected at the various VIMS wavelengths.

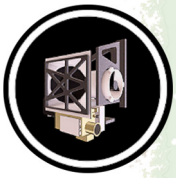

CONTENTS

Figures

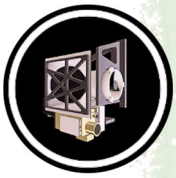

Tables

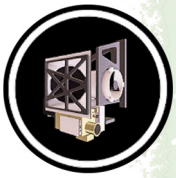

VIMS Science Performance Assessment

R. H. Brown, S. V. Badman, K. H. Baines, B. J. Buratti, R. N. Clark, P. D. Nicholson, C. Sotin and E. Joseph, April 27, 2018.

Instrument Description

The development, performance specifications and detailed design of the Cassini VIMS are well described in the literature and will not be repeated here. For detailed technical descriptions, the reader is referred to the refereed literature [Miller et al. 1996; Reininger et al. 1994; Brown et al. 2004] and Cassini project documents that describe the technical aspects of the VIMS instrument. For a complete discussion of the operational aspects of the Cassini VIMS the reader is directed to the VIMS User's Manual (JPL document D-14200).

> … the Team of people that eventually designed, built and used the VIMS instrument managed to extend the reach of the investigation well beyond what was envisioned by NASA … .

The VIMS instrument is an imaging spectrometer that is a composite of two channels: the VIMS visible (V) channel and the VIMS infrared (IR) channel. In its normal operating mode, the VIMS-V channel covers the wavelength region 0.35–1.05 μm in 96 spectral channels, with a spectral resolution of 0.0073 μm, an angular resolution of 0.5 microradians (mrad) and a 3.6 degree field of view. In its normal operating mode, the VIMS IR channel covers the wavelength region 0.85–5.1 μm in 256 channels at a spectral resolution of 0.0166 μm, an angular resolution of 0.5 mrad and a 3.6 degree field of view. The VIMS-V channel uses push-broom scanning to cover its 64 × 64 pixel field of view, while the IR instrument uses whisk-broom scanning to cover its 64 × 64 pixel field of view. The VIMS instrument is capable of a large range of operating modes, varying scan sizes and shapes, varying exposure times, and varying angular and spectral resolution, while incorporating a wide range of options for onboard processing of data such as spectral summing and spectral editing. For a detailed description of VIMS' various operating modes and parameters, the reader is again referred to the papers cited above. This document will focus on the scientific output of the VIMS investigation, and a few post-selection changes in the instrument and the investigation team that had a major effect on the scope and depth of the VIMS science investigation.

Several changes and developmental branches occurred during the designing and building of the VIMS instrument, and were not in the original specifications of the instrument as described in the Cassini Mission Announcement of Opportunity (AO), or in the original selection of the investigation team. Those changes, nevertheless, had dramatic and transformative effects on the science accomplished by the VIMS investigation. In essence, the Team of people that eventually designed, built and used the VIMS instrument managed to extend the reach of the investigation well beyond what was envisioned by NASA, the review panels that determined the original

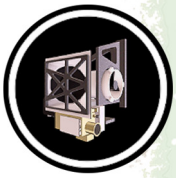

specifications of the instrument, its notional development budget, and the team of scientists originally chosen to use the instrument.

VIMS, as a facility instrument with its associated investigation team, was originally defined by several groups of people, most of whom had relevant expertise, but who would have no direct connection to the VIMS investigation, determination of its ultimate design and its development budget, or its overall scientific objectives. In addition, other individuals would judge the proposals submitted by scientists interested in becoming part of the VIMS science investigation team, and as such would determine to a great extent the depth and scope of the notional VIMS science investigation. Such an approach, though legitimate, necessarily cannot provide the deeply integrated vision and planning inherent in an instrument proposed by a principal investigator and a carefully picked team of associate scientists. Such teams have a more detailed and deeper understanding of the important scientific problems to be addressed, as well as the required specifications and capabilities of the instrumentation needed to achieve the science objectives, than that of a team and an instrument designed by committees. As such, though the committees that provided the initial input did as well as they could be given the constraints lain out by NASA, both the instrument configuration and the composition of the core VIMS science team changed significantly prior to and after Cassini's launch, reflecting the core team's vision of the scope and range of the eventual VIMS science investigation. As such, the VIMS investigation has far exceeded the scope and depth originally envisioned for it. For that, the entire team of scientists and engineers that have contributed to the development and use of VIMS on Cassini deserve a great amount of credit.

Changes to Hardware, Software and Personnel Post Announcement of Opportunity

There were several major changes made to the configuration of the VIMS instrument relative to that which was originally specified in the Cassini AO. The most significant of those changes were: i) incorporation of a separate channel to cover the visible spectral region from 0.35–1.05 microns; ii) incorporation of the ability to operate the VIMS instrument in a mode that resembled that of an occultation photometer; iii) the loss of the calibration plaque originally envisioned for the instrument, which drove the addition of a solar port to calibrate VIMS, along with the evolution of in-flight calibration strategies addressing that loss and the resulting capability to use the solar port to conduct solar-occultation studies of objects in the Saturn system; iv) the loss of Cassini's scan platform necessitating large changes in the operation plans envisioned for the entire package of remote-sensing instruments on Cassini; v) the addition of a second, orthogonal scanning direction for the VIMS secondary mirror, allowing for greater operational flexibility and scientific utility, specifically enabling collaborative studies with other remote sensing instruments having entrance slits; and vi) the use of H_3^+ emission measurements to study magnetospheric processes in the Saturn system. There were also several, minor changes to the flight software developed for the VIMS instrument, allowing for greater operational and scientific flexibility, among which were modes that allowed onboard processing of VIMS data such as data compression, spectral summing and spectral editing.

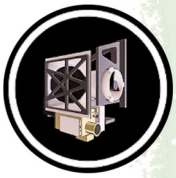

In addition to changes to both the hardware and software of the VIMS instrument relative to its AO configuration, after the original selections the VIMS core science team was embellished to better exploit the hardware and software changes. In particular, Dr. Phillip Nicholson was added to the team by NASA in response to a VIMS team request, specifically in the area of ring science and the use of occultation data to probe the structure and dynamics of Saturn's ring system. Dr. Alberto Adriani, Dr. Giancarlo Bellucci and Dr. Ezio Bussoletti were added to provide more expertise for scientific investigations using the VIMS-V channel. To enhance the expertise in the area of icy satellite surfaces, the VIMS team requested that Dr. Bonnie Buratti be added to the team. There have been other additions and subtractions to the VIMS core science team over the 29 years of its existence, but the aforementioned people were specifically added to expand the scope and depth of the VIMS investigation.

Another fundamental change in the scope of the VIMS investigation accrued from the realization that the lower atmosphere and surface of Titan could be imaged by VIMS. This opened up an entire sub discipline of the VIMS investigation concerning Titan geology, lakes, and methane cloud meteorology. The Titan sub-discipline grew explosively in the years following Cassini Saturn Orbit Insertion (SOI), eventually growing to become the largest of the VIMS sub-disciplines, both in number of investigators as well as production of scientific papers.

Stellar Occultation Mode

Were Cassini able to point its instruments at a specified celestial position (i.e., a star) with accuracy significantly better than 1 VIMS pixel, then occultation observations would be straightforward. In reality, however, the spacecraft's a priori pointing error was designed to be no worse than ~2 mrad, and in practice was approximately 1 mrad. It was thus impossible to predict in which VIMS pixel the stellar image would fall, though the uncertainty was at most 2–4 pixels. Fortunately, however, the spacecraft pointing was extremely stable once a new target was acquired, with typical pointing variations being only a few tens of narrow angle camera (NAC) pixels, or <<1 VIMS pixel. To solve the problem of initial targeting on board, the VIMS instrument was reprogrammed during cruise to first obtain a small image of the star 5–10 min before the predicted start of an occultation. Hardware constraints required this image to contain 64 pixels; in practice it was fixed at 16 × 4 pixels. The instrument's internal data compression software was then used to identify the brightest pixel in the scene (assumed to be the star of interest), and this was used to calculate the 2-D mirror offset necessary to place the star in the single pixel to be observed for the remainder of the occultation period. The star-finding cube was also returned to the ground, should it prove necessary to examine this later, as were the 2-D scanning mirror coordinates selected by the on-board star-finding software.

Although this simple procedure had its limitations, chiefly that it did not cope well with situations where the star fell more or less midway between two pixels, in practice it worked well in over 90% of the occultations we attempted. In only 4 cases out of 190 ring occultations did VIMS fail to acquire the star, or lose it after the initial acquisition, and in a further 11 cases (or 5% of the time) the occultation was recorded but the stellar signal was observed to be less than one-third of

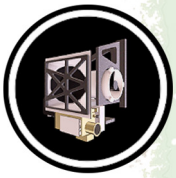

the predicted level, suggesting that the stellar image was not in fact centered within the pixel selected by the onboard algorithm.

Because the addition of both the stellar and solar occultation modes was such a substantial contributor to the overall VIMS science legacy, we detail the observation statistics in Table VIMS-1.

Table VIMS-1. Stellar and solar occultation mode observation statistics.

Type	Number tried	Successful	Failures	Comments
Ring stellar	190	182	8	~20 (10%) have poor SNR due to bad pointing
Saturn stellar	106	92	14	~10 (10%) have poor SNR due to bad pointing
Titan stellar	14	13	1	2 have poor SNR due to bad pointing
Ring solar	31	30	1	
Saturn solar	28	26	2	
Titan solar	16	12	1	3 were confused by bright limb in main port

A quick inspection of the above will reveal that VIMS attempted 310 stellar occultation measurements of Saturn, Saturn's rings and Titan, with only 23 failing to produce useful data. The remaining 287 produced data which was in general very high quality, resulting in 15 important scientific papers, and many new insights into the Saturn system. Those new insights ranged from atmospheric composition measurements for both Saturn and Titan, to studies of the structure and dynamics of Saturn's rings, to discovering features in Saturn's rings that resulted from gravitational perturbations driven by oscillations of Saturn's interior, thus allowing the VIMS team to virtually pioneer the field of space-based, observational Krono-seismology. In addition, VIMS attempted 75 solar occultation measurements of Saturn, Saturn's rings and Titan, all but four of which produced useful data, resulting in new insights into the composition and dynamics of those objects. It is useful to again note that the capabilities to conduct solar and stellar occultation measurements using VIMS were never envisioned by the committees that defined ether VIMS' notional design, or its complement of science team members. These capabilities, and the subsequent large contribution of scientific knowledge that resulted from their employ, were a huge bonus delivered to NASA by the talented people of the VIMS core science and engineering teams.

Impacts on the Scientific Community

As these efforts continue to grow over the next few years, the impact of the VIMS effort will continue to grow as well.

Further evidence of the seminality of the VIMS investigation is in the impact of its people and data on Planetary Science. At the time of writing, VIMS has had over 100 collaborators, postdocs and students associated with the investigation who are or have been participating in the analysis and publication of the data. Over 10 Ph.D. dissertations have made extensive use of the VIMS data, and there are at least four research groups studying Titan using VIMS data that have nucleated at the University of Idaho, M.I.T., Cornell, and The University of Paris around former students and postdocs who went on to become faculty at those institutions. As these efforts

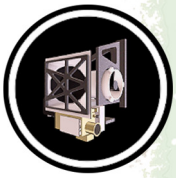

continue to grow over the next few years, the impact of the VIMS effort will continue to grow as well.

In the following we summarize the most significant of the VIMS science results in each of the disciplines where VIMS made contributions; i.e., atmospheres, magnetospheres, icy satellites, rings and Titan. After the science summaries follow detailed descriptions of the important results in the disciplines mentioned above. This document will then conclude with a bibliography of publications that have resulted from both the use of VIMS data and VIMS science results in scientific research driven and inspired by Cassini.

Summary of the Main Scientific Contributions of VIMS

In the following, we summarize in a list the most important scientific accomplishments of the VIMS investigation, organized by discipline.

Atmospheres and magnetospheres

1. Study and characterization of discrete clouds, silhouetted by 5-μm thermal radiation from Saturn's interior, resulting in important new insights into Saturn's atmospheric structure and circulation.

2. Study and characterization of Saturn's north-polar hexagon using 5-μm illumination while Saturn's north pole was in total darkness.

3. Discovery and characterization of Saturn's north polar vortex.

4. First spectral identification of ammonia ice in Saturn's clouds.

5. Discovery of carbon soot as a component of Saturn's dark clouds, likely produced by lightning in Saturn's atmosphere.

6. First detection of water ice in Saturn's clouds, from studies of the great storm of 2011–2012.

7. Determination of the abundance and spatial/temporal distribution of phosphine and arsine in Saturn's atmosphere.

8. Provision of additional constraints on Saturn's important He/H ratio.

9. Detailed mapping of the spatial and temporal character of Saturn's wind fields.

10. Discovery and characterization of Saturn's string of pearls storm system.

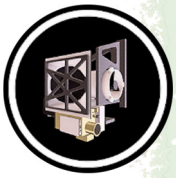

11. Extensive imaging of H_3^+ emission from Saturn's aurorae at the highest resolution ever resulting in new insights into Saturn's magnetospheric processes.

12. Discovery of a temperature asymmetry in Saturn's aurorae with the southern aurora being hotter than that of the north.

13. Elucidation of magnetospheric-ionospheric coupling in Saturn's aurorae.

14. First observations of surface emission features at sub-micron wavelengths on Venus.

15. Proved the existence of spectrally-identifiable ammonia and ammonium hydrosulfide ices in most zones and belts across Jupiter.

16. Provided new insights into the identity of the potential red chromophores responsible for the reddish tint of Jupiter and its Great Red Spot.

17. Discovery of a 3% asymmetry in Jupiter's thermal emission possibly due to hemispherical differences in the structure of Jupiter's interior.

Satellites

1. Discovery of widespread water on Earth's Moon at concentrations of 10 to 1000 parts per million, and locally higher.

2. Discovery of a surprisingly high opposition surge on Europa.

3. Discovery of a 3-μm feature in Himalia's spectrum of Jupiter's satellite Himalia, suggestive of the presence of water, either free, bound, or incorporated in layer-lattice silicates.

4. Provided the first near-IR phase curve of Europa, suggesting that neither coherent backscatter nor shadow hiding provide a complete description of Europa's opposition surge below 1°.

5. First spatially resolved spectra of Phoebe showing iron-bearing minerals, bound water, trapped CO_2, probable phyllosilicates, organics, and NH-bearing compounds, showing Phoebe to be one of the most compositionally diverse objects yet observed in our Solar System.

6. The recognition, through both chemical and isotopic composition measurements by VIMS, that Phoebe is very likely a captured object, probably from well beyond the orbit of Saturn.

7. The recognition that the water ice on the icy satellites is crystalline, rather than amorphous as had been thought.

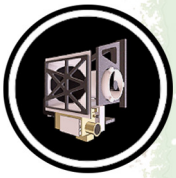

8. The discovery that CO_2 is present on the surface of most of Saturn's icy moons, extensive mapping of the spatial distribution of that CO_2, and elucidation of its physical state, both bound and free.

9. Discovery of spectral absorptions attributed to the presence of aromatic hydrocarbons on Iapetus and Phoebe.

10. Tentative identification of trapped H_2 and ammonia on the surfaces of several of Saturn's icy satellites.

11. Discovery of Deuterium on Phoebe, Iapetus, Hyperion, Rhea, Dione, Enceladus and the Saturn's rings, and measurement of the associated D/H ratios.

12. Detection of ^{13}C on Phoebe and Iapetus.

13. Recognition that VIMS' measurements of high D/H and $^{13}C/^{12}C$ isotopic ratios imply that the materials comprising Phoebe's surface came from a different reservoir than that of the other icy satellites of Saturn, and its rings.

14. Discovery that the plumes of Enceladus vary in intensity with mean anomaly over short-timescales in VIMS data, with subsequent attribution to tidal stresses induced by variations in Enceladus' orbital distance from Saturn.

15. Derived a temperature of 197 ±20 K, and a linear size of 9 meters for one of the plume sources on Enceladus using VIMS observations at 5 μm.

16. Discovered that the particulate component of Enceladus' plumes consist primarily of fine-grained water ice, ejected at velocities of 80 and 160 m/s, with size distributions strongly depleted in particles with radii larger than 3 μm, and that only a small fraction of 3-μm particles can escape from Enceladus.

17. Particle sizes on Enceladus are correlated with geologic features and surface ages, suggesting a stratigraphic relationship between tectonic features and cryovolcanic activity.

18. Constructed daytime temperature maps of the icy satellite surfaces using temperature-dependent spectral changes observed by VIMS in the spectrum of water ice on their surfaces.

19. Discovery of nano-phase iron oxides and metallic iron together explain the varied color and ultraviolet (UV) absorber on Iapetus, Phoebe, and Hyperion. The metallic iron must be embedded in another material like a silicate, thus characteristic of space-weathered meteoric dust. The 3-μm absorber in the Iapetus dark material is only matched by hydrated iron oxides. The 1.9-micron bound water absorption in

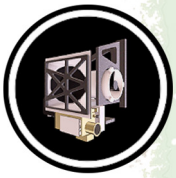

spectra of the dark material is also a constraining absorption characteristic of hydrated iron oxides.

Saturn's rings

1. VIMS spectral observations at SOI revealed that the mysterious red coloring agent in the rings resides within the water ice grains that make up the regolith on the ring particles.

2. Observations of ring occultations of o Ceti (aka Mira) in 2005 confirmed the existence of strong self-gravity wakes in the A-ring, leading to the first reliable estimates for the ring thickness of ~6 meters in this region.

3. Observations of multiple stellar and radio occultations in 2005–2009 leading to the discovery that the amplitude of the radial perturbations at the outer edge of the B-ring (due to the Mimas 2:1 resonance) varies from ~70 km to < 5 km, and that these may also be indirectly responsible for the regular spacing of the multiple gaps within the Cassini Division.

4. The observation of reststrahlen bands of H_2O ice in a stellar occultation by the F-ring permitted discrimination between clumps of macroscopic source bodies and the background of micron-sized dust.

5. A comparative analysis of visible-infrared (VIS-IR) spectral indicators (slopes and band depths) of rings, regular satellites and small moons has allowed VIMS to map the distribution of water ice and red contaminant materials across the Saturn system. However, in the main rings, the abundance of the red coloring agent is lower and there is at present no way to distinguish definitively between the nano-iron model and more traditional carbon-tholin models. Recent modeling results obtained with Hapke theory indicate that both intimate and intra-particle mixing of water ice, amorphous carbon and organic material (Titan tholins) can reproduce the observed ring spectra.

6. VIMS investigations of numerous small-scale wavelike structures in the C-ring have provided strong evidence that several of these are density waves driven by global oscillations within Saturn itself, opening up a new window on the planet's internal structure and rotation rate.

7. A pair of stellar occultations with turnaround radii in the inner A-ring yielded strong evidence for viscous over-stability in the denser parts of Saturn's rings, supporting previous work based on radio occultation data.

8. Together with occultation data from Radio Science Subsystem (RSS) and Ultraviolet Imaging Spectrograph (UVIS), VIMS data from more than 100 stellar occultations has led to the characterization of numerous non-circular features in the C-ring and

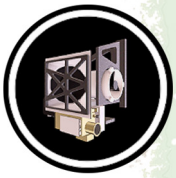

Cassini Division, including the discovery of a large number of normal mode oscillations on the edges of both narrow gaps and their associated ringlets.

9. Ring temperature maps have been built from VIMS spectra by using an indirect method based on the wavelength of the temperature-dependent reflectance peak at 3.6 μm.

10. Application of a new, phase-sensitive wavelet analysis technique to selected VIMS stellar occultation profiles has led to the identification of several satellite-driven density waves in the optically-thick B-ring, resulting in the first estimates of surface mass density in this most opaque part of Saturn's rings. The results are unexpectedly low, and imply a total mass for the rings of ~40 percent that of Mimas.

Titan

1. Observation and characterization of the first specular reflection from an extraterrestrial body of liquid.

2. Detection of liquid ethane in Ontario Lacus.

3. First observation and characterization of waves on Titanian lakes.

4. Discovery and characterization of cryovolcanic deposits near Hotei Regio and Tui Regio on Titan.

5. Discovery and characterization of evaporite deposits on Titan's surface.

6. Global mapping of Titan's surface composition.

7. Discovery of solid benzene on Titan.

8. Discovery of acetylene on Titan.

9. Mapping of the composition and distribution of material near or around Selk crater on Titan.

10. Discovery and characterization of dust storms on Titan.

11. Mapping, characterization and analysis of the global cloud distribution on Titan during the entire 13-year orbital tour.

12. Discovery and characterization of the extreme smoothness of Ontario Lacus during the early part of the Cassini orbital tour.

13. Discovery of CO nighttime emissions on Titan.

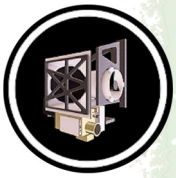

14. Discovery and characterization of precipitation-induced surface brightening seen on Titan.

15. Discovery of fog at the south pole of Titan.

16. Discovery of giant, infrared palimpsest on Titan's Xanadu region.

17. Observation and characterization of the shoreline of Ontario Lacus showing no changes over five years.

18. Discovery of ethane in Titan's rainfall.

19. Characterization of fluvial erosion and post-erosional processes on Titan.

20. Characterization of the evolution of Titan's north polar hood.

21. Evidence for tropical and temperate lakes on Titan.

Details of the Most Significant Scientific Results

Jupiter's Atmosphere, Saturn's Atmosphere and Aurorae

Cloud properties

Upon arrival at Saturn, VIMS used its 5-μm thermal spectral imaging capability to quickly discover that discrete clouds lie below the traditional levels observed in reflected sunlight. Across the planet, localized clouds were observed in silhouette against the planet's indigenous background thermal radiation and found to reside near the 1.5-bar level [Baines et al. 2005, 2009b; Fletcher et al. 2011a], revealing that a different dynamical atmospheric regime resides below the visible cloud tops. Upon observing the north polar region during the first set of inclined orbits in 2006 under full nighttime polar winter conditions, these clouds allowed the north polar hexagon to be clearly imaged for the first time and revealed the existence of a classical polar vortex via the determination of the north polar windfield by VIMS 5 μm cloud-tracking [Baines et al. 2009b].

Ammonia ice was found by VIMS to be a spectrally-identifiable component of thunderstorm-related clouds in southern mid-latitudes, the first spectral identification of ammonia ice in Saturn [Baines et al. 2009a]. Neighboring clouds were found to be exceptionally dark over all visible and near-IR reflective wavelengths, consistent with carbon soot being a significant component of these features, as perhaps produced by lightning observed in the region by Radio and Plasma Wave Spectrometer (RPWS) [Baines et al. 2009a]. More recent modeling by Sromovsky et al. [2018] confirms the excellent spectral fits for both the bright spectrally-identifiable ammonia-ice clouds and the dark neighboring features. This paper also finds excellent fits for the dark clouds via relatively bright cloud models characterized by depressed cloud tops, although depressed cloud tops are

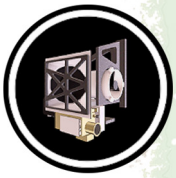

dynamically inconsistent with the anticyclonic nature of these features found by Imaging Science Subsystem (ISS).

Water ice was spectrally identified by VIMS in the cloud tops of the Great Storm of 2010–2011, the first identification of water ice on Saturn [Sromovsky et al. 2013]. The particle size, number density, and structure of the clouds in the nucleus of the Great Storm clouds were also determined from VIMS spectral imagery. The high cloud tops found (near 300 mbar) where the water ice is seen by VIMS implies that water is lofted over 150 km within this storm from its condensation level near the 20 bar level.

Composition

VIMS constrained the gaseous abundances of phosphine and arsine in Saturn's north polar region [Baines et al. 2009b], in the Great Storm of 2010–2011 [Fletcher et al. 2011b], and across the planet in various zonal structures [Fletcher et al. 2011a]. As noted above, VIMS also determined spectroscopically the presence of both ammonia and water ice in a variety of clouds. The He/H_2 ratio (important for understanding Saturn's internal heat) was constrained from VIMS 4– to 5-μm spectroscopy from a unique analysis of the unusually aerosol-free mid-northern-latitude band created in the aftermath of the Great Storm of 2010–2011, leveraging the effect of helium on the pressure/temperature gradient [Sromovsky et al. 2016].

Global and regional wind fields

The zonal wind field was mapped globally over the planet from ~60 degrees north latitude to 30 degrees south latitude by Choi et al. [2009]. In the north polar region, the zonal winds were mapped under winter nighttime conditions from Cassini's highly-inclined orbit in 2006, revealing the presence of a classical polar vortex [Baines et al. 2009b]. As well, a similar vortex structure was mapped by VIMS for the south pole [Dyudina et al. 2009] observed under the daylit conditions of southern summer, confirming the simultaneously-measured ISS cloud-tracked results obtained at significantly higher spatial resolution.

Synoptic cloud features and processes

VIMS followed the enigmatic String of Pearls which it discovered (and named) for five years, until its demise with the eruption of the Great Storm in December 2010 [Del Genio et al. 2009; Baines et al. 2018]. This feature was likely a Vortex Street, perhaps stimulated by undetected upwellings from below that eventually erupted into the Great Storm of 2010–2011.

The aftermath of the Great Storm of 2010–2011 left an unexpectedly clear atmosphere over the ~10 degrees of latitude that had been occupied by the storm. With its 5-μm observing capabilities, VIMS followed the evolution of this region, quantifying its rate of recovery back to its pre-storm state [Sromovsky et al. 2016].

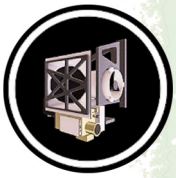

Auroral science

VIMS imaged Saturn's infrared aurora, emitted by the ionized molecule H_3^+, at unprecedented spatial and temporal resolution. New features were identified, including polar infilling for which no ultraviolet counterpart has yet been identified [Stallard et al. 2008]. Limb observations showed that the aurora peaks at ~1100 km altitude, similarly to the UV aurora, but has a narrower profile [Stallard et al. 2012a].

Observations of both hemispheres (not possible from Earth-based telescopes) revealed that the southern auroral oval was brighter than the north, implying a higher temperature [Badman et al. 2011b]. The southern temperature was estimated to be 440 ±50 K [Melin et al. 2011].

Comparison with UV observations showed that the infrared H_3^+ emission has a lifetime of ~500 s, and is morphologically identical to the UV H and H_2 emission only at the main auroral arc [Badman et al. 2011a; Melin et al. 2011, 2016].

Magnetosphere-ionosphere coupling was revealed in arcs conjugate with energetic ions and electrons [Badman et al. 2012a] and modulated by a rotating current system [Badman et al. 2012b; Lamy et al. 2013].

Venus science

During the Venus flyby in June 1999, the visual channel of VIMS was able to obtain the first observations of surface emission features at sub-micron wavelengths surface emission, proving the previously theorized existence of emissions at 0.85 and 0.90 μm [Baines et al. 2000]. This result extended the number of spectral windows useful for surface spectroscopy from 3 to 5 μm, expanding the useful surface-sensitive spectral range from 1.01 to 1.18 μm pre-VIMS/Cassini to 0.85–1.18 μm post-VIMS.

Jupiter science

During the Jupiter flyby of late 2000–early 2001, VIMS 0.35– to 5.1-μm spectral maps of the planet obtained at higher spatial resolution than available heretofore resulted in proving the existence of spectrally-identifiable ammonia and ammonium hydrosulfide ices in most zones and belts across the planet [Sromovsky et al. 2010]. Visual spectral imagery in the 0.35– to 0.6-μm range proved particularly useful for modeling the potential red chromophores responsible for the reddish tint of the planet [Sromovsky et al. 2017]. Spectral fits were particularly fine in the core of the Great Red Spot [Baines et al. 2019], providing significant clues to the centuries-long mystery of why the Great Red Spot is red.

Jupiter's emitted power was evaluated over latitude from a combination of VIMS and Composite Infrared Spectrometer (CIRS) and observations [Li et al. 2012]. The analysis found a north/south hemispherical difference of a 3% in emitted power, with the northern hemisphere being warmer. This is despite the low obliquity of the planet that theoretically prevents

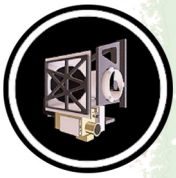

seasonal/hemispherical variations. The cause may then be due to hemispherical differences in the structure of Jupiter's thermally-emitting interior.

VIMS observed the night-side auroral emission with a peak at the equatorward edge of the main emission attributed to enhanced H_3^+ density, but very little emission, and hence particle precipitation, at the equator [Stallard et al. 2015].

Some open questions

1. What is the helium abundance on Saturn? The answer may still rest in the proper interpretation of the joint VIMS/CIRS data sets, but perhaps by better joint observational scenarios by future VIMS occultation and mid-IR thermal mapping instruments on a future mission are needed (or, finally, measured directly by an in situ atmospheric probe).

2. What, exactly, occurs in the initial development of major storms on Saturn? VIMS-like studies of the development of a major storm (particularly the composition of condensates seen in the early stages) would be able to determine more accurately what the energetics are in lofting materials from 100s of km down. Continued studies would then be able better constrain the energetics throughout the lifetime of a storm.

3. More studies are needed of smaller storms in the mid-southern-latitude storm alley, in particular, looking for and characterizing the dark carbon soot observed in storms in this region. VIMS had just one amazing set of images that revealed these, but that then limited us to just one set of lighting and viewing angles. Had we had some views of the these features near the limb or at a different phase angle we could have distinguished better between different scenarios of just how much of what we were seeing was actually due to soot vs unexpected but perhaps large depressions in both cloud tops and cloud thinning.

4. The String of Pearls. How often and why do such features appear? Like the Hexagon, this was a very strange phenomenon unseen on any other planet. The huge storm of 2010–2011, which actually erupted amongst the Pearls, obliterated it. Were these connected? Was the String of Pearls a harbinger of the Great Storm (somewhat like earthquakes can be a harbinger of volcanic eruptions).

5. The polar hexagon. What is its lifetime/variability? The very large shear in the winds rising from a more typical 10–20 m/s to over 125 m/s in just a few degrees of latitude, and then back down again to 10–20 m/s on the other side of the hexagon, is still perplexing. Why does not it diffuse away? Something is organizing it which is still very poorly understood. In addition, the whole north polar region seems to have some seasonal variability in its upper atmosphere aerosol coloring which should be studied by a VIMS or ISS instrument (or both) on a future mission. It is possible that Hubble

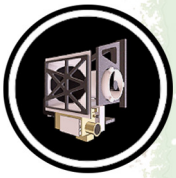

Space Telescope (HST) and some ground-based telescopes will continue to observe this, but as Saturn tilts back to its northern fall season it will be problematic to view.

6. What is Saturn's bulk rotation rate (or perhaps set of rates, if there are actually different rates for various 10,000 km depth-scale regimes, as some folks are starting to suggest)? The new Krono-seismology technique that Matt Hedman and Phil Nicholson have developed from VIMS observations may be a key contributor to answering this with future missions.

Icy Satellites and the Earth's Moon

Earth's moon

Clark [2009] wrote:

> *"Data from the Visual and Infrared Mapping Spectrometer (VIMS) on Cassini during its flyby of the Moon in 1999 show a broad absorption at 3 micrometers due to adsorbed water and near 2.8 μm attributed to hydroxyl in the sunlit surface on the Moon. The amounts of water indicated in the spectra depend on the type of mixing and the grain sizes in the rocks and soils but could be 10 to 1000 parts per million and locally higher. Water in the polar regions may be water that has migrated to the colder environments there. Trace hydroxyl is observed in the anorthositic highlands at lower latitudes."*

The discovery of widespread water on the Moon was evident in the data returned right after the Earth flyby, … .

See Figure VIMS-1 for image.

The discovery of widespread water on the Moon was evident in the data returned right after the Earth flyby, but calibration of the VIMS data was uncertain at that time. It was not until after Cassini orbit insertion at Saturn had the VIMS calibration been refined enough to be certain of the water signature. The VIMS results were later verified by the Moon Mineralogy Mapper on Chandrayan-1, and EPOXI on Deep Impact and the three instruments showed proof that the water signature was real, changing our understanding of the Moon.

Jupiter system

Brown et al. [2003] presented results from the Jupiter flyby. VIMS documented a surprisingly high opposition surge on Europa, the first visual-near-IR spectra of Himalia. Himalia has a slightly reddish spectrum, an apparent absorption near 3 μm, and a geometric albedo of 0.06 to 0.01 at 2.2 μm (assuming an 85 km radius). If the 3-μm feature in Himalia's spectrum is eventually confirmed, it would be suggestive of the presence of water in some form, either free, bound, or incorporated in layer-lattice silicates.

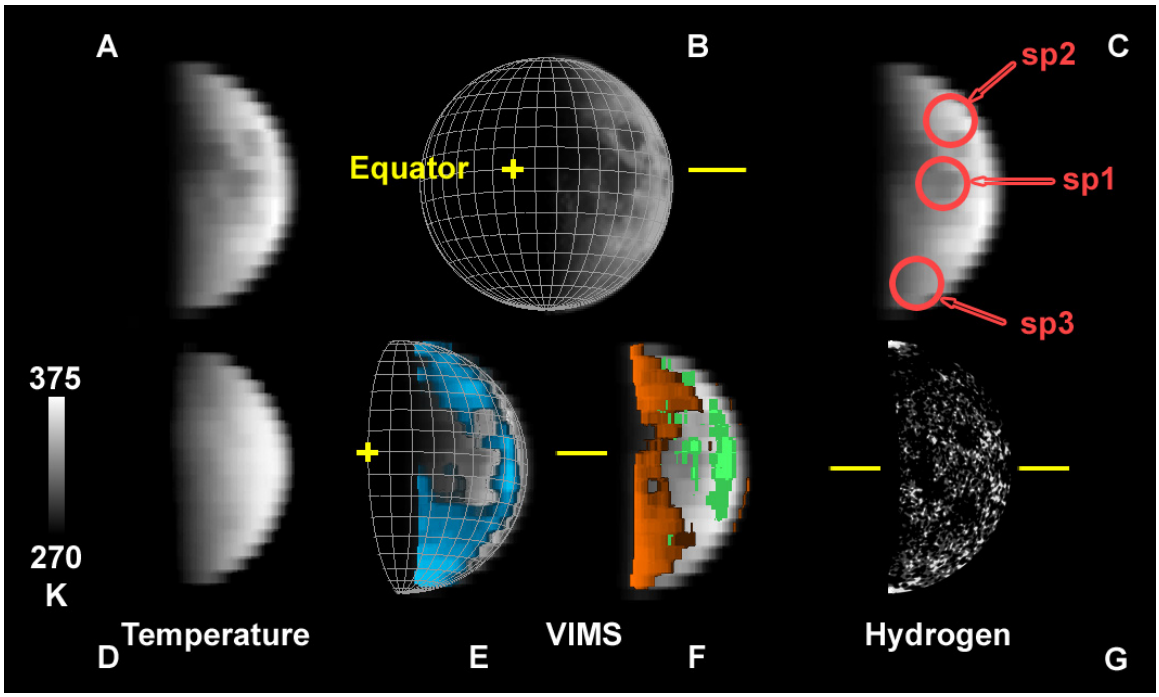

Figure VIMS-1. Cassini VIMS observations of the Moon on August 19, 1999. *A*: VIMS 2.4 μm apparent reflectance. *B*: Cassini Imaging Science Subsystem image obtained during the flyby. The yellow bars indicated the equator position. The yellow cross indicates latitude 0, longitude 0. *C*: Locations of VIMS spectra discussed in Clark [2009]. *D*: VIMS-derived temperatures. Maps of *E*: the 3 micron absorption strength (blue), and *F*: the 2.8 μm OH strength (orange and green). *G*: Hydrogen map from LP [Feldman et al. 2000] masked to give a similar view as the VIMS observation. Figure from Clark [2009].

VIMS spectra of the Galilean satellites confirmed the spectral features in the Near Infrared Mapping Spectrometer Subsystem (NIMS) data. Brown et al. [2003] also noted similar spectral structure as in NIMS data attributed to a CN bond near 4.5 μm. This structure was also seen in VIMS data of the Saturnian satellites—for example, Clark et al. [2005, 2008]—but as later found to be due to a calibration error [Clark et al. 2012]. VIMS data also provided the first near-IR phase curve of Europa. Europa exhibits a remarkable surge in brightness (~0.2 mag/deg) under 1°, comparable to the lunar opposition surge measured by Clementine [Buratti et al. 1996]. Furthermore, data at small phase angles show a clear trend with albedo, such that wavelengths corresponding to higher albedos have smaller surges, consistent with shadow illumination. The VIMS results suggest that neither CBE nor shadow hiding provide a complete description of Europa's opposition surge below 1° [Brown et al. 2003].

Saturn system

The first VIMS observations of the Saturnian satellites were of Phoebe on June 11, 2004, before Saturn orbit insertion [Clark et al. 2005]. VIMS spatially resolved the surface of Phoebe, and data have been registered and projected into simple cylindrical maps: low to medium resolution with near hemispheric coverage, and high resolution of a small area. Clark et al. [2005] mapped ferrous-

iron-bearing minerals, bound water, trapped CO_2, probable phyllosilicates, organics, nitriles and cyanide compounds. Detection of these compounds on Phoebe makes it one of the most compositionally diverse objects yet observed in our Solar System. It is likely that Phoebe's surface contains primitive materials from the outer Solar System, indicating a surface of cometary origin. Improved calibration [Clark et al. 2012] showed that the nitrile detection was due to an error in the calibration to reflectance. The ferrous-iron-bearing minerals was subsequently shown by Clark et al. [2012] to be nano-iron oxides plus nano-metallic iron (e.g., in space-weathered silicates) and scattering effects.

This nitrile identification error originated in the NIMS calibration and propagated into the VIMS calibration from cross instrument calibrations. A calibration target was descoped early in the mission, which led to the error. The diversity of targets and phase angles during the Cassini orbital tour led to continuing improvements in the VIMS calibration [Clark et al. 2016b, 2018]. Figure VIMS-2 shows the quality of spectra obtained using the new calibration.

We now know that the iron signatures in Phoebe's spectrum are due to a combination of nano-phase iron oxides and nano-metallic iron [Clark et al. 2012]. This is the same composition as the dark material on Iapetus (Figure VIMS-2). The 3-μm absorber was also identified as a definitive match by Clark et al. [2012] as a unique signature of hydrated nano-iron oxides (the water may be adsorbed water). The nano-phase metallic iron must be embedded in another matrix, e.g., silicates.

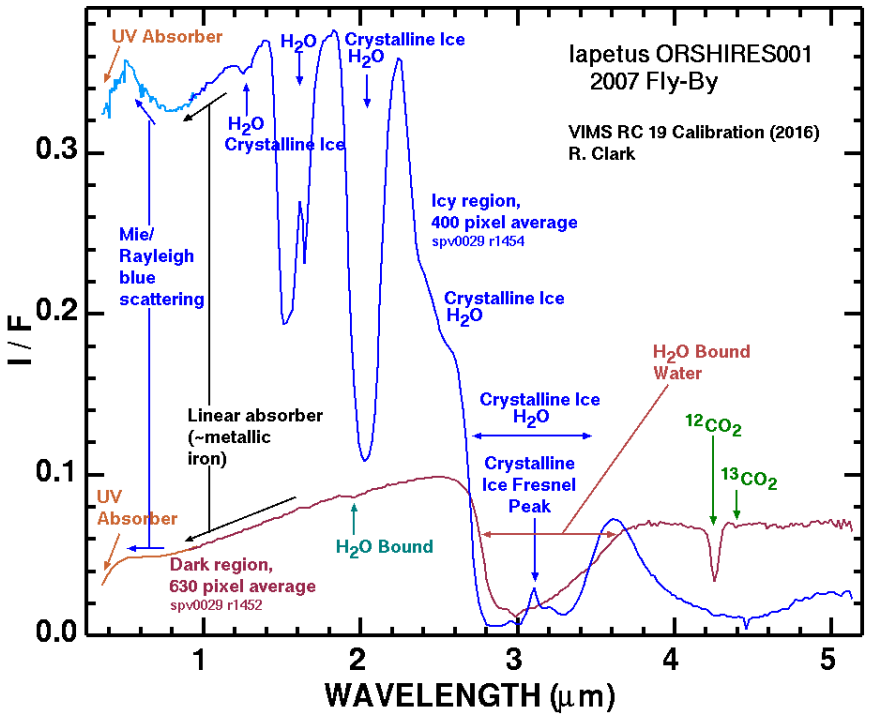

Figure VIMS-2. Illustration of VIMS spectra of two regions on Iapetus with causes of spectral features labeled. After Clark et al. [2012] with the RC 19 calibration [Clark et al. 2016b].

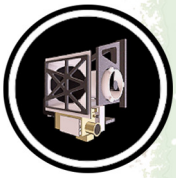

VIMS has shown that the water ice on the icy satellites is crystalline. While initial reports showed indications of amorphous ice, it was subsequently found that sub-micron ice grains modify the reflectance spectrum mimicking some aspects of amorphous ice signatures. Mastrapa et al. [2008] publication of crystalline and amorphous ice optical constants enabled better comparisons to observed spectra, and along with improved radiative transfer models that included diffraction effects of small particles [Clark et al. 2012], the differentiation between amorphous and crystalline ice could be made with more confidence. These results are summarized in Buratti et al. [2018a].

CO_2 is present on the surface of most of the moons [Buratti et al. 2005; Brown et al. 2006; Clark et al. 2005, 2008, 2012; Cruikshank et al. 2010 and references therein], but there are still spectral identifications that are uncertain. Clark et al. [2012] showed that a weak feature at 2.42 μm is due to trapped molecular hydrogen and is observed in dark material on multiple icy satellites, but this feature needs confirmation by an independent instrument. A weak absorption at 2.97 μm corresponds to ammonia [Clark et al. 2008, 2012] and is seen on multiple icy satellites, but the absorption overlaps an order-sorting filter gap in the VIMS instrument where instrument errors are larger. Observations of ammonia need confirmation either by a better calibration of the VIMS data, or by other instruments. Iapetus and Hyperion have many unidentified spectral bands in the 1- to 5-μm region [Cruikshank et al. 2007; Clark et al. 2012; Dalton et al. 2012] that may be the signature of higher order hydrocarbons, some of which have not been measured in the laboratory. Absorptions attributed to aromatic hydrocarbons have been detected in the spectrum of Iapetus and Phoebe [Cruikshank et al. 2008, 2014; Dalle Ore et al. 2012].

All of the icy Saturnian moons are absorbing in the ~0.2 to 0.5 μm region, making them dark at far ultraviolet channel (FUV) wavelengths. For instance, Filacchione et al. [2012, 2016] used Cassini VIMS data to show that the spectral slope (0.35–0.55 μm) increases (becomes redder) with distance from Enceladus. While the UV absorber causes reddening, sub-micron grains induce increased scattering, causing a bluing effect, so there are competing signatures of these two components throughout the Saturn system.

Deuterium has been found on Phoebe, Iapetus, Hyperion, Rhea, Dione, Enceladus and the Rings and carbon 13 has been detected on Phoebe and Iapetus (Figure VIMS-2) [Clark et al. 2018, 2017a, 2017b, 2016, 2012] and the D/H ratio derived. Phoebe is an outlier with D/H more than seven times higher than terrestrial, which the other satellites and rings are close to terrestrial ocean water values, an unexpected result not predicted by current models of Solar System formation.

The plumes of Enceladus were observed by VIMS to vary in intensity with mean anomaly over short-timescales [Hedman et al. 2013a]. Results from the VIMS, which measured the short-wavelength end of the blackbody curve for the south pole of Enceladus, calculated a temperature of 197 ±20 K and a linear size of 9 meters [Goguen et al. 2013]. Further analysis of VIMS data will enable this result to be refined and will place limits on additional emitting regions. The amount and/or size of particles spewing from the fissures varies as a function of the orbital position of Enceladus, implicating tidal forces as the source of energy driving eruptive activity [Hedman et al. 2013a; Nimmo et al. 2014]. Hedman et al. [2009] analyzed VIMS plume spectra as a function of altitude to derive composition and grain sizes. These spectra show that the particulate component

of the plume consists primarily of fine-grained water ice. The spectral data are used to derive profiles of particle densities versus height, which are in turn converted into measurements of the velocity distribution of particles launched from the surface between 80 and 160 m/s (i.e., between one-third and two-thirds of the escape velocity). The size distributions show that the parts of the plume observed by VIMS are strongly depleted in particles with radii larger than 3 μm. Furthermore, the velocity distributions indicate that only a small fraction of 3-μm particles can escape from Enceladus.

One of the most intriguing results of the mission was the discovery of global red streaks on Tethys and blue pearls on Rhea that do not appear to be connected to any underlying geologic structures [Schenk et al. 2011, 2015] VIMS analysis of the streaks on Tethys shows a clear spectral difference [Buratti et al. 2017], but it is not clear whether this difference is caused by composition, such as an enhanced amount of organic material, magnetospheric effects, or simply grain size.

Another intriguing result was the detection on December 15, 2004, of a transient aura-like ring around Dione at 2.65 μm that suggested the existence of an atmosphere [Clark et al. 2008] (Figure VIMS-3). Magnetometer data obtained on October 11, 2005, show a weak field perturbation in the upstream region, indicating a tenuous atmosphere [Simon et al. 2011]. Observing with Cassini Plasma Spectrometer (CAPS), Tokar et al. [2012] discovered a thin atmosphere (~0.01-0.09 particles/cm^3) of O_2^+ during the close (500 km) flyby on April 7, 2010. A search for forward scattered radiation at solar phase angles >150°, indicating a plume, was negative [Buratti et al. 2011]. No clear evidence of ongoing activity on Dione was discovered during the mission, although more thorough inspection of the 2.65-μm band is an ongoing task.

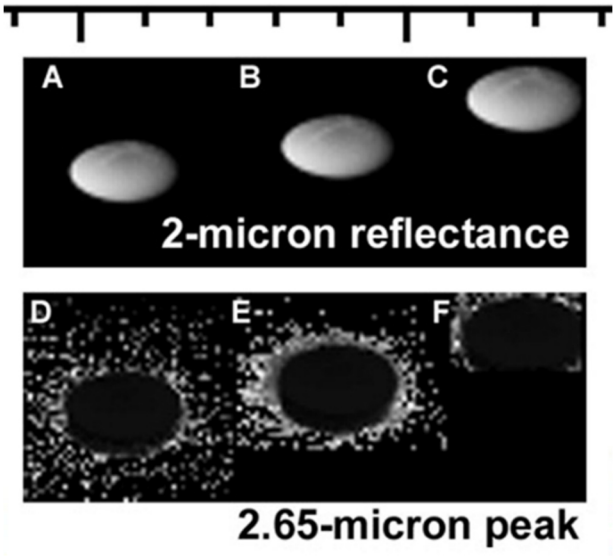

Figure VIMS-3. The 2.65-μm transient atmosphere on Dione [Clark et al. 2008].

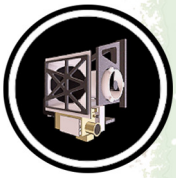

IR spectroscopy is sensitive to grain size of materials, and the multiple absorption in ice allow grain size mapping to be done with VIMS data. On Enceladus, the sizes of ice particles are generally well correlated with geologic features and surface ages, indicating a stratigraphic correlation between tectonic features and cryovolcanic activities [Jaumann et al. 2008b]. Grains much smaller than the wavelength of light cause enhanced blue scattering, including a Rayleigh scattering effect. This bluing effect is observed in the Saturn system and quantified by Clark et al. [2008, 2012].

Scipioni et al. [2017] produced image-cube maps of Enceladus,mapped ice grain sizes and identified plume deposits across the surface. The map showing the band-depths-ratio 1.50/2.02 μm overall shows a good agreement with the predicted plumes' deposits on the trailing side, where the amount of sub-micron particles decreases with increasing accumulation of ejecta material. However, this correlation is much weaker, or even absent, on the leading side of Enceladus, where the abundance of sub-micron particles is the highest across the entire surface.

Stephan et al. [2012] showed that the distribution of spectral endmembers as well as global band-depth variations of Dione's water-ice absorptions measurements imply that the bombardment with charged particles from Saturn's magnetosphere is one of at least two major global processes affecting Dione's surface. Ice deposits dominating its leading hemisphere appear rather associated with rays of the fresh impact crater Creusa on the northern leading hemisphere. These rays cross almost the whole hemisphere masking here any effects of possibly existent, but less dominant, processes as evident in the transition from the bright to dark regions on the Saturn-facing hemisphere (~0° W). CO_2 is evident in the dark material pointing to a possibly formation due to the interaction of the surface material with the impacting particles from Saturn's magnetosphere. Local spectral differences are consistent with impacting particles from the trailing side as described by Clark et al. [2008] with a pronounced ice signature on crater walls facing the leading side direction and shielded from impacting particles and dark material concentrated on interior crater walls facing the trailing hemisphere.

Spectra of ice also vary with temperature, so the surface temperatures of cold icy surfaces can be sensed without needing to measure longer wavelength thermal emission. Filachione et al. [2016] analyzed the ice spectra to produce daytime temperature maps of the satellite surfaces, just one more indication of the diversity of science that an imaging spectrometer can provide.

Observations of the small inner moons of Saturn were also obtained during the mission, including five best ever flybys of the ring moons Pan, Daphnis, Atlas, Pandora, and Epimetheus that were obtained between December 2016 and April 2017 during the Ring-grazing Orbits. An example of an observation is shown in Figure VIMS-4. Views of the moons' morphology, structure, particle environment, and composition were obtained, as well as VIMS maps in its full spectral range, except for Daphnis, which as of now is lacking a visible VIMS spectrum [Buratti et al. 2018b]. The optical properties of the moons are determined by two competing processes: contamination by a red chromophore in Saturn's main ring system, and accretion of bright particles from the E-ring originating from Enceladus.

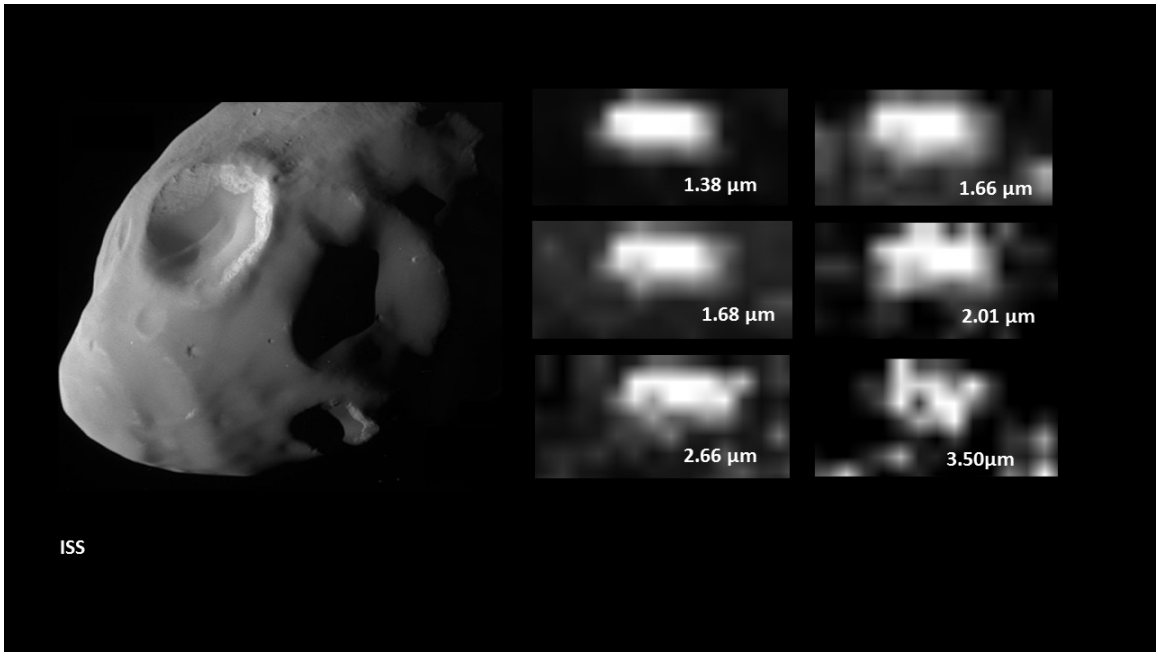

Figure VIMS-4. VIMS images of Pandora (*Right*), obtained on December 12, 2016 during a flyby that approached the shepherd moon to within a distance of 22,000 km. The ISS image is shown (*Left*) for context.

Open questions

Is there a connection between the composition of the plume and the regions on Enceladus where plume deposits exist, for example, Schenk et al. [2011]. How are the plume fallout zones compositionally different from the other zones on Enceladus that are affected by particles from the E-ring? What is the chemical make-up of the trailing side of Tethys, and why is it so reddish [Schenk et al. 2011] compared to regions dominated by the in-fall of E-ring grains?

What is the nature of possible activity on Dione? Is this moon still active, or has it been active in the recent past?

Similar to Dione, Tethys exhibits regions of smooth plains in which large craters have been removed. Cryovolcanic activity on Tethys is problematic: with a density even less than that of water, what is the driver for the activity?

What is the cause of the red streaks on Tethys and the blue dots on Rhea? Are they compositionally different, or can their appearance be explained solely by the effects of grain size?

What is the time scale for plume variability on Enceladus beyond the simple correlation with distance from Saturn, which is due to the magnitude of tidal effects? Is there a correlation with seasons? Can the variability be monitored from the ground?

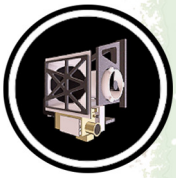

What is the identity of the red chromophore on the inner icy satellite surfaces? Is it nano-iron or organic material (tholins), and what are the transport processes to move this material around the Solar System? We have excellent evidence that Iapetus', Phoebe's and Hyperion's color is dominated by nano-iron and nano-iron oxide, but the red absorber is weaker on the inner satellites, and it cannot be established which possibility is correct for those satellites. Does radiation play a greater role in surface modification of these materials on the inner satellites?

What are some of the minor constituents of the Saturnian moons, and are the endogenic or exogenic? If exogenic, is the accretional process still ongoing?

How does the D/H ratio compare with that of other regions of the solar system, and what does that imply about the transport of volatiles on a large scale?

Is the detection of ammonia hydrate on the surfaces of the moons definitive?

Some of these unanswered questions might be answered with further research with the vast trove of archived data and with continuing ground-based observations, including the James Webb Space Telescope (JWST).

Science Assessment Summary

The VIMS instrument illustrated that the data an imaging spectrometer can deliver led to an amazing diversity in science. For icy satellites alone, from unexpected compositions, to geologic mapping, grain size distribution, temperature mapping, isotopic ratios, to plume dynamics, VIMS and the science team delivered far more than what was envisioned at the start of the mission. No single other instrument has shown such science diversity.

No single other instrument has shown such science diversity.

While the above science assessment documents huge accomplishments in satellite science with imaging spectroscopy data obtained by VIMS, interpretation of such data has been and remains difficult due to limited laboratory data and sophistication of models. For example, one of the main, seemingly simple, science questions yet to be answered is the nature of the coloring agent(s) on the inner icy Saturnian satellites and rings. While we obtained a definitive answer for the satellites beyond Titan, the origin of the coloring on the icy moons inside the orbit of Titan remain uncertain. This is largely due to lack of lab data and sophistication of radiative transfer models. Similarly, it was not until near the end of the prime mission before it was realized that the spectral effects of sub-micron ice particles affected the spectra in such profound ways, because there was no lab work or radiative transfer models for those conditions. Early on we wondered if there were calibration errors in VIMS causing unusual shapes of ice absorptions in VIMS data. If we had more extensive spectral libraries at the start of the mission, so much time would not have been lost going down blind alleys. Similar blind alleys were also traveled trying to identify other spectral features, like the 2.42 micron absorption. Initial thoughts were it was due to a C-N bond,

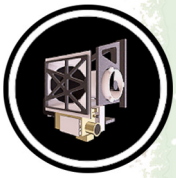

but the stronger absorptions of C-N bearing compounds at longer wavelengths were not seen. It took substantial resources to find the origin as trapped H_2. To date, the organics absorptions observed in VIMS data on several satellites still have not been precisely identified, only general categories like aliphatic versus aromatic can be determined. What major chemistry and implications are we missing with this lack of knowledge? Only additional resources put into lab work and modeling, funded by future NASA research programs will solve these problems. This should also be a lesson for future missions: the science output of the mission will be limited by current knowledge, including laboratory data and models.

Ring science

This part of the VIMS efforts had five principal components that are described below, along with their principal scientific goals, and major scientific results.

Ring macrostructure and dynamical processes

Our goal here was to study the radial structure of the main rings at the sub-km scale, at a variety of ring opening angles, and to examine their large-scale azimuthal variations (eccentricities, normal modes, etc.). Also of interest is the vertical structure of the rings, in those regions where it can be resolved.

Stellar occultations provide radial structure; over 170 were observed over the course of the mission, using ~40 different stars to provide different ring opening angles. A number of different investigations have been carried out using these data, as documented below. Particularly valuable for low-optical-depth regions such as the C-ring have been occultations of bright, low-latitude stars such as alpha Ori, omicron Ceti, and alpha CMa. But probably our most scientifically-productive data set is a sequence of ~17 occultations of the bright, high-latitude star gamma Crucis done on nearly-successive orbits with very similar geometry in 2008 and 2009.

Ring Plane Crossing observations were done on several near-equatorial orbits in order to provide measurements of the rings' photometric thickness as a function of radius and phase angle. Modeling of these data confirms that the ring's edge-on brightness is dominated by the vertically-extended F-ring.

Extended movies were obtained of the F-ring to study its complex azimuthal variations and also obtain high-quality spectra. Most of these observations were efficiently done as riders on ISS movies.

Ring microstructure and particle size distribution

Cassini observations, primarily radio and stellar occultations, have revealed the presence of various types of small-scale structure in the rings, notably self-gravity wakes (due to a completion between Keplerian shear and self-gravity) and radial oscillations caused by a viscous over-stability in dense

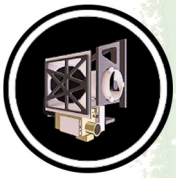

parts of the rings. The ring particle size distribution is critical to numerical models of ring structure and evolution, but can only be approached indirectly by Cassini.

Stellar occultations are again our main tool here, providing 100-m scale resolution or even better in some cases. The most useful observations here are occultations where the track of the star reaches a minimum radius in the rings. In hindsight, more of these events would have been useful. Occultations of low-latitude stars also provide quantitative data on the azimuthal variations in optical depth produced by self-gravity (S-G) wakes.

VIMS solar occultations by the main rings have provided valuable (and unique) information on the distribution of the smallest ring particles, in the mm–cm size range.

Spectral images of the rings obtained at phase angles of 165° or higher have provided very valuable data on the particle size distributions of the diffuse D-ring, F-ring, G-ring and E-ring that are not obtainable in any other way short of in situ sampling. Because the key scattering parameter in this geometry is the ratio $\Theta\lambda/r$, where Θ is the scattering angle, lambda is the wavelength, and r is the mean particle radius. VIMS 1– to 5-μm spectra effectively extend the range of observed scattering angles by a factor of 5.

Compositional variations

A primary goal of VIMS ring observations, not surprisingly, was to establish their composition and map radial variations in the fraction of non-icy material, suspected on the basis of Earth-based spectroscopy. This has turned out to be a very difficult problem, chiefly because of the very tiny amounts of non-icy material, estimated to be a few tenths of a per cent in most places. Although radial variations in the rings' spectral characteristics have been well-established, in the form of ice band depths and continuum slopes, there is still no consensus on the nature of the non-icy material. Recent Hapke modeling of spectra in selected regions indicate that both intimate and intra-particle mixing of water ice, amorphous carbon and organic material (modeled as Titan tholins) can reproduce the observed ring spectra, but nano-phase Fe-bearing materials such as these seen on Iapetus remain a possibility. A large variety of both Prime and Rider observations have been devoted to this problem.

VIMS radial scans generally provide the highest-quality data. This includes several high-resolution (30–60 km/pixel) complete radial scans obtained on the F-ring and Proximal orbits in 2017.

A unique set of radial scans were done at Saturn orbit insertion in 2004 that still provide our highest-resolution spectral data of the unlit side of the rings.

VIMS scans along the edge of Saturn's shadow on the rings are lower in resolution but were designed to minimize interference from Saturn-shine.

Several riders on ISS high-resolution radial scans also provide excellent-quality VIMS spectral data.

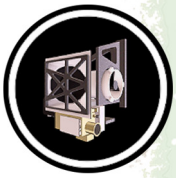

A large number of riders on lower-resolution CIRS radial scans provide useful data at a variety of ring opening and phase angles.

PHOTOMETRY AND LIGHT-SCATTERING PROCESSES

A number of observations were designed to provide lower spatial resolution spectral data on the rings at a wider range of observing geometries than are covered by the above compositional scans. The goal was to provide data with which to model light-scattering processes in the main rings, in particular the degree of multiple scattering between particles and the characteristics of the rings' well-known opposition brightening at low phase angles. The principal sets of observations are:

a. Standardized ring ansa mosaics done at ~20 R_S.

b. Scans and small mosaics at phase angles of 165° or higher.

c. Full system mosaics at distances of 30–40 R_S.

d. Radial scans across the rings immediately before and after the Equinox in August 2009, when the solar illumination was almost edge-on.

e. Riders on ISS photometry observations.

DIFFUSE RING STRUCTURE, PARTICLE SIZE, AND COMPOSITION

VIMS was well-suited to obtain reflected-light observations of Saturn's diffuse rings, including the D-ring, F-ring G-ring and E-ring as well as several smaller-scale structures such as narrow ringlets and clumps within gaps in the main rings and arcs associated with the small satellites such as Aegaeon. This is because of the instrument's very low level of scattered off-axis light (unlike the ISS-wide angle camera (WAC), which is also used for such studies), its spectral range, and its capacity to take long exposures. A mixture of VIMS-prime and ISS-rider observations was employed, with most observations being made at high phase angles where dust-sized particles are brightest. The principle sets of observations are:

a. Radial mosaics of one ansa of the E-ring at various phase angles.

b. Image cubes targeted to one ansa of the G-ring at various phase angles. Most E_ and GPHASE observations were made when the rings were viewed edge-on, on equatorial orbits, in order to increase the line-of-sight optical depth of these very diffuse structures.

c. Movies of the F-ring, intended to cover all (or most) co-moving longitudes of the ring in a single observation. This was done initially as VIMS-prime and later as ISS-riders, on non-equatorial orbits to resolve radial structure.

d. Riders on various ISS faint ring observations.

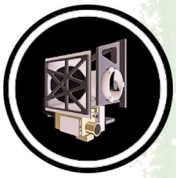

Cornell non-rings observations

In addition to observations of the rings, the Cornell group also took on responsibility for several categories of non-ring observations which used similar techniques or designs as some Rings observations.

> … VIMS proved to be an effective instrument for observing atmospheric occultations by Saturn and Titan.

Saturn and Titan stellar occultations

Using the same technique developed for ring stellar occultations, as discussed in the section entitled Saturn and Titan Stellar Occultations, VIMS proved to be an effective instrument for observing atmospheric occultations by Saturn and Titan. With sampling intervals of 20–40 msec, the altitude resolution is typically 100–400 m. The science obtained from such observations includes vertical profiles of temperature, atmospheric composition (chiefly methane) and aerosol abundance, as functions of latitude, as well as information on the shape of Saturn's geoid. Over the course of the mission ~70 stellar occultations by Saturn were planned, with all but 13 returning useful data. Another 35 were observed as bonuses at the end of ring occultations, but many of these were seen against a sunlit limb and suffer badly from background light from the planet. A total of 14 stellar occultations by Titan were observed, all but one successfully. Some of the latter show noticeable aerosol layers. An important limitation of such observations is atmospheric refraction, which eventually causes the star to leave the VIMS pixel. This limits the maximum depth of Saturn occultations to a pressure level of ~5 mbar.

Saturn and Titan solar occultations

Using the solar port originally designed for spectral calibrations, VIMS has observed 29 solar occultations by Saturn and 16 by Titan. Because the angular diameter of the sun exceeds the VIMS instantaneous field of view (IFOV) of 0.5 mrad, solar occultations were observed in IMAGE mode rather than in the special mode designed for stellar occultations, thus reducing the vertical resolution to10–30 km. All of these observations were done as riders on UVIS occultations. Analysis of several Titan solar occultations has led to vertical profiles of methane and CO, as well as characterization of the aerosol size distribution. All but one of the solar occultations attempted returned data, but in several cases the Titan observation were corrupted because the bright limb of Titan itself appeared in the main VIMS aperture while the sun was in the solarport.

Enceladus plume observations

VIMS made several important observations of the plumes of Enceladus, including both high-phase images that led to the discovery of the plumes' significant variations with orbital phase and a solar occultation from which the volume density of water ice particles could be measured directly.

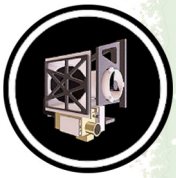

STELLAR CALIBRATIONS

In addition to regular observations of standard stars for instrumental calibration purposes, VIMS also obtained near-IR spectra for ~40 of the brightest stars in the sky, many of which were published in an IR spectral atlas. Many of the stars are late-type variables that exhibit strong absorptions due to CO and water vapor.

SOLAR PORT CALIBRATIONS

Over the course of the mission, a substantial number of calibration observations of the Sun were made with the VIMS solar port. Some of these simply provide routine monitoring of the solar spectrum, as check on instrumental sensitivity drifts while others were used to map the spatial variations in its throughput.

EXOPLANET AND VENUS TRANSITS

In 2010 and 2011 several attempts were made to observe stellar transits of the giant exoplanet, HD189533b. VIMS was used in 2 × 2 IMAGE mode in order to provide simultaneous background measurements and some insurance against pointing variations. Unfortunately the star was much fainter than normal VIMS point source targets and no transit was detected. Analysis of the data, however, demonstrated that VIMS sensitivity scaled with integration time as expected, even down to signal levels of order 0.1 DN. In December 2012 a very similar technique was used to monitor a predicted transit of Venus across the sun using the VIMS solar port. This observation, which involved a reduction in the solar flux of only 0.01% was successfully observed, though the signal-to-noise ratio was too low to detect the absorption signature of Venus' atmosphere in the transit spectra.

PRINCIPAL RESULTS

1. VIMS spectral observations at SOI revealed that the mysterious red coloring agent in the rings resides within the water ice grains that make up the regoliths on the ring particles [Nicholson et al. 2008].

2. Observations of ring occultations of o Ceti (aka Mira) in 2005 confirmed the existence of strong self-gravity wakes in the A-ring, leading to the first reliable estimates for the ring thickness of ~6 meters in this region [Hedman et al. 2007b].

3. Observations of multiple stellar and radio occultations in 2005–2009 led to the discovery that the amplitude of the radial perturbations at the outer edge of the B-ring (due to the Mimas 2:1 resonance) varies from ~70 km to < 5 km, and that these may also be indirectly responsible for the regular spacing of the multiple gaps within the Cassini Division [Hedman et al. 2010].

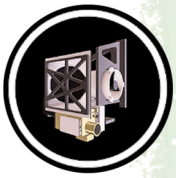

4. The observation of restrahlung bands of H_2O ice in a stellar occultation by the F-ring permitted discrimination between clumps of macroscopic source bodies and the background of micron-sized dust [Hedman et al. 2011].

5. A comparative analysis of VIS-IR spectral indicators (slopes and band depths) of rings, regular satellites and small moons has allowed VIMS to map the distribution of water ice and red contaminant materials across the Saturn system [Filacchione et al. 2012, 2013; Clark et al. 2012]. However, in the main rings, the abundance of the red coloring agent is lower and there is at present no way to distinguish definitively between the nano-iron model and more traditional carbon-tholin models. Recent modeling results obtained with Hapke theory indicate that both intimate and intraparticle mixing of water ice, amorphous carbon and organic material (Titan tholins) can reproduce the observed ring spectra [Ciarniello et al. 2019].

6. VIMS investigations of numerous, small-scale, wavelike structures in the C-ring have provided strong evidence that several of these are density waves driven by global oscillations within Saturn itself, opening up a new window on the planet's internal structure and rotation rate [Hedman and Nicholson 2013; Hedman and Nicholson 2014].

7. A pair of stellar occultations with turnaround radii in the inner A-ring yielded strong evidence for viscous over-stability in the denser parts of Saturn's rings, supporting previous work based on radio occultation data. [Hedman et al. 2014].

8. Together with occultation data from RSS and UVIS, VIMS data from more than 100 stellar occultations has led to the characterization of numerous non-circular features in the C-ring and Cassini Division, including the discovery of a large number of normal mode oscillations on the edges of both narrow gaps and their associated ringlets. [Nicholson et al. 2014a, 2014b; French et al. 2016].

9. Ring temperature maps have been built from VIMS spectra by using an indirect method based on the wavelength of the temperature-dependent reflectance peak at 3.6 μm [Filacchione et al. 2014].

10. Application of a new phase-sensitive wavelet analysis technique to selected VIMS stellar occultation profiles has led to the identification of several satellite-driven density waves in the optically-thick B-ring, resulting in the first estimates of surface mass density in this most opaque part of Saturn's rings. The results are unexpectedly low, and imply a total mass for the rings of ~40 percent that of Mimas [Hedman and Nicholson 2016].

EXAMPLES OF STELLAR OCCULTATION OBSERVATIONS

Figures VIMS-5 through VIMS-10 show examples of stellar occulation observations.

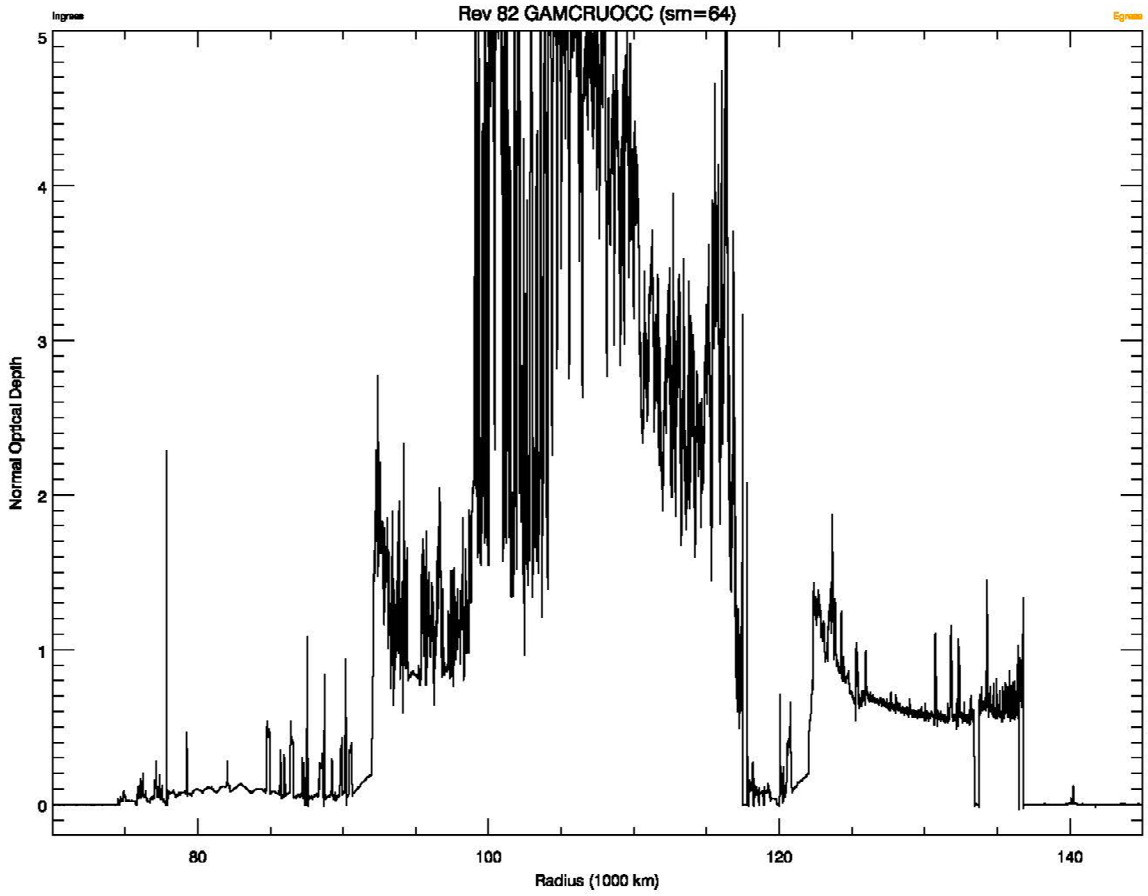

Figure VIMS-5. An optical depth profile of Saturn's rings at a wavelength of 2.92 microns, derived from a VIMS occultation of the star gamma Crucis on rev 82, obtained in August 2008. This is one of the highest-quality VIMS occultation observations, as evidenced by the very flat baselines exterior to the A-ring's edge at 136,770 km and interior to the C-ring at 74,500 km. Note that the optical depth exceeds 5 in some regions of the central B-ring.

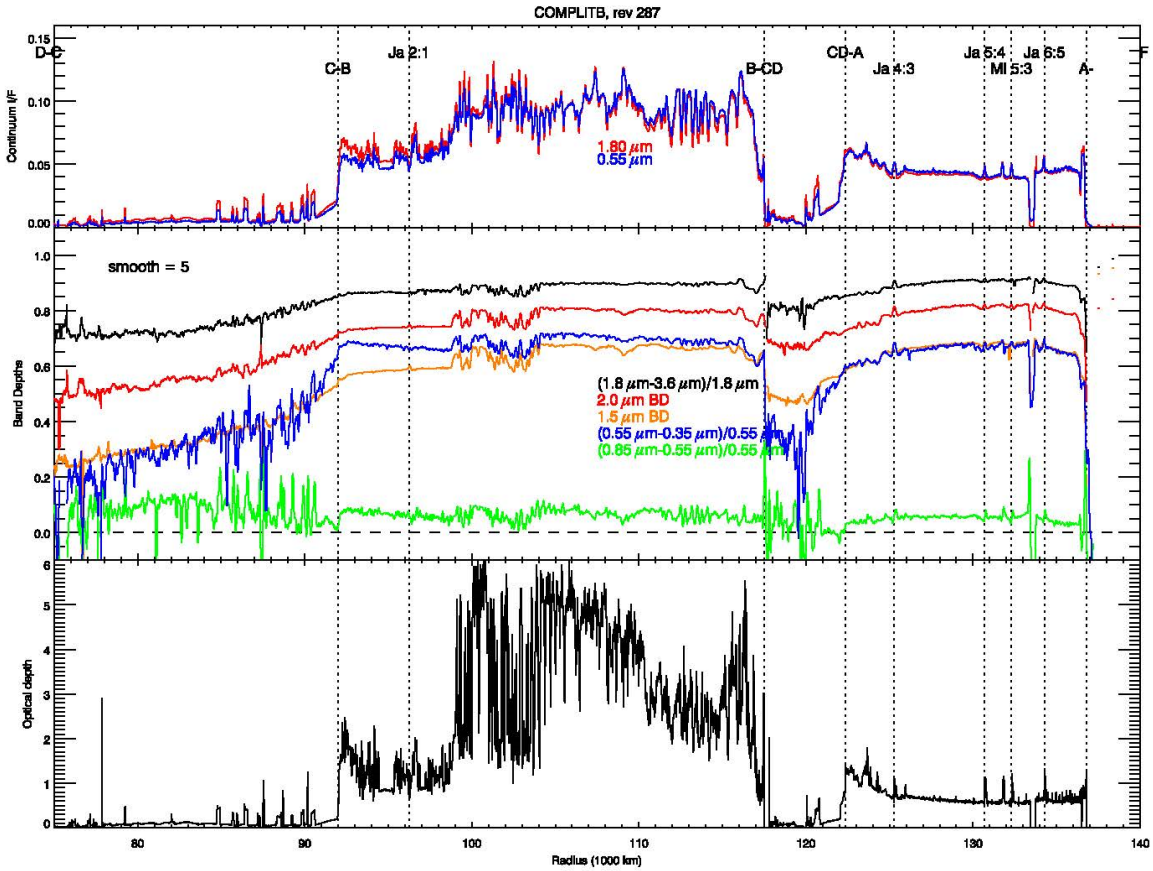

Figure VIMS-6. Radial profiles of IR spectral parameters derived from the final VIMS scan across the sunlit rings on rev 287, rebinned to a uniform sampling resolution of 20 km. *Upper panel*: shows the reflectivity of the rings at continuum wavelengths of 0.55 and 1.8 microns, with the locations of major ring boundaries and the strongest density waves identified by vertical dotted lines. *Middle panel*: shows the fractional depths of the IR water ice bands at 1.55, 2.0 and 3.6 microns, coded by line color, as well as the UV and red slopes measured with the visual channel, all smoothed to a resolution of 100 km. *Lower panel*: shows the optical depth profile of the rings obtained from a VIMS occultation of the star gamma Crucis on rev 82, binned to 10-km resolution, as context for the spectral scans.

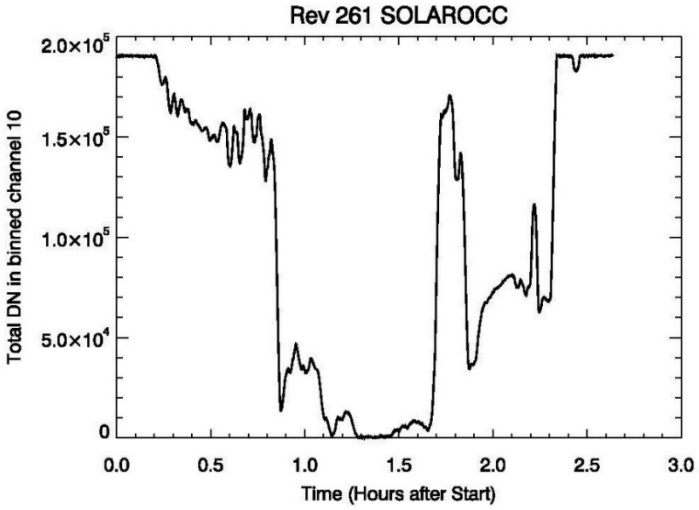

Figure VIMS-7. A transmission profile of the rings at a wavelength of 1.06 microns derived from a VIMS solar occultation on rev 261, obtained in February 2017. Note the lower spatial resolution compared to the stellar occultation in Figure VIMS-5, but the much higher signal-to-noise ratio.

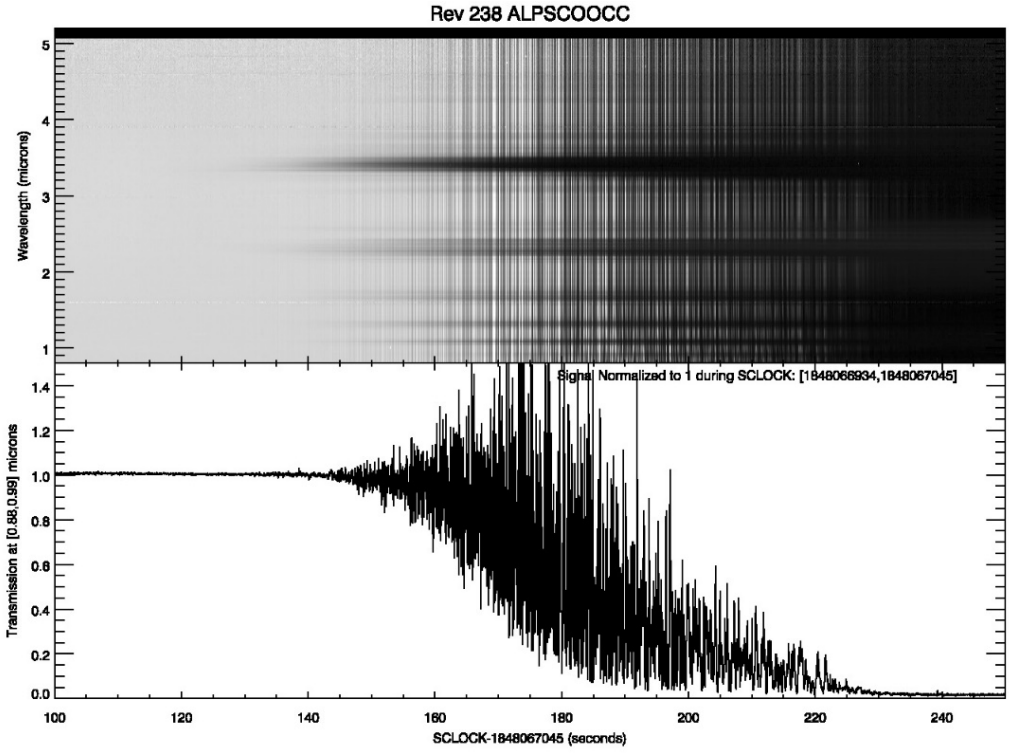

Figure VIMS-8. An ingress stellar occultation by Saturn's atmosphere at 63 deg south latitude on rev 238, obtained in July 2016. Time is shown on the abscissa, in seconds, with wavelength on the ordinate, from 0.85 to 5.1 microns. The greyscale indicates the measured stellar brightness, normalized to unity before the occultation began. In addition to a gradual loss of signal due to differential refraction, punctuated by rapid oscillations due to turbulent scintillation, one sees absorption at several discrete wavelengths (3.4, 2.3, 1.7 microns, etc.) due to stratospheric gasses, chiefly methane.

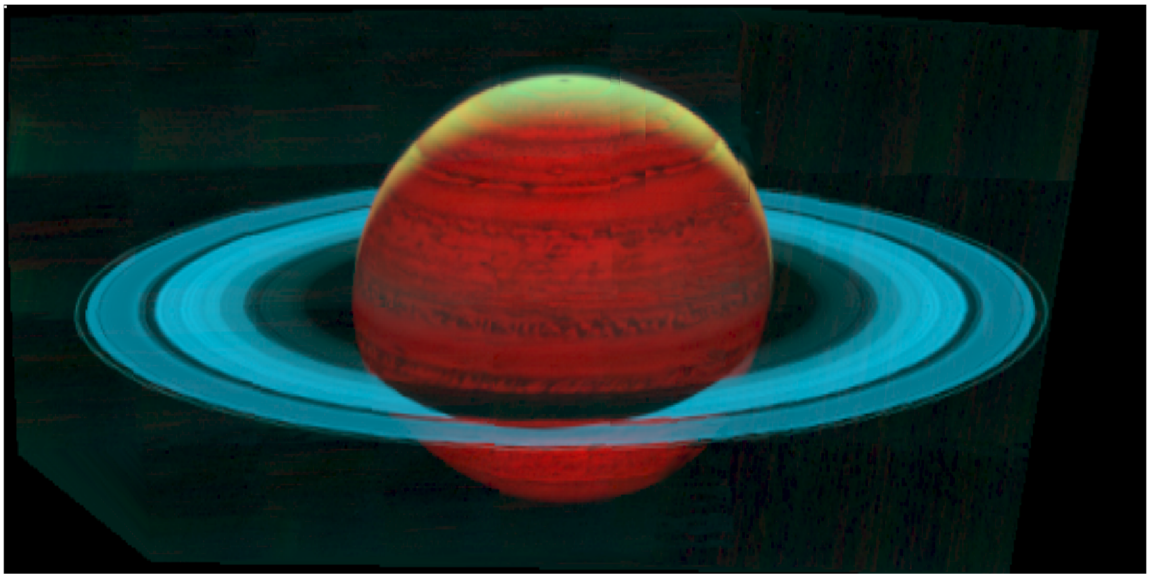

Figure VIMS-9. A mosaic of Saturn and its rings obtained by VIMS on revs 287/289, in August 2017. A total of 35 VIMS cubes were combined to produce this false-color image, with *Red* showing thermal emission from Saturn's deep atmosphere at 5 microns, *Green* showing reflected sunlight from the clouds at 3 microns, and *Blue* showing reflected sunlight from the icy rings at 1.8 microns. The view is at a phase angle of 140 degrees, with only a thin crescent in the north illuminated by sunlight. This close to summer solstice, the planet's shadow on the rings extends only just beyond the Cassini Division. Dark mottling on the planet is due to the variable thickness of clouds in the upper atmosphere. Saturn's oblateness is slightly exaggerated here by changes in the viewing geometry during the total observation period of almost 12 hours.

Open questions

A big unanswered question remains that of the nature of the non-icy component. We know that some of it is meteoritic (or cometary) debris, but the true nature of the UV-absorbing component(s) remains elusive. More sophisticated spectral modeling might eventually solve this problem, as we certainly have acquired plenty of spectra.

Titan

Before Cassini, Titan's surface was unknown territory because aerosols in its dense nitrogen and methane atmosphere hide the surface in the optical wavelengths. It was believed that only radar waves would be able to cross the atmosphere and provide images of the surface, thus it was not expected that the VIMS instrument would be able to image Titan's surface. During Cassini's cruise phase, telescopic observations hinted that Titan's surface may be observable by VIMS at 1.6 and 2.0 μm [Meier et al. 2000], providing impetus for VIMS prime time observations during the first Titan flyby (T00A). Since it had been added to solve the issue of the transmission between the Huygens probe and the Cassini spacecraft, this flyby had not yet been allocated to any instrument. During that first flyby, the VIMS instrument demonstrated its potential to observe Titan's surface in seven atmospheric windows [Sotin et al. 2005]. The 5-μm band in particular was shown to have very little

scattering from atmospheric aerosols, while the 2-μm band proved to be the best compromise between solar flux, atmospheric scattering, and detector sensitivity. That discovery propelled the VIMS instrument into a key mapping role for Titan, and provided information very complementary to radar images. Most of the VIMS images of Titan's surface were acquired during the extended mission because the flybys during the Prime Mission were already allocated.

As history has shown, VIMS made some fundamental observations of Titan's atmosphere with implications for both its composition and dynamics. A solar port, aligned with the UVIS solar port, was set up to allow for solar occultation as riding along with UVIS, and a dozen solar occultation observations of Titan were performed at different latitudes and seasons, providing key information on the aerosol content of the atmosphere. Finally, specular reflections from Titan's seas were observed at 5 μm and have provided key information on the presence and dynamics of Titan's seas. The following three sections provide the main scientific results obtained by the VIMS instrument.

TITAN'S SOLID SURFACE

The VIMS instrument can see Titan's surface through seven atmospheric windows in the near infrared between 0.9 and 5 μm [Sotin et al. 2005; Rodriguez et al. 2006]. Because atmospheric scattering decreases with wavelength, and observations of specular reflection (Figure VIMS-10) show that there is very little scattering at 5 μm, it was determined that optimum imaging occurred at 2 μm. RGB, synthetic color images can be constructed by choosing three out of the seven wavelengths from a VIMS image cube, enhancing the visibility of geological features, which can be

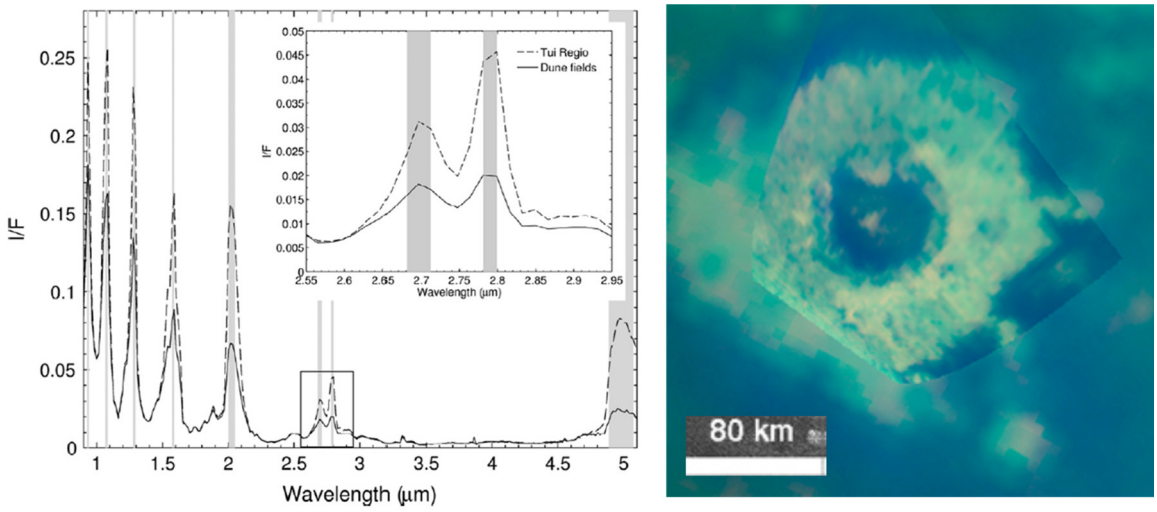

Figure VIMS-10. Titan's surface. *Left*: Typical spectrum of Titan's surface with the dark spectrum taken over dune fields and the bright spectrum taken on the bright feature known as Tui regio. *Right*: Sinlap crater is considered as the least altered impact crater on Titan [Neish et al. 2015]. Resolution ranges from 1 to 4 km. The RGB image was constructed with R=4.8–5.2 μm, G=2.00 μm, B=1.28 μm.

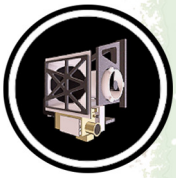

observed with pixel size as small as 500 m in a few spots. The resolution depends on the distance between the Cassini spacecraft and Titan's surface and the global maps are mosaics of images with very different pixel scales and viewing geometry. The VIMS images enable detailed comparisons to be carried out with Titan Radar Mapper (RADAR) images, for example, Soderblom et al. [2007a] demonstrated the very strong correlation of the dark brown VIMS units with the radar dune fields. They suggested that the bright areas surrounded by these dune fields are deposits of bright, fine, precipitating tholin-aerosol-dust, and hypothesized that chemical/mechanical processes may be converting the bright, fine-grained aerosol deposits into the dark, saltating, hydrocarbon and/or nitrile grains. Alternatively the dark dune materials may be derived from a different type of air aerosol photochemical product than Titan's bright materials.

VIMS mapped a few impact craters [Le Mouélic et al. 2008; Buratti et al. 2012; Neish et al. 2015]. These impact craters exhibit various degrees of degradation, with Sinlap being the least degraded. Buratti et al. [2012] studied the crater Paxsi, located in the dune field known as Senkyo. This crater's dark brown interior was attributed to infilling by dune material. The number density of impact craters on Titan is small suggesting a young surface.

At the end of the Cassini mission, it is not clear that Titan's surface displays cryovolcanic features. 5-µm-bright lobate features at Tui regio [Barnes et al. 2006] suggest an endogenic origin, but, other authors have attributed this 5-µm-bright feature to evaporitic material [MacKenzie et al. 2014], which suggests that Tui regio may be located in a depression near Titan's equator. Similarly, Hotei Regio, also located in the Xanadu area to the East of Hotei, exhibits a 5 µm bright feature also interpreted as evaporitic material. The interpretation that the 5-µm-bright feature is evaporitic material comes from the observation of such features at the North poles, next to the large hydrocarbons seas.

The composition of Titan's surface has stimulating much debate since the observation of the surface at seven infrared wavelengths, and one, important unsettled question is the presence or absence of convincing water ice deposits on Titan's surface. Water ice has a clear spectral signature in the 2.7-µm window, characterized by two peaks at 2.7 and 2.8 µm. Its spectrum shows a strong decrease in albedo between 2.7 and 2.8, suggesting that the 2.8-µm peak should be much less pronounced than the 2.7-µm peak. This is not what is observed, suggesting that Titan's surface is covered by organic material which masks the spectral signature of water ice. The composition of Titan's surface has been studied by Clark et al. [2010], using absorption bands in the 5-µm atmospheric window. They discovered a benzene absorption (5.05 µm), alkane absorptions (near 4.97 µm), and a component yet to be identified which has an absorption at 5.01 µm.

TITAN'S SEAS

Titan is the only place in the solar system, other than Earth, that has seas of liquids at its surface. That many very dark areas on Titan are bodies of liquid was confirmed by the solar glint (secular reflection) at 5 µm (Figure VIMS-11), first observed by Stephan et al. [2010d] over Jingpo Lacus.

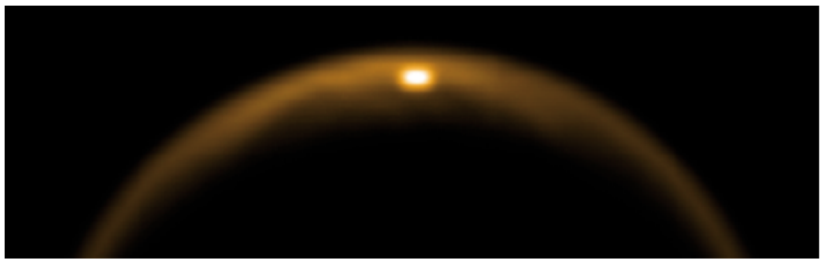

Figure VIMS-11. The 5 µm solar glint during the T58 flyby.

This glint demonstrated that the lake's surface is smooth and free of scatterers, at the observation wavelength of 5 µm. Just before Cassini arrived at Saturn, Lorenz and Lunine [2005] wrote:

> *"The glint may be observable at longer wavelengths by VIMS (although this will not be trivial, since the specular point moves across the surface as the sub-spacecraft point moves, and VIMS is a mapping spectrometer, not a framing camera, so its image is not built instantaneously)".*

Despite these difficulties, several observations of 5-µm specular reflections have been made. Measuring the intensity of specular reflections was employed by Barnes et al. [2011b], to demonstrate that the surfaces of many of Titan's lake and seas are very smooth, with waves which have slopes 2 orders of magnitude lower than those on Earthly lakes and seas.

Titan's lakes and seas are very dark in Titan's atmospheric windows, and their distribution correlates very well with the radar observations [Sotin et al. 2012]. Besides the specular points that provide information on the waves, VIMS observations also provide information on transport processes operating to move liquids between Kraken Mare and Ligeia Mare through a channel known as Trevize fretum [Sotin et al. 2015].

VIMS also determined that ethane is one of the components present in a large lake, Ontario lacus, located in the southern hemisphere [Brown et al. 2008]. The VIMS instrument cannot determine whether methane is present because of its abundance in the atmosphere. However, in the solid surface, liquid ethane/methane was detected by VIMS in some non-polar locations [Clark et al. 2010].

TITAN'S ATMOSPHERE

VIMS provided data important to understanding on Titan's climate by observing the appearance and evolution of clouds [Rodriguez et al. 2009, 2011], as well as determining their composition using solar occultation observations [Bellucci et al. 2009; Maltagliati et al. 2015]. Two types of clouds were detected during the period 2005–2009 during northern winter (Figure VIMS-12). Initially the north pole was covered by a polar hood, while later clouds with a short lifetime were detected at southern mid-latitudes.

The composition of Titan's atmosphere was derived from solar occultation observations by Bellucci et al. [2009], who determined the mixing ration of methane above an altitude of 200 km to

be between 1.4 and 1.7%, while the amount of CO was 33 ±10 ppm. Maltagliati et al. [2015] used solar occultation observations to refine measurement of the mixing ratio of CH_4, finding it be 1.28% ±0.08% and the CO abundance equal to 46 ±1 6 ppm, comparable with the previous measurements. Their work showed the presence of ethane, explaining many of the remaining, and previously unattributed absorption bands.

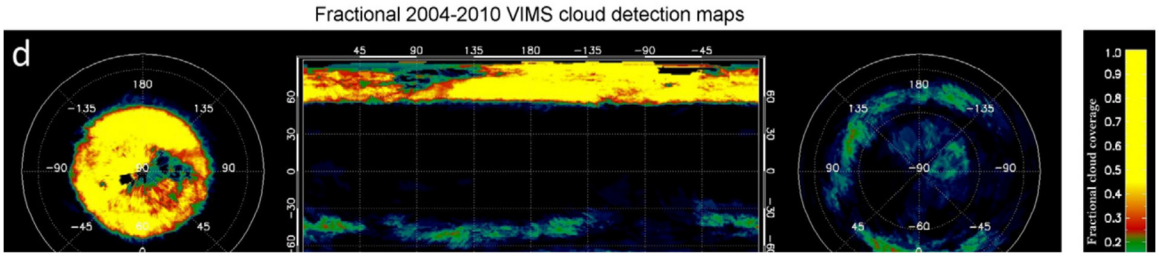

Figure VIMS-12. Fraction of cloud coverage on Titan during the period 2004–2010.

Conclusion

The VIMS instrument exceeded all expectations with regard to its studies of Titan, with major advances in understanding of Titan's surface and atmosphere. It made fundamental discoveries regarding the composition of Titan's surface and atmosphere, the dynamics of Titan's atmosphere, and the morphology of its surface. VIMS paved the way for the development of an infrared camera that may eventually enable us to obtain global maps of Titan's surface at 25-meter resolution (Huygens type resolution), providing important information on unanswered questions about Titan's geology, such as why is the surface so young; why are there geomorphological features that trace outgassing; is there fluvial erosion; what are the ages of any methane outbursts; are there tectonic features; is there aeolian transport of organics?

Open questions

Are there water ice outcrops on the surface?

What is the composition of the river beds?

Where are located the ethane reservoirs?

Are there morphological features related to the release of methane in the atmosphere?

What is the nature of the organic material covering Titan's surface?

What is the nature of the very bright deposits?

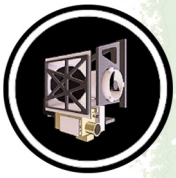

ACRONYMS

Note: For a complete list of Acronyms, refer to Cassini Acronyms – Attachment A.

AO	Announcement of Opportunity
CAPS	Cassini Plasma Spectrometer
CIRS	Composite Infrared Spectrometer
D/H	Deuterium to Hydrogen
FUV	far ultraviolet channel
HST	Hubble Space Telescope
IFOV	instantaneous field of view
IR	infrared
ISS	Imaging Science Subsystem
JWST	James Webb Space Telescope
mrad	microradians
NAC	narrow angle camera
NIMS	Near Infrared Mapping Spectrometer Subsystem
RADAR	Titan Radar Mapper
RPWS	Radio and Plasma Wave Spectrometer
RSS	Radio Science Subsystem
S-G	self-gravity
SNR	signal to noise ratio
SOI	Saturn Orbit Insertion
UV	ultraviolet
UVIS	Ultraviolet Imaging Spectrograph
V	visible
VIMS	Visual and Infrared Mapping Spectrometer
VIS-IR	visible-infrared
WAC	wide angle camera

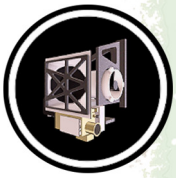

THE VIMS BIBLIOGRAPHY SUMMARY

The Cassini VIMS and its team contributed to 373 peer-reviewed articles, book chapters, and reviewed conference proceedings. The publications span 29 years (and counting) from 1990 to 2018.

This bibliography was compiled from the online databases Scopus, Science Direct, and the SAO/NASA Astrophysics Data System. Generally, the databases were searched for “Cassini VIMS” as a keyword, and the returned entries were evaluated to determine if VIMS data were the main driver of a publication or made significant contributions to its scientific conclusions. Publications were also considered for inclusion at the recommendation of VIMS Science Team members based on the above criteria. These entries were assembled in an EndNote Database (available on request), and further organized and analyzed (also available on request).

The contributions appeared in 54 different publications in at least 5 different countries. Icarus published 198 of the references (53%), and 48 (15%) appeared in Planetary & Space Science. Geophysical Research Letters had 17 articles, all other sources had 10 or less. Twenty journals had only a single paper. Also represented were the proceedings of three conferences, eight books, and four graduate dissertations.

The references were categorized based on their target, discipline of study, and technique. Almost the same number of publications was contributed on the study of Saturn and on the study of Titan, 164 & 167 respectively. Also represented were Venus (2), Earth & its moon (5), Mars (1), Jupiter (23), stars (7), and the hardware and software systems used by the instrument (10).

There are 3,272 author listings in the bibliography, representing over 720 individuals. Three hundred and ninty-six of them appear only once, while P.D. Nicholson is the most prolific with 129 entries (Appearing in 35% of the references, representing 4% of the total author listings). The largest number of authors on a single paper is 34. The median number of authors for a reference is 7, the mode is 3.

Almost 190 different people lead the publications, with M. M. Hedman appearing as first author most often (15 times).

Citation numbers were collected for all but two of the entries. The VIMS h-index as calculated from the 371 references with available data is 47. The highest number of reported citations is 248, and the average is 21.

Further details of analysis are available on request. Please direct any requests, additions, or corrections to ejoseph@lpl.arizona.edu.

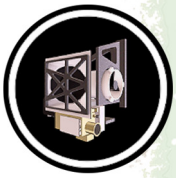

REFERENCES

Disclaimer: The partial list of references below correspond with in-text references indicated in this report. For all other Cassini references, refer to Attachment B – References & Bibliographies; Attachment C – Cassini Science Bibliographies; the sections entitled References contributed by individual Cassini instrument and discipline teams located in Volume 1 Sections 3.1 and 3.2 Science Results; and other resources outside of the Cassini Final Mission Report.

Ádámkovics, M., J. W. Barnes, M. Hartung, I. de Pater, (2010), Observations of a stationary mid-latitude cloud system on Titan, Icarus, 208, 2, 868–877, doi: 10.1016/j.icarus.2010.03.006.

Ádámkovics, M., I. de Pater, M. Hartung, J. W. Barnes, (2009), Evidence for condensed-phase methane enhancement over Xanadu on Titan, Planetary and Space Science, 57, 13, 1586–1595, doi: 10.1016/j.pss.2009.07.001.

Adriani, A., B. M. Dinelli, M. López-Puertas, M. García-Comas, M. L. Moriconi, E. D'Aversa, B. Funke, A. Coradini, (2011), Distribution of HCN in Titan's upper atmosphere from Cassini/VIMS observations at 3μm, Icarus, 214, 2, 584–595, doi: 10.1016/j.icarus.2011.04.016.

Adriani, A., A. Gardini, E. D'Aversa, A. Coradini, M. L. Moriconi, G. L. Liberti, R. Orosei, G. Filacchione, (2005), Titan's ground reflectance retrieval from Cassini-VIMS data taken during the July 2nd, 2004 fly-by at 2 am ut, Earth, Moon and Planets, 96, 3–4, 109–117, doi: 10.1007/s11038-005-9057-3.

Anderson, C. M., R. E. Samuelson, D. Nna-Mvondo, (2018), Organic Ices in Titan's Stratosphere, Space Science Reviews, 214, 8, doi:10.1007/s11214-018-0559-5.

Anderson, C. M., R. E. Samuelson, R. K. Achterberg, J. W. Barnes, F. M. Flasar, (2014), Subsidence-induced methane clouds in Titan's winter polar stratosphere and upper troposphere, Icarus, 243, 129–138, doi: 10.1016/j.icarus.2014.09.007.

Atreya, S. K., E. Y. Adams, H. B. Niemann, J. E. Demick-Montelara, T. C. Owen, M. Fulchignoni, F. Ferri, E. H. Wilson, (2006), Titan's methane cycle, Planetary and Space Science, 54, 12, 1177–1187, doi: 10.1016/j.pss.2006.05.028.

Badman, S. V., G. Provan, E. J. Bunce, D. G. Mitchell, H. Melin, S. W. H. Cowley, A. Radioti, et al., (2016), Saturn's auroral morphology and field-aligned currents during a solar wind compression, Icarus, 263, 83–93, doi: 10.1016/j.icarus.2014.11.014.

Badman, S. V., N. Achilleos, C. S. Arridge, K. H. Baines, R. H. Brown, E. J. Bunce, A. J. Coates, et al., (2012a), Cassini observations of ion and electron beams at Saturn and their relationship to infrared auroral arcs, Journal of Geophysical Research: Space Physics, 117, no. A1.

Badman, S. V., D. J. Andrews, S. W. H. Cowley, L. Lamy, G. Provan, C. Tao, S. Kasahara, et al., (2012b), Rotational modulation and local time dependence of Saturn's infrared H_3^+ auroral intensity, Journal of Geophysical Research: Space Physics, 117, 9, doi: 10.1029/2012JA017990.

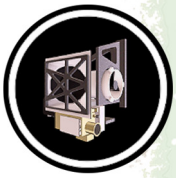

Badman, S. V., N. Achilleos, K. H. Baines, R. H. Brown, E. J. Bunce, M. K. Dougherty, H. Melin, J. D. Nichols, T. Stallard, (2011a), Location of Saturn's northern infrared aurora determined from Cassini VIMS images, Geophysical Research Letters, 38, 3, doi: 10.1029/2010GL046193.

Badman, S. V., C. Tao, A. Grocott, S. Kasahara, H. Melin, R. H. Brown, K. H. Baines, M. Fujimoto, T. Stallard, (2011b), Cassini VIMS observations of latitudinal and hemispheric variations in Saturn's infrared auroral intensity, Icarus, 216, 2, 367–375, doi: 10.1016/j.icarus.2011.09.031.

Baines, K. H., L. A. Sromovsky, R. W. Carlson, T. W. Momary, P. M. Fry, (2019), The visual spectrum of Jupiter’s Great Red Spot accurately modeled with aerosols produced by photolyzed ammonia reacting with acetylene, Icarus, 330, 217–229, doi: 10.1016/j.icarus.2019.04.008.

Baines, K. H., L. A. Sromovsky, R. W. Carlson, T. W. Momary, P. M. Fry, (2019) The visual spectrum of Jupiter's Great Red Spot accurately modeled with aerosols produced by photolyzed ammonia reacting with acetylene, Icarus, 330, 217–229.

Baines, K. H., L. A. Sromovsky, P. M. Fry, T. W. Momary, R. H. Brown, B. J. Buratti, R. N. Clark, P. D. Nicholson, C. Sotin, (2018), The eye of Saturn's north polar vortex: Unexpected cloud structures observed at high spatial resolution by Cassini/VIMS, Geophysical Research Letters, 45, 12, 5867–5875, doi:10.1029/2018GL078168.

Baines, K. H., P. A. Yanamandra-Fisher, T. W. Momary, G. S. Orton, G. G. Villar Iii, L. N. Fletcher, H. Campins, A. S. Rivkin, M. Shara, (2013), The temporal evolution of the July 2009 Jupiter impact cloud, Planetary and Space Science, 77, 25–39, doi: 10.1016/j.pss.2012.05.007.

Baines, K. H., M. L. Delitsky, T. W. Momary, R. H. Brown, B. J. Buratti, R. N. Clark, P. D. Nicholson, (2009a), Storm clouds on Saturn: Lightning-induced chemistry and associated materials consistent with Cassini/VIMS spectra, Planetary and Space Science, 57, 1650–1658, doi: 10:1016/j.pss.2009.06.025.

Baines, K. H., T. W. Momary, L. N. Fletcher, A. P. Showman, M. Roos-Serote, R. H. Brown, B. J. Buratti, R. N. Clark, P. D. Nicholson, (2009b), Saturn’s north polar cyclone and hexagon at depth revealed by Cassini/VIMS. Planetary and Space Science, 57, 1671–1681, doi: 10.1016/j.pss.2009.06.026.

Baines, K. H., S. Atreya, R. W. Carlson, D. Crisp, P. Drossart, V. Formisano, S. S. Limaye, W. J. Markiewicz, G. Piccioni, (2006a), To the depths of Venus: Exploring the deep atmosphere and surface of our sister world with Venus Express, Planetary and Space Science, 54, 13–14, 1263–1278, doi: 10.1016/j.pss.2006.04.034.

Baines, K. H., P. Drossart, M. A. Lopez-Valverde, S. K. Atreya, C. Sotin, T. W. Momary, R. H. Brown, B. J. Buratti, R. N. Clark, P. D. Nicholson, (2006b), On the discovery of CO nighttime emissions on Titan by Cassini/VIMS: Derived stratospheric abundances and geological

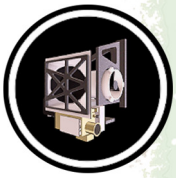

implications, Planetary and Space Science, 54, 15, 1552–1562, doi: 10.1016/j.pss.2006.06.020.

Baines, K. H., P. Drossart, T. W. Momary, V. Formisano, C. Griffith, G. Bellucci, J. P. Bibring, et al., (2006c), The atmospheres of Saturn and Titan in the near-infrared: First results of Cassini/Vims, Earth, Moon and Planets, 96, 3–4, 119–147, doi: 10.1007/s11038-005-9058-2.

Baines, K. H., P. Drossart, T. W. Momary, V. Formisano, C. Griffith, G. Bellucci, J. P. Bibring, et al., (2005), The atmospheres of Saturn and Titan in the near-infrared: First results of Cassini/VIMS, Earth, Moon, and Planets, 96, no. 3–4, 119–147.

Baines, K. H., G. Bellucci, J.-P. Bibring, R. H. Brown, B. J. Buratti, E. Bussoletti, F. Capaccioni, et al., (2000), Detection of Sub-Micron Radiation from the Surface of Venus by Cassini/VIMS, Icarus, 148, 1, 307–311, doi: 10.1006/icar.2000.6519.

Banfield, D., B. J. Conrath, P. J. Gierasch, P. D. Nicholson, K. Matthews, (1998), Near-IR Spectrophotometry of Jovian Aerosols - Meridional and Vertical Distributions, Icarus, 134, 1, 11–23, doi: 10.1006/icar.1998.5942.

Barbosa Aguiar, A. C., P. L. Read, R. D. Wordsworth, T. Salter, Y. Hiro Yamazaki, (2010), A laboratory model of Saturn’s north polar hexagon, Icarus, 206, 2, 755–763, doi: 10.1016/j.icarus.2009.10.022.

Barnes, J. W., S. M. Mackenzie, E. F. Young, L. E. Trouille, S. Rodriguez, T. Cornet, B. K. Jackson, M. Ádámkovics, C. Sotin, J. M. Soderblom, (2018), Spherical radiative transfer in C++ (SRTC++): A parallel Monte Carlo radiative transfer model for Titan, The Astronomical Journal, 155, 6, doi:10.3847/1538-3881/aac2db.

Barnes, J. W., C. Sotin, J. M. Soderblom, R. H. Brown, A. G. Hayes, (2014), Cassini/VIMS observes rough surfaces on Titan's Punga Mare in specular reflection, Planetary Science, 3, 1, doi: 10.1186/s13535-014-0003-4.

Barnes, J. W., B. J. Buratti, E. P. Turtle, J. Bow, P. A. Dalba, J. Perry, R. H. Brown, et al., (2013a), Precipitation-induced surface brightenings seen on Titan by Cassini VIMS and ISS, Planetary Science, 2, 1, doi: 10.1186/2191-2521-2-1.

Barnes, J. W., R. N. Clark, C. Sotin, M. Ádámkovics, T. Appéré, S. Rodriguez, J. M. Soderblom, et al., (2013b), A transmission spectrum of Titan's north polar atmosphere from a specular reflection of the Sun, The Astrophysical Journal, 777, 2, 161, doi: 10.1088/0004-637X/777/2/161.

Barnes, J. W., J. Bow, J. Schwartz, R. H. Brown, J. M. Soderblom, A. G. Hayes, G. Vixie, et al., (2011a), Organic sedimentary deposits in Titan's dry lakebeds: Probable evaporite, Icarus, 216, 1, 136–140, doi: 10.1016/j.icarus.2011.08.022.

Barnes, J. W., J. M. Soderblom, R. H. Brown, L. A. Soderblom, K. Stephan, R. Jaumann, S. Le Mouélic, et al., (2011b), Wave constraints for Titan's Jingpo Lacus and Kraken Mare from VIMS specular reflection lightcurves, Icarus, 211, 1, 722–731, doi: 10.1016/j.icarus.2010.09.022.

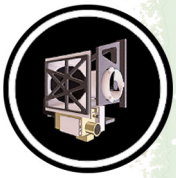

Barnes, J. W., R. H. Brown, J. M. Soderblom, L. A. Soderblom, R. Jaumann, B. Jackson, S. Le Mouélic, et al., (2009a), Shoreline features of Titan's Ontario Lacus from Cassini/VIMS observations, Icarus, 201, 1, 217–225, doi: 10.1016/j.icarus.2008.12.028.

Barnes, J. W., J. M. Soderblom, R. H. Brown, B. J. Buratti, C. Sotin, K. H. Baines, R. N. Clark, et al., (2009b), VIMS spectral mapping observations of Titan during the Cassini prime mission, Planetary and Space Science, 57, 14–15, 1950–1962, doi: 10.1016/j.pss.2009.04.013.

Barnes, J. W., R. H. Brown, L. Soderblom, C. Sotin, S. Le Mouèlic, S. Rodriguez, R. Jaumann, et al., (2008), Spectroscopy, morphometry, and photoclinometry of Titan's dunefields from Cassini/VIMS, Icarus, 195, 1, 400–414, doi: 10.1016/j.icarus.2007.12.006.

Barnes, J. W., R. H. Brown, L. Soderblom, B. J. Buratti, C. Sotin, S. Rodriguez, S. Le Mouèlic, K. H. Baines, R. Clark, P. Nicholson, (2007a), Global-scale surface spectral variations on Titan seen from Cassini/VIMS, Icarus, 186, 1, 242–258, doi: 10.1016/j.icarus.2006.08.021.

Barnes, J. W., J. Radebaugh, R. H. Brown, S. Wall, L. Soderblom, J. Lunine, D. Burr, et al., (2007b), Near-infrared spectral mapping of Titan's mountains and channels, Journal of Geophysical Research E: Planets, 112, 11, doi: 10.1029/2007JE002932.

Barnes, J. W., R. H. Brown, J. Radebaugh, B. J. Buratti, C. Sotin, S. Le Mouelic, S. Rodriguez, et al, (2006), Studies of Titan's 5-Micron-Bright Regions Using Combined VIMS and ISS Observations, American Geophysical Union (AGU) Fall Meeting, abstract.

Barstow, J. K., P. G. J. Irwin, L. N. Fletcher, R. S. Giles, C. Merlet, (2016), Probing Saturn's tropospheric cloud with Cassini/VIMS, Icarus, 271, 400–417, doi: 10.1016/j.icarus.2016.01.013.

Barth, E. L., (2017), Modeling survey of ices in Titan's stratosphere, Planetary and Space Science, 137, 20–31, doi: 10.1016/j.pss.2017.01.003.

Barth, E. L. and S. C. R. Rafkin, (2010), Convective cloud heights as a diagnostic for methane environment on Titan, Icarus, 206, 2, 467–484, doi: 10.1016/j.icarus.2009.01.032.

Bauerecker, S. and E. Dartois, (2009), Ethane aerosol phase evolution in Titan's atmosphere, Icarus, 199, 2, 564–567, doi: 10.1016/j.icarus.2008.09.014.

Bellini, B., G. Bellucci, V. Formisano, (1998), Atmospheric studies with spectro-imaging: Prospects for the VIMS experiment on Cassini, Planetary and Space Science, 46, 9–10, 1305–1314, doi: 10.1016/S0032-0633(98)00004-X.

Bellucci, A. S., B., Drossart, P., Rannou, P., Nicholson, P. D., Hedman, M., Baines, K. H., Burrati, B., (2009), Titan solar occultation observed by Cassini/VIMS: Gas absorption and constraints on aerosol composition, Icarus, 201(1), 198–216, doi: 10.1016/j.icarus.2008.12.024.

Bellucci, A., (2008), Analyse d'occultations solaires et stellaires par Titan observées par l'instrument Cassini/VIMS, Université Paris VI - Pierre et Marie Curie.

Bellucci, G., E. D'Aversa, V. Formisano, D. Cruikshank, R. M. Nelson, R. N. Clark, K. H. Baines, et al., (2004a), Cassini/VIMS observation of an Io post-eclipse brightening event, Icarus, 172, 1, 141–148, doi: 10.1016/j.icarus.2004.05.012.

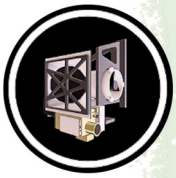

Bellucci, G. F., V., D'Aversa, E., Brown, R. H., Baines, K. H., Bibring, J. P., Buratti, B. J., Capaccioni, F., Cerroni, P., Clark, R. N., Coradini, A., Cruikshank, D. P., Drossart, P., Jaumann, R., Langevin, Y., Matson, D. L., McCord, T. B., Mennella, V., Nelson, R. M., Nicholson, P. D., Sicardy, B., Sotin, C., Chamberlain, M. C., Hansen, G., Hibbits, K., Showalter, M., Filacchione, G., (2004b), Principal components analysis of Jupiter VIMS spectra, Advances in Space Research, 34, 8, 1640–1646, doi: 10.1016/j.asr.2003.05.062.

Bellucci, G., R. H. Brown, V. Formisano, K. H. Baines, J.-P. Bibring, B. J. Buratti, F. Capaccioni, et al., (2002), Cassini/VIMS observations of the moon, Advances in Space Research, 30, 8, 1889–1894, doi: 10.1016/S0273-1177(02)00484-2.

Bellucci, G. and V. Formisano, (1997), Regional mapping of planetary surfaces with imaging spectroscopy, Planetary and Space Science, 45, 11, 1371–1381, doi: 10.1016/S0032-0633(97)00074-3.

Bernard, J. M., E. Quirico, O. Brissaud, G. Montagnac, B. Reynard, P. McMillan, P. Coll, M. J. Nguyen, F. Raulin, B. Schmitt, (2006), Reflectance spectra and chemical structure of Titan's tholins: Application to the analysis of Cassini–Huygens observations, Icarus, 185, 1, 301–307, doi: 10.1016/j.icarus.2006.06.004.

Bézard, B., S. Vinatier, R. K. Achterberg, (2018), Seasonal radiative modeling of Titan's stratospheric temperatures at low latitudes, Icarus, 302, 437–450, doi: 10.1016/j.icarus.2017.11.034.

Birch, S. P. D., A. G. Hayes, P. Corlies, E. R. Stofan, J. D. Hofgartner, R. M. C. Lopes, R. D. Lorenz, et al., (2017), Morphological evidence that Titan’s southern hemisphere basins are paleoseas, Icarus, doi: 10.1016/j.icarus.2017.12.016.

Blackburn, D. G., (2011), An analysis of the stability and transport of carbon dioxide on Mars and Iapetus: Increasing accuracy via experiments and photometry, University of Arkansas.

Blackburn, D. G., B. J. Buratti, R. Ulrich, (2011), A bolometric Bond albedo map of Iapetus: Observations from Cassini VIMS and ISS and Voyager ISS, Icarus, 212, 1, 329–338, doi: 10.1016/j.icarus.2010.12.022.

Blackburn, D. G., B. J. Buratti, R. Ulrich, J. A. Mosher, (2010), Solar phase curves and phase integrals for the leading and trailing hemispheres of Iapetus from the Cassini Visual Infrared Mapping Spectrometer, Icarus, 209, 2, 738–744, doi: 10.1016/j.icarus.2010.04.011.

Bonnefoy, L. E., A. G. Hayes, P. O. Hayne, M. J. Malaska, A. Le Gall, A. Solomonidou, A. Lucas, (2016), Compositional and spatial variations in Titan dune and interdune regions from Cassini VIMS and RADAR, Icarus, 270, 222–237, doi: 10.1016/j.icarus.2015.09.014.

Bourke, M. C., N. Lancaster, L. K. Fenton, E. J. R. Parteli, J. R. Zimbelman, J. Radebaugh, (2010), Extraterrestrial dunes: An introduction to the special issue on planetary dune systems, Geomorphology, 121, 1–2, 1–14, doi: 10.1016/j.geomorph.2010.04.007.

Brassé, C., O. Muñoz, P. Coll, F. Raulin, (2015), Optical constants of Titan aerosols and their tholins analogs: Experimental results and modeling/observational data, Planetary and Space Science, 109–110, 159–174, doi: 10.1016/j.pss.2015.02.012.

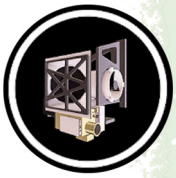

Brossier, J. F., S. Rodriguez, T. Cornet, Antoine Lucas, J. Radebaugh, L. Maltagliati, S. Le Mouélic, et al., (2018), Geological evolution of Titan's equatorial regions: Possible nature and origin of the dune material, Journal of Geophysical Research: Planets, 123, 5, 1089–1112, doi: 10.1029/2017JE00539.

Brown, A. J., (2014), Spectral bluing induced by small particles under the Mie and Rayleigh regimes, Icarus, 239, 85–95, doi: 10.1016/j.icarus.2014.05.042.

Brown, M. E., J. E. Roberts, E. L. Schaller, (2010), Clouds on Titan during the Cassini prime mission: A complete analysis of the VIMS data, Icarus, 205, 2, 571–580, doi: 10.1016/j.icarus.2009.08.024.

Brown, M. E., A. L. Smith, C. Chen, M. Ádámkovics, (2009), Discovery of fog at the south pole of Titan, The Astrophysical Journal Letters, 706, no. 1, L110, doi: 10.1088/0004-637X/706/1/L110.

Brown, R. H., J. W. Barnes, H. J. Melosh, (2011), On Titan’s Xanadu region, Icarus, 214, 2, 556–560, doi: 10.1016/j.icarus.2011.03.018.

Brown, R. H., L. A. Soderblom, J. M. Soderblom, R. N. Clark, R. Jaumann, J. W. Barnes, C. Sotin, B. Buratti, K. H. Baines, P. D. Nicholson, (2008), The identification of liquid ethane in Titan's Ontario Lacus, Nature, 454, 7204, 607–610, doi: 10.1038/nature07100.

Brown, R. H. B., K. H., Bellucci, G., Buratti, B. J., Capaccioni, F., Cerroni, P., Clark, R. N., Coradini, A., Cruikshank, D. P., Drossart, P., Formisano, V., Jaumann, R., Langevin, Y., Matson, D. L., McCord, T. B., Mennella, V., Nelson, R. M., Nicholson, P. D., Sicardy, B., Sotin, C., Baugh, N., Griffith, C. A., Hansen, G. B., Hibbitts, C. A., Momary, T. W., Showalter, M. R., (2006), Observations in the Saturn system during approach and orbital insertion, with Cassini's visual and infrared mapping spectrometer (VIMS), Astronomy and Astrophysics, 446, 2, 707–716, doi: 10.1051/0004-6361:20053054.

Brown, R. H., K. H. Baines, G. Bellucci, J.-P. Bibring, B. J. Buratti, F. Capaccioni, P. Cerroni, et al., (2004), The Cassini visual and infrared mapping spectrometer (VIMS) investigation, Space Science Reviews, 115, 1–4, 111–168, doi: 10.1007/s11214-004-1453-x.

Brown, R. H. B., K. H., Bellucci, G., Bibring, J. P., Buratti, B. J., Capaccioni, F., Cerroni, P., Clark, R. N., Coradini, A., Cruikshank, D. P., Drossart, P., Formisano, V., Jaumann, R., Langevin, Y., Matson, D. L., McCord, T. B., Mennella, V., Nelson, R. M., Nicholson, P. D., Sicardy, B., Sotin, C., Amici, S., Chamberlain, M. A., Filacchione, G., Hansen, G., Hibbitts, K., Showalter, M., (2003), Observations with the Visual and Infrared Mapping Spectrometer (VIMS) during Cassini's flyby of Jupiter, Icarus, 164, 2, 461–470, doi: 10.1016/S0019-1035(03)00134-9.

Buratti, B. J., R. N. Clark, F. Crary, C. J. Hansen, A. R. Hendrix, C. J. A.Howett, J. Lunine, C. Paranicas, (2018a), Cold cases: What we don't know about Saturn's Moons, Planetary and Space Science, vol. 155, pp. 41–49, doi.org/10.1016/j.pss.2017.11.017.

Buratti, B. J., C. J. Hansen, A. R. Hendrix, L. W. Esposito, J. A. Mosher, R. H. Brown, R. N. Clark, K. H. Baines, P. D. Nicholson, (2018b), The search for activity on Dione and Tethys with

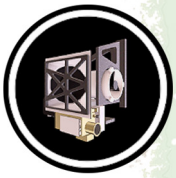

Cassini VIMS and UVIS, Geophysical Research Letters, 45, 12, 5860–5866, doi: 10.1029/2018GL078165.

Buratti, B. J., R. H. Brown, R. N. Clark, D. P. Cruikshank, G. Filacchione, (2017), Spectral analyses of Saturn's moons using Cassini-VIMS, In Remote Sensing, (eds.) J. Bishop, J. Bell, Cambridge, In press.

Buratti, B. J., C. Sotin, K. Lawrence, R. H. Brown, S. Le Mouélic, J. M. Soderblom, J. Barnes, R. N. Clark, K. H. Baines, P. D. Nicholson, (2012), A newly discovered impact crater in Titan's Senkyo: Cassini VIMS observations and comparison with other impact features, Planetary and Space Science, 60, 1, 18–25, doi: 10.1016/j.pss.2011.05.004.

Buratti, B. J., S. P. Faulk, J. Mosher, K. H. Baines, R. H. Brown, R. N. Clark, P. D. Nicholson, (2011), Search for and limits on plume activity on Mimas, Tethys, and Dione with the Cassini Visual Infrared Mapping Spectrometer (VIMS), Icarus, 214, 2, 534–540, doi: 10.1016/j.icarus.2011.04.030.

Buratti, B. J., J. M. Bauer, M. D. Hicks, J. A. Mosher, G. Filacchione, T. Momary, K. H. Baines, R. H. Brown, R. N. Clark, P. D. Nicholson, (2010), Cassini spectra and photometry 0.25-5.1 μm of the small inner satellites of Saturn, Icarus, 206, 2, 524–536, doi: 10.1016/j.icarus.2009.08.015.

Buratti, B. J., K. Soderlund, J. Bauer, J. A. Mosher, M. D. Hicks, D. P. Simonelli, R. Jaumann, et al., (2008), Infrared (0.83-5.1 μm) photometry of Phoebe from the Cassini Visual Infrared Mapping Spectrometer, Icarus, 193, 2, 309–322, doi: 10.1016/j.icarus.2007.09.014.

Buratti, B. J., C. Sotin, R. H. Brown, M. D. Hicks, R. N. Clark, J. A. Mosher, T. B. McCord, et al., (2006), Titan: Preliminary results on surface properties and photometry from VIMS observations of the early flybys, Planetary and Space Science, 54, 15, 1498–1509, doi: 10.1016/j.pss.2006.06.015.

Buratti, B. J., D. P. Cruikshank, R. H. Brown, R. N. Clark, J. M. Bauer, R. Jaumann, T. B. McCord, et al., (2005), Cassini Visual and Infrared Mapping Spectrometer observations of Iapetus: Detection of CO_2, The Astrophysical Journal Letters, 622, 2, L149–L152, doi: 10.1086/429800.

Buratti, B. J., J. K. Hillier, M. Wang, (1996), The lunar opposition surge: Observations by Clementine, Icarus, 124, no. 2, 490–499.

Buratti, B. J., J. A. Mosher, T. V. Johnson, (1990), Albedo and color maps of the Saturnian satellites, Icarus, 87, 2, 339–357, doi: 10.1016/0019-1035(90)90138-Y.

Campargue, A., L. Wang, D. Mondelain, S. Kassi, B. Bézard, E. Lellouch, A. Coustenis, C. De Bergh, M. Hirtzig, P. Drossart, (2012), An empirical line list for methane in the 1.26–1.71 μm region for planetary investigations (T = 80–300 K). Application to Titan, Icarus, 219, 1, 110–128, doi: 10.1016/j.icarus.2012.02.015.

Campbell, J., P. Sidiropoulos, J. P. Muller, (2016), IR spectral mapping of the martian south polar residual cap using CRISM, The International Archives of the Photogrammetry, Remote Sensing and Spatial Information Sciences, XXIII ISPRS Congress, 12–19 July 2016, Prague, Czech Republic, vol. XLI-B7, doi: 10.5194/isprsarchives-XLI-B7-71-2016

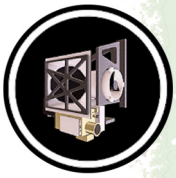

Capaccioni, F., A. Coradini, P. Cerroni, S. Amici, (1998), Imaging spectroscopy of Saturn and its satellites: VIMS-V onboard Cassini, Planetary and Space Science, 46, 9-10, 1263–1276, doi: 10.1016/S0032-0633(98)00037-3.

Carlson, R. E., (2010), Spatial and seasonal variations in Saturn's haze and vertical phosphine distribution at 3 microns from 2005 to 2010, New Mexico State University.

Carlson, R. W., K. H. Baines, M. S. Anderson, G. Filacchione, A. A. Simon, (2016), Chromophores from photolyzed ammonia reacting with acetylene: Application to Jupiter's Great Red Spot, Icarus, 274, 106–115, doi: 10.1016/j.icarus.2016.03.008.

Castillo-Rogez, J. C., D. L. Matson, C. Sotin, T. V. Johnson, J. I. Lunine, P. C. Thomas, (2007), Iapetus' geophysics: Rotation rate, shape, and equatorial ridge, Icarus, 190, 1, 179–202, doi: 10.1016/j.icarus.2007.02.018.

Chaban, G. M., M. Bernstein, D. P. Cruikshank, (2007), Carbon dioxide on planetary bodies: Theoretical and experimental studies of molecular complexes, Icarus, 187, 2, 592–599, doi: 10.1016/j.icarus.2006.10.010.

Chamberlain, M. A. and R. H. Brown, (2004), Near-infrared spectroscopy of Himalia, Icarus, 172, 163–169, doi: 10.1016/j.icarus.2003.12.016.

Chauhan, P., P. Kaur, N. Srivastava, R. K. Sinha, N. Jain, S. V. S. Murty, (2015), Hyperspectral remote sensing of planetary surfaces: An insight into composition of inner planets and small bodies in the solar system, Current Science, 108, 5, 915–924.

Choi, D. S., A. P. Showman, R. H. Brown, (2009), Cloud features and zonal wind measurements of saturn's atmosphere as observed by Cassini/VIMS, Journal of Geophysical Research: Planets, 114, 4, doi: 10.1029/2008JE003254.

Ciarniello, M., G. Filacchione, E. D'Aversa, F. Capaccioni, P. D. Nicholson, J. N. Cuzzi, R. N. Clark, et al., (2019), Cassini-VIMS observations of Saturn's main rings: II. A spectrophotometric study by means of Monte Carlo ray-tracing and Hapke's theory, Icarus, 317, 242–265.

Ciarniello, M., F. Capaccioni, G. Filacchione, R. N. Clark, D. P. Cruikshank, P. Cerroni, A. Coradini, et al., (2011), Hapke modeling of Rhea surface properties through Cassini-VIMS spectra, Icarus, 214, 2, 541–555, doi: 10.1016/j.icarus.2011.05.010.

Clark, R. N., R. H. Brown, D. P. Cruikshank, G. A. Swayze, (2019), Isotopic ratios of Saturn's rings and satellites: Implications for the origin of water and Phoebe, Icarus, 321, 791–802, doi: 10.1016/j.icarus.2018.11.029.

Clark, R. N., R. H. Brown, D. M. Lytle, M. Hedman, (2018), The VIMS Wavelength and Radiometric Calibration 19, Final Report, NASA Planetary Data System.

Clark, R. N., R. H. Brown, G. A. Swayze, D. P. Cruikshank, (2017a), Detecting Isotopic Signatures and Measuring Isotopic Ratios on Solid Icy Surfaces: Implications for Origin and Evolution, American Geophysical Union (AGU) Fall Meeting, abstracts.

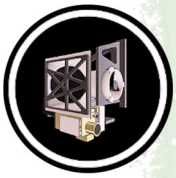

Clark, R. N., R. H. Brown, G. A. Swayze, D. P. Cruikshank, (2017b), Detection of Deuterium in Icy Surfaces and the D/H Ratio of Icy Objects, American Astronomical Society (AAS)/Division for Planetary Sciences Meeting, abstract 49, vol. 49.

Clark, R. N., R. H. Brown, D. P. Cruikshank, (2016a), CO_2 and ^{12}C: ^{13}C Isotopic Ratios on Phoebe and Iapetus, AGU Fall Meeting, abstract.

Clark, R. N., R. H. Brown, D. M. Lytle, (2016b), The VIMS wavelength and radiometric calibration, NASA Planetary Data System, The Planetary Atmospheres Node.

Clark, R. N., G. A. Swayze, R. Carlson, W. Grundy, K. Noll, (2014), Spectroscopy from Space, Reviews in Mineralogy and Geochemistry, pp. 399–446, doi: 10.2138/rmg.2014.78.10.

Clark, R. N., R. Carlson, W. Grundy, K. Noll, (2013), Observed Ices in the Solar System, In The Science of Solar System Ices, (eds.) M. Gudipati, J. Castillo-Rogez, Astrophysics and Space Science Library (ASSL), Springer, NY, vol. 356, Part 1, pp. 3–46, doi: 10.1007/978-1-4614-3076-6_1.

Clark, R. N., D. P. Cruikshank, R. Jaumann, R. H. Brown, K. Stephan, C. M. Dalle Ore, K. E. Livo, N. Pearson, J. M. Curchin, T. M. Hoefen, B. J. Buratti, G. Filacchione, K. H. Baines, P. D. Nicholson, (2012), The surface composition of Iapetus: Mapping results from Cassini VIMS, Icarus, 218, 831–860, doi: 10.1016/j.icarus.2012.01.008.

Clark, R. N., J. M. Curchin, J. W. Barnes, R. Jaumann, L. Soderblom, D. P. Cruikshank, R. H. Brown, S. Rodriguez, J. Lunine, K. Stephan, T. M. Hoefen, (2010), Detection and mapping of hydrocarbon deposits on Titan, Journal of Geophysical Research: Planets, 115, 10, doi: 10.1029/2009JE003369.

Clark, R. N., (2009), Detection of adsorbed water and hydroxyl on the Moon, Science, 326, 562–564, doi: 10.1126/science.1178105.

Clark, R. N., R. H. Brown, R. Jaumann, D. P. Cruikshank, B. Buratti, K. H. Baines, R. M. Nelson, P. D. Nicholson, J. M. Moore, J. Curchin, T. Hoefen, K. Stephan, (2008), Compositional mapping of Saturn's satellite Dione with Cassini VIMS and implications of dark material in the Saturn system, Icarus, 193, p 372–386, doi: 10.1016/j.icarus.2007.08.035.

Clark, R. N., R. H. Brown, R. Jaumann, D. P. Cruikshank, R. M. Nelson, B. J. Buratti, T. B. McCord, J. Lunine, K. H. Baines, G. Bellucci, J.-P. Bibring, F. Capaccioni, P. Cerroni, A. Coradini, V. Formisano, Y. Langevin, D. L. Matson, V. Mennella, P. D. Nicholson, B. Sicardy, C. Sotin, T. M. Hoefen, J. M. Curchin, G. Hansen, K. Hibbits, K.-D. Matz, (2005), Compositional maps of Saturn's moon Phoebe from imaging spectroscopy, Nature, doi: 10.1038/nature03558.

Cohen-Zada, A. L., D. G. Blumberg, S. Maman, (2016), Earth and planetary aeolian streaks: A review, Aeolian Research, 20, 108–125, doi: 10.1016/j.aeolia.2015.12.002.

Colwell, J. E., P. D. Nicholson, M. S. Tiscareno, C. D. Murray, R. G. French, E. A. Marouf, (2009), The structure of Saturn's rings, Chapter 13, In Saturn from Cassini-Huygens, (eds.) M. Dougherty, L. Esposito, S. Krimigis, Springer Dordrecht, pp. 375– 412, doi: 10.1007/978-1-4020-9217-6_13.

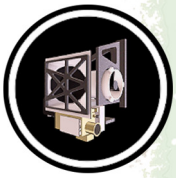

Combe, J. P., T. B. McCord, D. L. Matson, T. V. Johnson, A. G. Davies, F. Scipioni, F. Tosi, (2019), Nature, distribution and origin of CO_2 on Enceladus, Icarus, 317, 491–508, doi: 10.1016/j.icarus.2018.08.007.

Cooper, J. F., P. D. Cooper, E. C. Sittler, S. J. Sturner, A. M. Rymer, (2009), Old faithful model for radiolytic gas-driven cryovolcanism at Enceladus, Planetary and Space Science, 57, 13, 1607–1620, doi: 10.1016/j.pss.2009.08.002.

Coradini, A., F. Capaccioni, P. Cerroni, G. Filacchione, G. Magni, R. Orosei, F. Tosi, D. Turrini, (2009), Saturn satellites as seen by Cassini Mission, Earth, Moon and Planets, 105, no. 2–4, pp. 289–310, doi: 10.1007/s11038-009-9334-7.

Coradini, A., F. Tosi, A. I. Gavrishin, F. Capaccioni, P. Cerroni, G. Filacchione, A. Adriani, et al., (2008), Identification of spectral units on Phoebe, Icarus, 193, 1, 233–251, doi: 10.1016/j.icarus.2007.07.023.

Coradini, A., (2005), Planetary observations and landers, Chapter 8, In Payload and Mission Definition in Space Sciences, (eds.) V. M. Pillet, A. Aparicio, F. Sanchez, Cambridge University Press, pp. 323–394, doi: 10.1017/CBO9780511550591.009.

Coradini, A., G. Filacchione, F. Capaccioni, P. Cerroni, A. Adriani, Robert H. Brown, Y. Langevin, B. Gondet, (2004), Cassini/VIMS-V at Jupiter: Radiometric calibration test and data results, Planetary and Space Science, 52, 7, 661–670, doi: 10.1016/j.pss.2003.11.005.

Cordier, D., T. Cornet, J. W. Barnes, S. M. MacKenzie, T. Le Bahers, D. Nna-Mvondo, P. Rannou, A. G. Ferreira, (2016), Structure of Titan’s evaporites, Icarus, 270, 41–56, doi: 10.1016/j.icarus.2015.12.034.

Cordier, D., J. W. Barnes, A. G. Ferreira, (2013), On the chemical composition of Titan’s dry lakebed evaporites, Icarus, 226, 2, 1431–1437, doi: 10.1016/j.icarus.2013.07.026.

Cordier, D., O. Mousis, J. I. Lunine, S. Lebonnois, P. Rannou, P. Lavvas, L. Q. Lobo, A. G. M. Ferreira, (2012), Titan's lakes chemical composition: Sources of uncertainties and variability, Planetary and Space Science, 61, 1, 99–107, doi: 10.1016/j.pss.2011.05.009.

Cornet, T., O. Bourgeois, S. Le Mouélic, S. Rodriguez, T. Lopez Gonzalez, C. Sotin, G. Tobie, et al, (2012a), Geomorphological significance of Ontario Lacus on Titan: Integrated interpretation of Cassini VIMS, ISS and RADAR data and comparison with the Etosha Pan (Namibia), Icarus, 218, 2, 788–806, doi: 10.1016/j.icarus.2012.01.013.

Cornet, T., O. Bourgeois, S. Le Mouélic, S. Rodriguez, C. Sotin, J. W. Barnes, R. H. Brown et al., (2012b), Edge detection applied to Cassini images reveals no measurable displacement of Ontario Lacus' margin between 2005 and 2010, Journal of Geophysical Research: Planets, 117, 7, doi: 10.1029/2012JE004073.

Cours, T., P. Rannou, A. Coustenis, A. Hamdouni, (2010), A new analysis of the ESO very large telescope (VLT) observations of Titan at 2 μm, Planetary and Space Science, 58, 13, 1708–1714, doi: 10.1016/j.pss.2009.12.009.

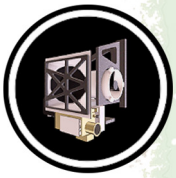

Courtin, R., H. Feuchtgruber, S. J. Kim, E. Lellouch, (2016), The 6–7 μm spectrum of Titan from ISO/SWS observations, Icarus, 270, 389–398, doi: 10.1016/j.icarus.2015.07.021.

Courtin, R., S. J. Kim, A. Bar-Nun, (2015), Three-micron extinction of the Titan haze in the 250–700 km altitude range: Possible evidence of a particle-aging process, Astronomy & Astrophysics, 573, A21, doi: 10.1051/0004-6361/201424977.

Couturier-Tamburelli, I., M. S. Gudipati, A. Lignell, R. Jacovi, N. Piétri, (2014), Spectroscopic studies of non-volatile residue formed by photochemistry of solid C_4N_2: A model of condensed aerosol formation on Titan, Icarus, 234, 81–90, doi: 10.1016/j.icarus.2014.02.016.

Cruikshank, D. P., C. M. Dalle Ore, R. N. Clark, Y. J. Pendleton, (2014), Aromatic and aliphatic organic materials on Iapetus: Analysis of Cassini VIMS data, Icarus, 233, 306–315, doi: 10.1016/j.icarus.2014.02.011.

Cruikshank, D. P., J. P. Emery, K. A. Kornei, G. Bellucci, E. d'Aversa, (2010a), Eclipse reappearances of Io: Time-resolved spectroscopy (1.9–4.2 μm), Icarus, 205, 2, 516–527, doi: 10.1016/j.icarus.2009.05.035.

Cruikshank, D. P., A. W. Meyer, R. H. Brown, R. N. Clark, R. Jaumann, K. Stephan, C. A. Hibbitts, et al, (2010b), Carbon dioxide on the satellites of Saturn: Results from the Cassini VIMS investigation and revisions to the VIMS wavelength scale, Icarus, 206, 561–572, doi: 10.1016/j.icarus.2009.07.012.

Cruikshank, D. P., A. W. Meyer, R. H. Brown, R. N. Clark, R. Jaumann, K. Stephan, C. A. Hibbitts, et al., (2010), Carbon dioxide on the satellites of Saturn: Results from the Cassini VIMS investigation and revisions to the VIMS wavelength scale, Icarus 206, no. 2, 561–572.

Cruikshank, D. P., E. Wegryn, C. M. Dalle Ore, R. H. Brown, K. H. Baines, J.-P. Bibring, B. J. Buratti, R. N. Clark, T .B. McCord, P. D. Nicholson, Y. J. Pendleton, T. C. Owen, G. Filacchione, VIMS Team, (2008), Hydrocarbons on Saturn's Satellites Iapetus and Phoebe, Icarus, Icarus, 193, 334–343, doi: 10.1016/j.icarus.2007.04.036.

Cruikshank, D. P., J. B. Dalton, C. M. Dalle Ore, J. Bauer. K. Stephan, G. Filacchione, A. R. Hendrix, C. J. Hansen, A. Coradini, P. Cerroni, F. Tosi, F. Capaccioni, R. Jaumann, B. J. Buratti, R. N. Clark, R. H. Brown, R. M. Nelson, T. B. McCord, K. H. Baines, P. D. Nicholson, C. Sotin, A. W. Meyer, G. Bellucci, M. Combes, J.-P. Bibring, Y. Langevin, B. Sicardy, D. L. Matson, V. Formisano, P. Drossart, V. Mennella, (2007), Surface composition of Hyperion, Nature, 448, pp. 54–56, doi: 10.1038/nature05948.

Cruikshank, D. P., T. C. Owen, C. M. Dalle Ore, T. R. Geballe, T. L. Roush, C. De Bergh, S. A. Sandford, F. Poulet, G. K. Benedix, J. P. Emery, (2005), A spectroscopic study of the surfaces of Saturn's large satellites: H_2O ice, tholins, and minor constituents, Icarus, 175, 1, 268–283, doi: 10.1016/j.icarus.2004.09.003.

Cuzzi, J., R. Clark, G. Filacchione, R. French, R. Johnson, E. Marouf, L. Spilker, (2009), Ring particle composition and size distribution, Chapter 15, In Saturn from Cassini-Huygens, (eds.) M. Dougherty, L. Esposito, S. Krimigis, Springer Dordrecht, pp. 459–510, doi: 10.1007/978-1-4020-9217-6_15.

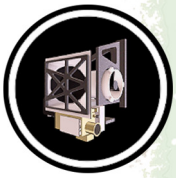

Dalba, P. A., P. S. Muirhead, J. J. Fortney, M. M. Hedman, P. D. Nicholson, M. J. Veyette, (2015), The transit transmission spectrum of a cold gas giant planet, The Astrophysical Journal, 814, 154, doi: 10.1088/0004-637X/814/2/154.

Dalba, P. A., B. J. Buratti, R. H. Brown, J. W. Barnes, K. H. Baines, C. Sotin, R. N. Clark, K. J. Lawrence, P. D. Nicholson, (2012), Cassini VIMS observations show ethane is present in Titan's rainfall, The Astrophysical Journal Letters, 761, 2, doi: 10.1088/2041-8205/761/2/L24.

Dalle Ore, C. M., D. P. Cruikshank, R. M. E. Mastrapa, E. Lewis, O. L. White, (2015), Impact craters: An ice study on Rhea, Icarus, 261, 80–90, doi: 10.1016/j.icarus.2015.08.008.

Dalle Ore, C. M., D. P. Cruikshank, R. N. Clark, (2012), Infrared spectroscopic characterization of the low-albedo materials on Iapetus, Icarus, 221, 2, 735–743, doi: 10.1016/j.icarus.2012.09.010.

Dalton III, J. B., D. P. Cruikshank, R. N. Clark, (2012), Compositional analysis of Hyperion with the Cassini Visual and Infrared Mapping Spectrometer, Icarus, 220, 752–776, doi: 10.1016/j.icarus.2012.05.003.

D'Aversa, E., G. Bellucci, F. Altieri, F. G. Carrozzo, G. Filacchione, F. Tosi, P. D. Nicholson, M. M. Hedman, R. H. Brown, M. R. Showalter, (2011), Spectral characteristics of a spoke on the Saturn Rings, Memorie della Societa Astronomica Italiana Supplementi, 16, 70.

D'Aversa, E., G. Bellucci, P. D. Nicholson, M. M. Hedman, R. H. Brown, M. R. Showalter, F. Altieri, F. G. Carrozzo, G. Filacchione, F. Tosi, (2010), The spectrum of a Saturn ring spoke from Cassini/VIMS, Geophysical Research Letters, 37, 1, doi: 10.1029/2009GL041427.

Davies, A. G., C. Sotin, M. Choukroun, D. L. Matson, T. V. Johnson, (2016), Cryolava flow destabilization of crustal methane clathrate hydrate on Titan, Icarus, 274, 23–32, doi: 10.1016/j.icarus.2016.02.046.

Davies, A. G., L. P. Keszthelyi, A. J. L. Harris, (2010a), The thermal signature of volcanic eruptions on Io and Earth, Journal of Volcanology and Geothermal Research, 194, 4, 75–99, doi: 10.1016/j.jvolgeores.2010.04.009.

Davies, A. G., C. Sotin, D. L. Matson, J. Castillo-Rogez, T. V. Johnson, M. Choukroun, K. H. Baines, (2010b), Atmospheric control of the cooling rate of impact melts and cryolavas on Titan’s surface, Icarus, 208, 2, 887–895, doi: 10.1016/j.icarus.2010.02.025.

De Bergh, C., R. Courtin, B. Bézard, A. Coustenis, E. Lellouch, M. Hirtzig, P. Rannou, et al., (2012), Applications of a new set of methane line parameters to the modeling of Titan's spectrum in the 1.58 μm window, Planetary and Space Science, 61, 1, 85–98, doi: 10.1016/j.pss.2011.05.003.

de Kok, R., P. G. J. Irwin, N. A. Teanby, (2010a), Far-infrared opacity sources in Titan’s troposphere reconsidered, Icarus, 209, 2, 854–857, doi: 10.1016/j.icarus.2010.06.035.

de Kok, R., P. G. J. Irwin, N. A. Teanby, S. Vinatier, F. Tosi, A. Negrão, S. Osprey, A. Adriani, M. L. Moriconi, A. Coradini, (2010b), A tropical haze band in Titan’s stratosphere, Icarus, 207, 1, 485–490, doi: 10.1016/j.icarus.2009.10.021.

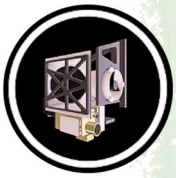

Déau, E., L. Dones, M. I. Mishchenko, R. A. West, P. Helfenstein, M. M. Hedman, C. C. Porco, (2018), The opposition effect in Saturn's main rings as seen by Cassini ISS: 4. Correlations of the surge morphology with surface albedos and VIMS spectral properties, Icarus, 305, 324–349, doi:10.1016/j.icarus.2017.12.025.

Degruyter, W. and M. Manga, (2011), Cryoclastic origin of particles on the surface of Enceladus, Geophysical Research Letters, 38, 16, doi: 10.1029/2011GL048235.

Del Genio, A. D., R. K. Achterberg, K. H. Baines, F. M. Flasar, P. L. Read, A. Sánchez-Lavega, A. P. Showman, (2009), Saturn atmospheric structure and dynamics, Chapter 6, In Saturn from Cassini-Huygens, (eds.) M. K. Dougherty, L. W. Esposito, S. M. Krimigis, Springer Dordrecht, pp. 113–159, doi:10.1007/978-1-4020-9217-6_6.

Dhingra, R. D., J. W. Barnes, R. H. Brown, B. J. Burrati, C. Sotin, P. D. Nicholson, K. H. Baines, et al., (2019), Observational evidence for summer rainfall at Titan's north pole, Geophysical Research Letters, 46, 3, 1205–1212, doi:10.1029/2018GL080943.

Dhingra, R. D., J. W. Barnes, B. J. Yanites, R. L. Kirk, (2018), Large catchment area recharges Titan's Ontario Lacus, Icarus, 299, 331–338, doi:10.1016/j.icarus.2017.08.009

Dhingra, D., M. M. Hedman, R. N. Clark, P. D. Nicholson, (2017), Spatially resolved near infrared observations of Enceladus' tiger stripe eruptions from Cassini VIMS, Icarus, 292, 1–12, doi: 10.1016/j.icarus.2017.03.002.

Dinelli, B. M., M. Lõpez-Puertas, A. Adriani, M. L. Moriconi, B. Funke, M. García-Comas, E. D'Aversa, (2013), An unidentified emission in Titan's upper atmosphere, Geophysical Research Letters, 40, 8, 1489–1493, doi: 10.1002/grl.50332.

Dyudina, U. A., A. P. Ingersoll, S. P. Ewald, D. Wellington, (2016), Saturn's aurora observed by the Cassini camera at visible wavelengths, Icarus, 263, 32–43, doi: 10.1016/j.icarus.2015.05.022.

Dyudina, U. A., A. P. Ingersoll, S. P. Ewald, A.R. Vasavada, R. A. West, K. H. Baines, T. W. Momary, A. D. Del Genio, J. M. Barbara, C. C. Porco, R. K. Achterberg, F. M. Flasar, A. A. Simon-Miller, L. N. Fletcher, (2009), Saturn's south pole vortex compared to other large vortices in the solar system, Icarus, 202, 240–248, doi:10.1016/j.icarus.2009.02.014.

El Moutamid, M., P. D. Nicholson, R. G. French, M. S. Tiscareno, C. D. Murray, M. W. Evans, C. M. French, M. M. Hedman, J. A. Burns, (2016), How Janus' orbital swap affects the edge of Saturn's A-ring?, Icarus, 279, 125–140, doi: 10.1016/j.icarus.2015.10.025.

Esposito, L. W., B. K. Meinke, J. E. Colwell, P. D. Nicholson, M. M. Hedman, (2008), Moonlets and clumps in Saturn's F ring, Icarus, 194, 1, 278–289, doi: 10.1016/j.icarus.2007.10.001.

Fabiano, F., M. López Puertas, A. Adriani, M. L. Moriconi, E. D'Aversa, B. Funke, M. A. López-Valverde, M. Ridolfi, B. M. Dinelli, (2017), CO concentration in the upper stratosphere and mesosphere of Titan from VIMS dayside limb observations at 4.7 μm, Icarus, 293, 119–131, doi: 10.1016/j.icarus.2017.04.014.

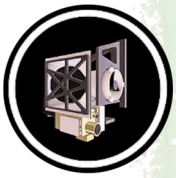

Feldman, W. C., D. J. Lawrence, R. C. Elphic, B. L. Barraclough, S. Maurice, I. Genetay, A. B. Binder, (2000), Polar hydrogen deposits on the Moon, Journal of Geophysical Research: Planets, 105, no. E2, 4175–4195.

Filacchione, G., M. Ciarniello, E. D'Aversa, F. Capaccioni, P. Cerroni, B. Buratti, R. N. Clark, K. Stephan, C. Plainaki, (2018a), Photometric modeling and VIS-IR albedo maps of Tethys from Cassini-VIMS, Geophysical Research Letters, 45, 13, 6400–6407, doi: 10.1029/2018GL078602.

Filacchione, G., M. Ciarniello, E. D'Aversa, F. Capaccioni, P. Cerroni, B. J. Buratti, R. N. Clark, K. Stephan, C. Plainaki, (2018b), Photometric modeling and VIS-IR albedo maps of Dione from Cassini-VIMS, Geophysical Research Letters, 45, 5, 2184–2192, doi: 10.1002/2017GL076869.

Filacchione, G., E. D'Aversa, F. Capaccioni, R. N. Clark, D. P. Cruikshank, M. Ciarniello, P. Cerroni, et al., (2016), Saturn's icy satellites investigated by Cassini-VIMS, IV, Daytime temperature maps, Icarus, 271, 292–313, doi: 10.1016/j.icarus.2016.02.019.

Filacchione, G., M. Ciarniello, F. Capaccioni, R. N. Clark, P. D. Nicholson, M. M. Hedman, J. N. Cuzzi, et al., (2014), Cassini-VIMS observations of Saturn's main rings: I, Spectral properties and temperature radial profiles variability with phase angle and elevation, Icarus, 241, 45–65, doi: 10.1016/j.icarus.2014.06.001.

Filacchione, G., F. Capaccioni, R. N. Clark, P. D. Nicholson, D. P. Cruikshank, J. N. Cuzzi, J. I. Lunine, et al., (2013), The radial distribution of water ice and chromophores across Saturn's system, The Astrophysical Journal, 766, 2, doi: 10.1088/0004-637X/766/2/76.

Filacchione, G., F. Capaccioni, M. Ciarniello, R. N. Clark, J. N. Cuzzi, P. D. Nicholson, D. P. Cruikshank, et al., (2012), Saturn's icy satellites and rings investigated by Cassini-VIMS: III - Radial compositional variability, Icarus, 220, 2, 1064–1096, doi: 10.1016/j.icarus.2012.06.040.

Filacchione, G., F. Capaccioni, R. N. Clark, J. N. Cuzzi, D. P. Cruikshank, A. Coradini, P. Cerroni, et al., (2010), Saturn's icy satellites investigated by Cassini-VIMS, II, Results at the end of nominal mission, Icarus, 206, 2, 507–523, doi: 10.1016/j.icarus.2009.11.006.

Filacchione, G., F. Capaccioni, T. B. McCord, A. Coradini, P. Cerroni, G. Bellucci, F. Tosi, et al., (2007), Saturn's icy satellites investigated by Cassini-VIMS – I, Full-disk properties: 350–5100 nm reflectance spectra and phase curves, Icarus, 186, 1, 259–290, doi: 10.1016/j.icarus.2006.08.001.

Fischer, G., U. A. Dyudina, W. S. Kurth, D. A. Gurnett, P. Zarka, T. Barry, M. Delcroix, et al., (2011), Overview of Saturn lightning observations, Planetary Radio Emissions VII, (eds.) H. O. Rucker, W. S. Kurth, P. Louarn, G. Fischer, Austrian Academy of Sciences Press, Vienna, 135–144, arXiv:1111.4919.

Flasar, F. M., K. H. Baines, M. K. Bird, T. Tokano, R. A. West, (2009), Atmospheric dynamics and meteorology, Chapter 13, In Titan from Cassini-Huygens, (eds.) R. H. Brown, J.-P. Lebreton, J. H. Waite, Springer Dordrecht, pp. 323–352, doi: 10.1007/978-1-4020-9215-2_13.

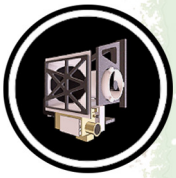

Fletcher, L. N., K. H. Baines, T. W. Momary, A. P. Showman, P. G. J. Irwin, G. S. Orton, M. Roos-Serote, C. Merlet, (2011a), Saturn's tropospheric composition and clouds from Cassini/VIMS 4.6-5.1 μm nightside spectroscopy, Icarus, 214, 2, 510–533, doi: 10.1016/j.icarus.2011.06.006.

Fletcher, L. N., B. E. Hesman, P. G. J. Irwin, K. H. Baines, T. W. Momary, A. Sanchez-Lavega, F. M. Flasar et al, (2011b), Thermal structure and dynamics of Saturn’s northern springtime disturbance, Science, 332, no. 6036, 1413–1417.

Fleury, B., M. S. Gudipati, I. Couturier-Tamburelli, N. Carrasco, (2019), Photoreactivity of condensed acetylene on Titan aerosols analogues, Icarus, 321, 358–366, doi: 10.1016/j.icarus.2018.11.030.

Formisano, V., E. D'Aversa, G. Bellucci, K. H. Baines, J. P. Bibring, Robert H. Brown, B. J. Buratti et al., (2003), Cassini-VIMS at Jupiter: Solar occultation measurements using Io, Icarus, 166, 1, 75–84, doi: 10.1016/S0019-1035(03)00178-7.

Formisano, V., A. Adriani, G. Bellucci, (1992), The VNIR-VIMS experiment for Craf/Cassini, Il Nuovo Cimento C, 15, 6, 1179–1192, doi: 10.1007/BF02506711.

Fortes, A. D., P. M. Grindrod, S. K. Trickett, L. Vočadlo, (2007), Ammonium sulfate on Titan: Possible origin and role in cryovolcanism, Icarus, 188, 1, 139–153, doi: 10.1016/j.icarus.2006.11.002.

French, R. G., C. A. McGhee-French, P. D. Nicholson, M. M. Hedman, (2019), Kronoseismology III: Waves in Saturn's inner C ring, Icarus, 319, 599–626, doi:10.1016/j.icarus.2018.10.013.

French, R. G., C. A. McGhee-French, K. Lonergan, T. Sepersky, R. A. Jacobson, P. D. Nicholson, M. M. Hedman, E. A. Marouf, J. E. Colwell, (2017), Noncircular features in Saturn's rings IV: Absolute radius scale and Saturn's pole direction, Icarus, 290, 14–45, doi: 10.1016/j.icarus.2017.02.007.

French, R. G., P. D. Nicholson, M. M. Hedman, J. M. Hahn, C. A. McGhee-French, J. E. Colwell, E. A. Marouf, N. J. Rappaport, (2016a), Deciphering the embedded wave in Saturn’s Maxwell ringlet, Icarus, 279, 62–77, doi: 10.1016/j.icarus.2015.08.020.

French, R. G., P. D. Nicholson, C. A. McGhee-French, K. Lonergan, T. Sepersky, M. M. Hedman, E. A. Marouf, J. E. Colwell, (2016b), Noncircular features in Saturn's rings III: The Cassini Division, Icarus, 274, 131–162, doi: 10.1016/j.icarus.2016.03.017.

French, R. G., P. D. Nicholson, C. A. McGhee-French, K. Lonergan, T. Sepersky, M. M. Hedman, E. A. Marouf, J. E. Colwell, (2016), Noncircular features in saturn’s rings III: the cassini division, Icarus, 274, 131–162.

French, R. S., M. R. Showalter, R. Sfair, C. A. Argüelles, M. Pajuelo, P. Becerra, M. M. Hedman, P. D. Nicholson, (2012), The brightening of Saturn's F ring, Icarus, 219, 1, 181–193, doi: 10.1016/j.icarus.2012.02.020.

García-Comas, M., M. López-Puertas, B. Funke, B. M. Dinelli, M. Luisa Moriconi, A. Adriani, A. Molina, A. Coradini, (2011), Analysis of Titan CH_4 3.3μm upper atmospheric emission as measured by Cassini/VIMS, Icarus, 214, 2, 571–583, doi: 10.1016/j.icarus.2011.03.020.

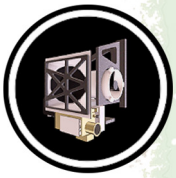

Gautier, T., J. A. Sebree, X. Li, V. T. Pinnick, A. Grubisic, M. J. Loeffler, S. A. Getty, M. G. Trainer, W. B. Brinckerhoff, (2017), Influence of trace aromatics on the chemical growth mechanisms of Titan aerosol analogues, Planetary and Space Science, 140, 27–34, doi: 10.1016/j.pss.2017.03.012.

Gautier, T., N. Carrasco, A. Mahjoub, S. Vinatier, A. Giuliani, C. Szopa, C. M. Anderson, J. J. Correia, P. Dumas, G. Cernogora, (2012), Mid- and far-infrared absorption spectroscopy of Titan's aerosols analogues, Icarus, 221, 1, 320–327, doi: 10.1016/j.icarus.2012.07.025.

Giles, R. S., L. N. Fletcher, P. G. J. Irwin, (2015), Cloud structure and composition of Jupiter's troposphere from 5-μm Cassini VIMS spectroscopy, Icarus, 257, 457–470, doi: 10.1016/j.icarus.2015.05.030.

Gilliam, A. E. and A. Lerman, (2016), Formation mechanisms of channels on Titan through dissolution by ammonium sulfate and erosion by liquid ammonia and ethane, Planetary and Space Science, 132, 13–22, doi: 10.1016/j.pss.2016.08.009.

Goguen, J. D., B. J. Buratti, R. H. Brown, R. N. Clark, P. D. Nicholson, M. M. Hedman, R. R. Howell, C. Sotin, D. P. Cruikshank, K. H. Baines, K. J. Lawrence, J. R. Spencer, D. G. Blackburn, (2013), The temperature and width of an active fissure on Enceladus measured with Cassini VIMS during the 14 April 2012, south pole flyover, Icarus, 226 p1128–1137, doi: 10.1016/j.icarus.2013.07.012.

Griffith, C. A., P. F. Penteado, J. D. Turner, C. D. Neish, G. Mitri, N. J. Montiel, A. Schoenfeld, R. M. C. Lopes, (2019), A corridor of exposed ice-rich bedrock across Titan’s tropical region, Nature Astronomy, doi: 10.1038/s41550-019-0756-5.

Griffith, C. A., L. Doose, M. G. Tomasko, P. F. Penteado, C. See, (2012), Radiative transfer analyses of Titan's tropical atmosphere, Icarus, 218, 2, 975–988, doi: 10.1016/j.icarus.2011.11.034.

Hansen, C. J., S. J. Bolton, D. L. Matson, L. J. Spilker, J.-P. Lebreton, (2004), The Cassini–Huygens flyby of Jupiter, Icarus, 172, 1, 1–8, doi: 10.1016/j.icarus.2004.06.018.

Hansen, G. B., E. C. Hollenbeck, K. Stephan, S. K. Apple, E. J. Z. Shin-White, (2012), Water ice abundance and CO_2 band strength on the saturnian satellite Phoebe from Cassini/VIMS observations, Icarus, 220, 2, 331–338, doi: 10.1016/j.icarus.2012.05.004.

Hansen, G. B., (2009), Calculation of single-scattering albedos: Comparison of Mie results with Hapke approximations, Icarus, 203, 2, 672–676, doi: 10.1016/j.icarus.2009.05.025.

Harbison, R. A., P. D. Nicholson, M. M. Hedman, (2013), The smallest particles in Saturn's A and C rings, Icarus, 226, 2, 1225–1240, doi: 10.1016/j.icarus.2013.08.015.

Hayes, A. G., J. M. Soderblom, M. Ádámkovics, (2016), Titan’s surface and atmosphere, Icarus, 270, 1, doi: 10.1016/j.icarus.2016.02.029.

Hayes, A. G., R. D. Lorenz, M. A. Donelan, M. Manga, J. I. Lunine, T. Schneider, M. P. Lamb, et al., (2013), Wind driven capillary-gravity waves on Titan’s lakes: Hard to detect or non-existent?, Icarus, 225, 1, 403–412, doi: 10.1016/j.icarus.2013.04.004.

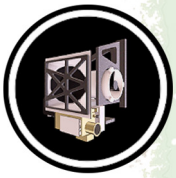

Hayne, P. O., T. B. McCord, C. Sotin, (2014), Titan's surface composition and atmospheric transmission with solar occultation measurements by Cassini VIMS, Icarus, 243, 158–172, doi: 10.1016/j.icarus.2014.08.045.

Hedman, M. M., P. D. Nicholson, R. G. French, (2019), Kronoseismology. IV. Six Previously Unidentified Waves in Saturn’s Middle C Ring, The Astronomical Journal, 157, 1, 18, doi: 10.3847/1538-3881/aaf0a6.

Hedman, M. M., D. Dhingra, P. D. Nicholson, C. J. Hansen, G. Portyankina, S. Ye, Y. Dong, (2018a), Spatial variations in the dust-to-gas ratio of Enceladus’ plume, Icarus, 305, 123–138, doi: 10.1016/j.icarus.2018.01.006.

Hedman, M. M., F. Postberg, D. P. Hamilton, S. Renner, H. W. Hsu, (2018b), Dusty rings, Chapter 12, In Planetary Ring Systems: Properties, Structure, and Evolution, (eds.) M. S. Tiscareno, C. D. Murraypp, Cambridge University Press, pp. 308–337, doi: 10.1017/9781316286791.012.

Hedman, M. M., (2018), An introduction to planetary ring dynamics, Chapter 2, In Planetary Ring Systems: Properties, Structure, and Evolution, (eds.) M. S. Tiscareno, C. D. Murraypp, Cambridge University Press, pp. 30–47, doi: 10.1017/9781316286791.002.

Hedman, M. M. and P. D. Nicholson, (2016), The B-ring's surface mass density from hidden density waves: Less than meets the eye?, Icarus, 279, 109–124, doi: 10.1016/j.icarus.2016.01.007.

Hedman, M. M. and P. D. Nicholson, (2014), More Kronoseismology with Saturn's rings, Monthly Notices of the Royal Astronomical Society, 444, 1369–1388, doi: 10.1093/mnras/stu1503.

Hedman, M. M., P. D. Nicholson, H. Salo, (2014), Exploring overstabilities in Saturn's A-ring using two stellar occultations, The Astronomical Journal, 148, 15, doi: 10.1088/0004-6256/148/1/15.

Hedman, M. M., C. M. Gosmeyer, P. D. Nicholson, C. Sotin, R. H. Brown, R. N. Clark, K. H. Baines, B. J. Buratti, M. R. Showalter, (2013a), An observed correlation between plume activity and tidal stresses on Enceladus, Nature, 500, 182–184, doi: 10.1038/nature12371.

Hedman, M. M., P. D. Nicholson, J. N. Cuzzi, R. N. Clark, G. Filacchione, F. Capaccioni, M. Ciarniello, (2013b), Connections between spectra and structure in Saturn's main rings based on Cassini VIMS data, Icarus, 223, 1, 105–130, doi: 10.1016/j.icarus.2012.10.014.

Hedman, M. M. and P. D. Nicholson, (2013c), Kronoseismology: Using density waves in Saturn's C ring to Probe the planet's interior, The Astronomical Journal, 146, 12, doi: 10.1088/0004-6256/146/1/12.

Hedman, M. M., P. D. Nicholson, M. R. Showalter, R. H. Brown, B. J. Buratti, R. N. Clark, K. Baines, C. Sotin, (2011), The Christiansen Effect in Saturn's narrow dusty rings and the spectral identification of clumps in the F ring, Icarus, 215, 2, 695–711, erratum in Icarus 218, 735, doi: 10.1016/j.icarus.2011.02.025.

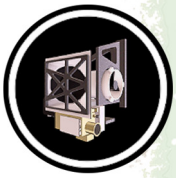

Hedman, M. M., P. D. Nicholson, K. H. Baines, B. J. Buratti, C. Sotin, R. N. Clark, R. H. Brown, R. G. French, E. A. Marouf, (2010), The architecture of the Cassini Division, The Astronomical Journal, 139, 228–251, doi: 10.1088/0004-6256/139/1/228.

Hedman, M. M., P. D. Nicholson, M. R. Showalter, R. H. Brown, B. J. Buratti, R. N. Clark, (2009), Spectral observations of the enceladus plume with Cassini-VIMS, The Astrophysical Journal, 693, 2, 1749–1762, doi: 10.1088/0004-637X/693/2/1749.

Hedman, M. M., J. A. Burns, M. R. Showalter, C. C. Porco, P. D. Nicholson, A. S. Bosh, M. S. Tiscareno, et al., (2007a), Saturn's dynamic D ring, Icarus, 188, 1, 89–107, doi: 10.1016/j.icarus.2006.11.017.

Hedman, M. M., P. D. Nicholson, H. Salo, B. D. Wallis, B. J. Buratti, K. H. Baines, R. H. Brown, R. N. Clark, (2007b), Self-gravity wake structures in Saturn's A-ring revealed by Cassini VIMS, The Astronomical Journal, 133, 6, 2624–2629, doi: 10.1086/516828.

Hendrix, A. R., G. Filacchione, C. Paranicas, P. Schenk, F. Scipioni, (2018), Icy Saturnian satellites: Disk-integrated UV-IR characteristics and links to exogenic processes, Icarus, 300, 103–114, doi: 10.1016/j.icarus.2017.08.037.

Hendrix, A. R., T. A. Cassidy, B. J. Buratti, C. Paranicas, C. J. Hansen, B. Teolis, E. Roussos, E. Todd Bradley, P. Kollmann, R. E. Johnson, (2012), Mimas' far-UV albedo: Spatial variations, Icarus, 220, 2, 922–931, doi: 10.1016/j.icarus.2012.06.012.

Hirtzig, M., B. Bézard, E. Lellouch, A. Coustenis, C. De Bergh, P. Drossart, A. Campargue, et al., (2013a), Corrigendum to– Titan's surface and atmosphere from Cassini/VIMS data with updated methane opacity, Icarus, vol. 226, Issue 1, p. 1182, doi: 10.1016/j.icarus.2013.07.015.

Hirtzig, M., B. Bézard, E. Lellouch, A. Coustenis, C. De Bergh, P. Drossart, A. Campargue, et al., (2013b), Titan's surface and atmosphere from Cassini/VIMS data with updated methane opacity, Icarus, vol. 226, Issue 1, pp. 470–486, doi: 10.1016/j.icarus.2013.05.033.

Hodyss, R., P. V. Johnson, J. V. Stern, J. D. Goguen, I. Kanik, (2009), Photochemistry of methane–water ices, Icarus, 200, 1, 338–342, doi: 10.1016/j.icarus.2008.10.024.

Hofgartner, J. D., A. G. Hayes, J. I. Lunine, H. Zebker, R. D. Lorenz, M. J. Malaska, M. Mastrogiuseppe, C. Notarnicola, J. M. Soderblom, (2016), Titan's "Magic Islands": Transient features in a hydrocarbon sea, Icarus, 271, 338–349, doi:10.1016/j.icarus.2016.02.022.

Imanaka, H., D. P. Cruikshank, B. N. Khare, C. P. McKay, (2012), Optical constants of Titan tholins at mid-infrared wavelengths (2.5–25 μm) and the possible chemical nature of Titan's haze particles, Icarus, 218, 1, 247–261, doi: 10.1016/j.icarus.2011.11.018.

Ingersoll, A. P. and S. P. Ewald, (2017), Decadal timescale variability of the Enceladus plumes inferred from Cassini images, Icarus, 282, 260–275, doi: 10.1016/j.icarus.2016.09.018.

Izawa, M. R. M., E. A. Cloutis, D. M. Applin, M. A. Craig, P. Mann, M. Cuddy, (2014), Laboratory spectroscopic detection of hydration in pristine lunar regolith, Earth and Planetary Science Letters, 390, 157–164, doi: 10.1016/j.epsl.2014.01.007.

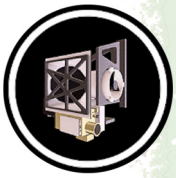

Jaumann, R., R. H. Brown, K. Stephan, J. W. Barnes, L. A. Soderblom, C. Sotin, S. Le Mouélic, et al., (2008a), Fluvial erosion and post-erosional processes on Titan, Icarus, 197, 2, 526–538, doi: 10.1016/j.icarus.2008.06.002.

Jaumann, R., K. Stephan, G. B. Hansen, R. N. Clark, B. J. Buratti, R. H. Brown, K. H. Baines, G. Bellucci, A. Coradini, D. P. Cruikshank, C. A. Griffith, C. A. Hibbitts, T. B. McCord, R. M. Nelson, P. D. Nicholson, C. Sotin, R. Wagner, (2008b), Distribution of icy particles across Enceladus' surface as derived from Cassini-VIMS measurements, Icarus 193, 407–419, doi: 10.1016/j.icarus.2007.09.013.

Jaumann, R., K. Stephan, R. H. Brown, B. J. Buratti, R. N. Clark, T. B. McCord, A. Coradini, (2006), High-resolution Cassini-VIMS mosaics of Titan and the icy Saturnian satellites, Planetary and Space Science, 54, 12, 1146–1155, doi: 10.1016/j.pss.2006.05.034.

Jerousek, R. G., J. E. Colwell, L. W. Esposito, P. D. Nicholson, M. M. Hedman, (2016), Small particles and self-gravity wakes in Saturn's rings from UVIS and VIMS stellar occultations, Icarus, 279, 36–50, doi: 10.1016/j.icarus.2016.04.039.

Juergens, D. W., J. E. Duval, R. F. Lockhart, Y. Langevin, V. Formisano, G. Bellucci, (1991), Visible and infrared mapping spectrometer for exploration of comets, asteroids, and the saturnian system of rings and moons, International Journal of Imaging Systems and Technology, 3, 2, 108–120, doi: 10.1002/ima.1850030207.

Karkoschka, E. and S. E. Schröder, (2016), Eight-color maps of Titan's surface from spectroscopy with Huygens' DISR, Icarus, 270, 260–271, doi: 10.1016/j.icarus.2015.06.010.

Kazeminejad, B., D. H. Atkinson, J. P. Lebreton, (2011), Titan's new pole: Implications for the Huygens entry and descent trajectory and landing coordinates, Advances in Space Research, 47, 9, 1622–1632, doi: 10.1016/j.asr.2011.01.019.

Kim, S. J., C. K. Sim, T. S. Stallard, R. Courtin, (2019), Spectral characteristics and formation of high-altitude haze in the south-polar regions of Saturn, Icarus, 321, 436–444, doi: 10.1016/j.icarus.2018.12.004.

Kim, S. J., D. W. Lee, C. K. Sim, K. I. Seon, R. Courtin, T. R. Geballe, (2018), Retrieval of haze properties and HCN concentrations from the three-micron spectrum of Titan, Journal of Quantitative Spectroscopy and Radiative Transfer, 210, 197–203, doi: 10.1016/j.jqsrt.2018.02.024.

Kim, S. J. and R. Courtin, (2013), Spectral characteristics of the Titanian haze at 1–5 micron from Cassini/VIMS solar occultation data, Astronomy & Astrophysics, 557, doi: 10.1051/0004-6361/201322173.

Kim, S. J., C. K. Sim, D. W. Lee, R. Courtin, J. I. Moses, Y. C. Minh, (2012), The three-micron spectral feature of the Saturnian haze: Implications for the haze composition and formation process, Planetary and Space Science, 65, 1, 122–129, doi: 10.1016/j.pss.2012.02.013.

Kim, S. J., A. Jung, C. K. Sim, R. Courtin, A. Bellucci, B. Sicardy, I. O. Song, Y. C. Minh, (2011), Retrieval and tentative indentification of the 3 μm spectral feature in Titans haze, Planetary and Space Science, 59, 8, 699–704, doi: 10.1016/j.pss.2011.02.002.

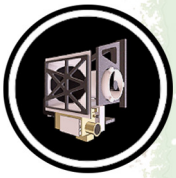

Kim, Y. S., C. Ennis, S. J. Kim, (2013), Simulating the 3.4-micron feature of titan's haze, Bulletin of the Korean Chemical Society, 34, 3, 759–762, doi: 10.5012/bkcs.2013.34.3.759.

Kolokolova, L., L. Liu, B. Buratti, M. I. Mishchenko, (2011), Modeling variations in near-infrared spectra caused by the coherent backscattering effect, Journal of Quantitative Spectroscopy and Radiative Transfer, 112, 13, 2175–2181, doi: 10.1016/j.jqsrt.2011.03.010.

Kolokolova, L., B. Buratti, V. Tishkovets, (2010), Impact of coherent backscattering on the spectra of icy satellites of Saturn and the implications of its effects for remote sensing, The Astrophysical Journal Letters, 711, L71–L74, doi: 10.1088/2041-8205/711/2/L71.

Lamy, L., R. Prangé, W. Pryor, Jacques Gustin, S. V. Badman, H. Melin, T. Stallard, D. G. Mitchell, P. C. Brandt, (2011), Multispectral simultaneous diagnosis of Saturn's aurorae throughout a planetary rotation, Journal of Geophysical Research: Space Physics, 118, no. 8, 4817–4843.

Langhans, M., J. I. Lunine, G. Mitri, (2013), Titan’s Xanadu region: Geomorphology and formation scenario, Icarus, 223, 2, 796–803, doi: 10.1016/j.icarus.2013.01.016.

Langhans, M. H., R. Jaumann, K. Stephan, R. H. Brown, B. J. Buratti, R. N. Clark, K. H. Baines, et al., (2012), Titan's fluvial valleys: Morphology, distribution, and spectral properties, Planetary and Space Science, 60, 1, 34–51, doi: 10.1016/j.pss.2011.01.020.

Langhans, M., (2011), Erosion on saturn's moon Titan - Analyses of the distribution, morphology, and spectral properties of Titan's fluvial valleys, Ph.D. dissertation, doi: 10.17169/refubium-6689.

Larson, E. J. L., O. B. Toon, A. J. Friedson, (2014), Simulating Titan’s aerosols in a three dimensional general circulation model, Icarus, 243, 400–419, doi: 10.1016/j.icarus.2014.09.003.

Launeau, P., C. Sotin, J. Girardeau, (2002), Cartography of the Ronda peridotite (Spain) by hyperspectral remote sensing, Bulletin de la Societe Geologique de France, 173, 6, 491–508, doi: 10.2113/173.6.491.

Le Corre, L., S. Le Mouélic, C. Sotin, J.-P. Combe, S. Rodriguez, J. W. Barnes, R. H. Brown, et al., (2009), Analysis of a cryolava flow-like feature on Titan, Planetary and Space Science, 57, 7, 870–879, doi: 10.1016/j.pss.2009.03.005.

Le Gall, A., M. A. Janssen, L. C. Wye, A. G. Hayes, J. Radebaugh, C. Savage, H. Zebker, et al., (2011), Cassini SAR, radiometry, scatterometry and altimetry observations of Titan's dune fields, Icarus, 213, 2, 608–624, doi: 10.1016/j.icarus.2011.03.026.

Le Mouélic, S., T. Cornet, S. Rodriguez, C. Sotin, B. Seignovert, J. W. Barnes, R. H. Brown, et al., (2019), The Cassini VIMS archive of Titan: From browse products to global infrared color maps, Icarus, 319, 121–132, doi: 10.1016/j.icarus.2018.09.017.

Le Mouélic, S., S. Rodriguez, R. Robidel, B. Rousseau, B. Seignovert, C. Sotin, J. W. Barnes, et al., (2018), Mapping polar atmospheric features on Titan with VIMS: From the dissipation of

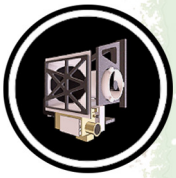

the northern cloud to the onset of a southern polar vortex, Icarus, 311, 371–383, doi: 10.1016/j.icarus.2018.04.028.

Le Mouélic, S., T. Cornet, S. Rodriguez, C. Sotin, J. W. Barnes, K. H. Baines, R. H. Brown, et al., (2012a), Global mapping of Titan′s surface using an empirical processing method for the atmospheric and photometric correction of Cassini/VIMS images, Planetary and Space Science, 73, 1, 178–190, doi: 10.1016/j.pss.2012.09.008.

Le Mouélic, S., P. Rannou, S. Rodriguez, C. Sotin, C. A. Griffith, L. Le Corre, J. W. Barnes, et al., (2012b), Dissipation of Titans north polar cloud at northern spring equinox, Planetary and Space Science, 60, 1, 86–92, doi: 10.1016/j.pss.2011.04.006.

Le Mouélic, S., P. Paillou, M. A. Janssen, J. W. Barnes, S. Rodriguez, C. Sotin, R. H. Brown, et al., (2008), Mapping and interpretation of Sinlap crater on Titan using Cassini VIMS and RADAR data, Journal of Geophysical Research: Planets, 113, 4, doi: 10.1029/2007JE002965.

Lee, J. S., B. J. Buratti, M. Hicks, J. Mosher, (2010), The roughness of the dark side of Iapetus from the 2004 to 2005 flyby, Icarus, 206, 2, 623–630, doi: 10.1016/j.icarus.2009.11.008.

Li, L., K. H. Baines, M. A. Smith, R. A. West, S. Pérez-Hoyos, H. J. Trannell, A. A. Simon-Miller, B. J. Conrath, G. S. Orton, C. A. Nixon, G. Filacchione, P. M. Fry, T. W. Momary, (2012), Emitted power of Jupiter based on Cassini CIRS and VIMS observations, Journal of Geophysical Research: Planets, doi: 10.1029/2012JE004191.

Loeffler, J. and A. Baragiola, (2009), Is the 3.5 μm infrared feature on Enceladus due to hydrogen peroxide?, The Astrophysical Journal, 694, L92–L94, doi: 10.1088/0004-637X/694/1/L92.

Lopes, R. M. C., M. J. Malaska, A. Solomonidou, A. Le Gall, M. A. Janssen, C. D. Neish, E. P. Turtle, et al., (2016), Nature, distribution, and origin of Titan's Undifferentiated Plains, Icarus, 270, 162–182, doi: 10.1016/j.icarus.2015.11.034.

Lopes, R. M. C., R. L. Kirk, K. L. Mitchell, A. LeGall, J. W. Barnes, A. Hayes, J. Kargel, et al., (2013), Cryovolcanism on Titan: New results from Cassini RADAR and VIMS, Journal of Geophysical Research: Planets, 118, 3, 416–435, doi: 10.1002/jgre.20062.

Lopes, R. M. C., B. J. Buratti, A. R. Hendrix, (2008), The Saturn system's icy satellites: New results from Cassini, Icarus, 193, 2, 305–308, doi: 10.1016/j.icarus.2007.11.002.

Lora, J. M., J. I. Lunine, J. L. Russell, (2015), GCM simulations of Titan’s middle and lower atmosphere and comparison to observations, Icarus, 250, 516–528, doi: 10.1016/j.icarus.2014.12.030.

Lorenz, R. D., J. I. Lunine, (2005), Titan's surface before Cassini, Planetary and Space Science, 53, no. 5, 557–576.

MacKenzie, S. M., J. W. Barnes, C. Sotin, J. M. Soderblom, S. Le Mouélic, S. Rodriguez, K. H. Baines, et al., (2014), Evidence of Titan's climate history from evaporite distribution, Icarus, 243, 191–207, doi: 10.1016/j.icarus.2014.08.022.

Mahjoub, A., M. Choukroun, R. Hodyss, C. Sotin, P. Beauchamp, M. Barmatz, (2018), Titan Lakes Simulation System (TiLSS): A cryogenic experimental setup to simulate Titan's liquid

hydrocarbon surfaces, Review of Scientific Instruments, 89, 12, 124502, doi: 10.1063/1.5053126.

Mahjoub, A., M. Schwell, N. Carrasco, Y. Benilan, G. Cernogora, C. Szopa, M. C. Gazeau (2016), Characterization of aromaticity in analogues of titan's atmospheric aerosols with two-step laser desorption ionization mass spectrometry, Planetary and Space Science, 131, 1–13, doi: 10.1016/j.pss.2016.05.003.

Mahjoub, A., N. Carrasco, P. R. Dahoo, T. Gautier, C. Szopa, G. Cernogora, (2012), Influence of methane concentration on the optical indices of Titan's aerosols analogues, Icarus, 221, 2, 670–677, doi: 10.1016/j.icarus.2012.08.015.

Malaska, M. J., R. M. C. Lopes, D. A. Williams, C. D. Neish, A. Solomonidou, J. M. Soderblom, A. M. Schoenfeld, et al., (2016), Geomorphological map of the Afekan Crater region, Titan: Terrain relationships in the equatorial and mid-latitude regions, Icarus, 270, 130–161, doi: 10.1016/j.icarus.2016.02.021.

Malathy Devi, V., I. Kleiner, R. L. Sams, L. R. Brown, D. C. Benner, L. N. Fletcher, (2014), Line positions and intensities of the phosphine (PH_3) Pentad near 4.5 μm, Journal of Molecular Spectroscopy, 298, 11–23, doi: 10.1016/j.jms.2014.01.013.

Maltagliati, L., B. Bézard, S. Vinatier, M. M. Hedman, E. Lellouch, P. D. Nicholson, C. Sotin, R. J. de Kok, B. Sicardy, (2015), Titan's atmosphere as observed by Cassini/VIMS solar occultations: CH_4, CO and evidence for C_2H_6 absorption, Icarus, 248, 1–24, doi: 10.1016/j.icarus.2014.10.004.

Mastrapa, R. M., M. P. Bernstein, S. A. Sandford, T. L. Roush, D. P. Cruikshank, C. M. Dalle Ore, (2008), Optical constants of amorphous and crystalline H_2O-ice in the near infrared from 1.1 to 2.6 μm, Icarus, 197, no. 1, 307–320.

Mastrogiuseppe, M., A. G. Hayes, V. Poggiali, J. I. Lunine, R. D. Lorenz, R. Seu, A. Le Gall, et al., (2018), Bathymetry and composition of Titan's Ontario Lacus derived from Monte Carlo-based waveform inversion of Cassini RADAR altimetry data, Icarus, 300, 203–209, doi: 10.1016/j.icarus.2017.09.009.

Mathé, C., T. Gautier, M. G. Trainer, N. Carrasco, (2018), Detection Opportunity for Aromatic Signature in Titan's Aerosols in the 4.1–5.3 μm Range, The Astrophysical Journal Letters, 861, 2, doi:10.3847/2041-8213/aacf88.

Matson, D. L., A. G. Davies, T. V. Johnson, J. P. Combe, T. B. McCord, J. Radebaugh, S. Singh, (2018), Enceladus' near-surface CO_2 gas pockets and surface frost deposits, Icarus, 302, 18–26, doi: 10.1016/j.icarus.2017.10.025.

McCord, T. B., et al., (2008), Titan's surface: Search for spectral diversity and composition using the Cassini VIMS investigation, Icarus, 194(1), 212–242, doi: 10.1016/j.icarus.2007.08.039.

McCord, T. B., P. Hayne, J.-P. Combe, G. B. Hansen, J. W. Barnes, S. Rodriguez, S. Le Mouélic, et al., (2006), Composition of Titan's surface from Cassini VIMS, Planetary and Space Science, 54, 15, 1524–1539, doi: 10.1016/j.pss.2006.06.007.

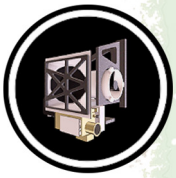

McCord, T. B., A. Coradini, C. A. Hibbitts, F. Capaccioni, G. B. Hansen, G. Filacchione, R. N. Clark, et al., (2004), Cassini VIMS observations of the Galilean satellites including the VIMS calibration procedure, Icarus, 172, 104–126, doi: 10.1016/j.icarus.2004.07.001.

Meier, R., B. A. Smith, T. C. Owen, R. J. Terrile, (2000), The surface of Titan from NICMOS observations with the Hubble Space Telescope, Icarus, 145, no. 2, 462–473.

Melin, H., S. V. Badman, T. S. Stallard, U. Dyudina, J. D. Nichols, G. Provan, J. O'Donoghue, W. R. Pryor, K. H. Baines, S. Miller, J. Gustin, A. Radioti, C. Tao, C. J. Meredith, J. S. D. Blake, (2016), Simultaneous multi-scale and multiinstrument observations of Saturn's aurorae during the 2013 Observing Campaign, Icarus, 263, 56–74, doi: 10.1016/j.icarus.2015.08.021.

Melin, H., T. Stallard, S. Miller, J. Gustin, M. Galand, S. V. Badman, W. R. Pryor, J. O'Donoghue, R. H. Brown, K. H. Baines, (2011), Simultaneous Cassini/VIMS and UVIS observations of Saturn's southern aurora: Comparing emissions from H, H_2 and H_3^+ at a high spatial resolution, Geophysical Research Letters, 38, L15203, doi: 10.1029/2011GL048457.

Miller, E. A., G. Klein, D. W. Juergens, K. Mehaffey, J. M. Oseas, R. A. Garcia, A. Giandomenico, et al., (1996), The visual and infrared mapping spectrometer for Cassini, In Cassini/Huygens: A Mission to the Saturnian Systems, International Symposium on Optical Science, Engineering, and Instrumentation, Denver, CO, vol. 2803, pp. 206–220, doi: 10.1117/12.253421.

Moore, J. M. and R. T. Pappalardo, (2011), Titan: An exogenic world?, Icarus, 212, 2, 790–806, doi: 10.1016/j.icarus.2011.01.019.

Moore, J. M. and A. D. Howard, (2010), Are the basins of Titan's Hotei Regio and Tui Regio sites of former low latitude seas?, Geophysical Research Letters, 37, 22, doi: 10.1029/2010GL045234.

Morales-Juberías, R., K. M. Sayanagi, T. E. Dowling, A. P. Ingersoll, (2011), Emergence of polar-jet polygons from jet instabilities in a Saturn model, Icarus, 211, 2, 1284–1293, doi: 10.1016/j.icarus.2010.11.006.

Moriconi, M. L., A. Adriani, E. D'Aversa, G. L. Liberti, G. Filacchione, F. Oliva, (2016), Unbiased estimations of atmosphere vortices: The Saturn's storm by Cassini VIMS-V as case study, Journal of Signal and Information Processing, 7, no. 02, 75–83, doi: 10.4236/jsip.2016.72009.

Moriconi, M. L., J. I. Lunine, A. Adriani, E. D'Aversa, A. Negrão, G. Filacchione, A. Coradini, (2010), Characterization of Titan's Ontario Lacus region from Cassini/VIMS observations, Icarus, 210, 2, 823–831, doi: 10.1016/j.icarus.2010.07.023.

Neish, C. D., J. W. Barnes, C. Sotin, S. MacKenzie, J. M. Soderblom, S. Le Mouélic, R. L. Kirk, et al., (2015), Spectral properties of Titan's impact craters imply chemical weathering of its surface, Geophysical Research Letters, 42, 10, 3746–3754, doi:10.1002/2015gl063824.

Nelson, R. M., L. W. Kamp, R. M. C. Lopes, D. L. Matson, R. L. Kirk, B. W. Hapke, S. D. Wall., et al., (2009a), Photometric changes on Saturn's Titan: Evidence for active cryovolcanism, Geophysical Research Letters, 36, 4, doi: 10.1029/2008GL036206.

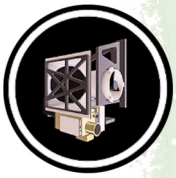

Nelson, R. M., L. W. Kamp, D. L. Matson, P. G. J. Irwin, K. H. Baines, M. D. Boryta, F. E. Leader, et al., (2009b), Saturn's Titan: Surface change, ammonia, and implications for atmospheric and tectonic activity, Icarus, 199, 2, 429–441, doi: 10.1016/j.icarus.2008.08.013.

Nelson, R. M., R. H. Brown, B. W. Hapke, W. D. Smythe, L. Kamp, M. D. Boryta, F. Leader, et al., (2006), Photometric properties of Titan's surface from Cassini VIMS: Relevance to titan's hemispherical albedo dichotomy and surface stability, Planetary and Space Science, 54, 15, 1540–1551, doi: 10.1016/j.pss.2006.06.014.

Nelson, R. M., W. D. Smythe, B. W. Hapke, A. S. Hale, (2002), Low phase angle laboratory studies of the opposition effect: search for wavelength dependence, Planetary and Space Science, 50, 9, 849–856, doi: 10.1016/S0032-0633(02)00059-4.

Nelson, R. M., B. W. Hapke, W. D. Smythe, L. J. Horn, (1998), Phase curves of selected particulate materials: The contribution of coherent backscattering to the opposition surge, Icarus, 131, 1, 223–230, doi: 10.1006/icar.1997.5850.

Newman, S. F., B. J. Buratti, R. H. Brown, R. Jaumann, J. Bauer, T. Momary, (2009), Water ice crystallinity and grain sizes on Dione, Icarus, 203, 2, 553–559, doi: 10.1016/j.icarus.2009.04.034.

Newman, S. F., B. J. Buratti, R. H. Brown, R. Jaumann, J. Bauer, T. Momary, (2008), Photometric and spectral analysis of the distribution of crystalline and amorphous ices on Enceladus as seen by Cassini, Icarus, 193, 2, 397–406, doi: 10.1016/j.icarus.2007.04.019.

Newman, S. F., B. J. Buratti, R. Jaumann, J. M. Bauer, T. W. Momary, (2007), Hydrogen peroxide on Enceladus, The Astrophysical Journal, 670, L143–L146, doi: 10.1086/524403.

Nichols, J. D., S. V. Badman, E. J. Bunce, J. T. Clarke, S. W. H. Cowley, G. J. Hunt, G. Provan, (2016), Saturn’s northern auroras as observed using the Hubble Space Telescope, Icarus, 263, 17–31, doi: 10.1016/j.icarus.2015.09.008.

Nicholson, P. D., R. G. French, J. N. Spitale, (2018), Narrow rings, gaps and sharp edges, Chapter 11, In Planetary Ring Systems: Properties, Structure, and Evolution, (eds.) M. S. Tiscareno, C. D. Murraypp, Cambridge University Press, pp. 276–307, doi: 10.1017/9781316286791.011.

Nicholson, P. D. and M. M. Hedman, (2016), A vertical rift in Saturn's inner C ring, Icarus, 279, 78–99, doi: 10.1016/j.icarus.2016.01.024.

Nicholson, P. D., R. G. French, M. M. Hedman, E. A. Marouf, J. E. Colwell, (2014a), Noncircular features in Saturn’s rings I: The edge of the B ring, Icarus, 227, 152–175, doi: 10.1016/j.icarus.2013.09.002.

Nicholson, P. D., R. G. French, C. A. McGhee-French, M. M. Hedman, E. A. Marouf, J. E. Colwell, K. Lonergan, T. Sepersky, (2014b), Noncircular features in Saturn’s rings II: The C ring, Icarus, 241, 373–396, doi: 10.1016/j.icarus.2014.06.024.

Nicholson, P. D. and M. M. Hedman, (2010), Self-gravity wake parameters in Saturn's A and B rings, Icarus, 206, 2, 410–423, doi: 10.1016/j.icarus.2009.07.028.

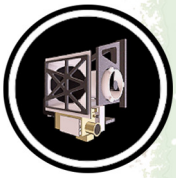

Nicholson, P. D., M. M. Hedman, R. N. Clark, M. R. Showalter, D. P. Cruikshank, J. N. Cuzzi, G. Filacchione et al., (2008), A close look at Saturn's rings with Cassini VIMS, Icarus 193, 182–212, doi: 10.1016/j.icarus.2007.08.036.

Nimmo, F., C. Porco, C. Mitchell, (2014), Tidally modulated eruptions on Enceladus: Cassini ISS observations and models, The Astronomical Journal, 148, no. 3, 46.

Nordheim, T. A., K. P. Hand, C. Paranicas, C. J. A. Howett, A. R. Hendrix, G. H. Jones, A. J. Coates, (2017), The near-surface electron radiation environment of Saturn's moon Mimas, Icarus, 286, 56–68, doi: 10.1016/j.icarus.2017.01.002.

Oancea, A., O. Grasset, E. Le Menn, O. Bollengier, L. Bezacier, S. Le Mouélic, G. Tobie, (2012), Laboratory infrared reflection spectrum of carbon dioxide clathrate hydrates for astrophysical remote sensing applications, Icarus, 221, 2, 900–910, doi: 10.1016/j.icarus.2012.09.020.

Oliva, F., A. Adriani, M. L. Moriconi, G. L. Liberti, E. D'Aversa, G. Filacchione, (2016), Clouds and hazes vertical structure of a Saturn's giant vortex from Cassini/VIMS-V data analysis, Icarus, 278, 215–237, doi: 10.1016/j.icarus.2016.06.021.

Orton, G. S., L. N. Fletcher, C. M. Lisse, P. W. Chodas, A. Cheng, P. A. Yanamandra-Fisher, K. H. Baines, et al., (2011), The atmospheric influence, size and possible asteroidal nature of the July 2009 Jupiter impactor, Icarus, 211, 1, 587–602, doi: 10.1016/j.icarus.2010.10.010.

Palmer, E. E. and R. H. Brown, (2011), Production and detection of carbon dioxide on Iapetus, Icarus, 212, 2, 807–818, doi: 10.1016/j.icarus.2010.12.007.

Palmer, E. E. and R. H. Brown, (2008), The stability and transport of carbon dioxide on Iapetus, Icarus, 195, 1, 434–446, doi: 10.1016/j.icarus.2007.11.020.

Pasek, V. and Lytle, D., (2011), Mission-critical software development for a distributed and diverse user base, paper presented at IEEE Aerospace Conference Proceedings.

Penteado, P. F. and C. A. Griffith, (2010), Ground-based measurements of the methane distribution on Titan, Icarus, 206, 1, 345–351, doi: 10.1016/j.icarus.2009.08.022.

Penteado, P. F., C. A. Griffith, M. G. Tomasko, S. Engel, C. See, L. Doose, K. H. Baines, et al., (2010), Latitudinal variations in Titan's methane and haze from Cassini VIMS observations, Icarus, 206, 1, 352–365, doi: 10.1016/j.icarus.2009.11.003.

Penteado, P. F., (2009), Study of Titan's methane cycle, University of Arizona.

Pinilla-Alonso, N., T. L. Roush, G. A. Marzo, D. P. Cruikshank, C. M. Dalle Ore, (2011), Iapetus surface variability revealed from statistical clustering of a VIMS mosaic: The distribution of CO2, Icarus, 215, 1, 75–82, doi: 10.1016/j.icarus.2011.07.004.

Pirim, C., R. D. Gann, J. L. McLain, T. M. Orlando, (2015), Electron-molecule chemistry and charging processes on organic ices and Titan's icy aerosol surrogates, Icarus, 258, 109–119, doi: 10.1016/j.icarus.2015.06.006.

Pitman, K. M., L. Kolokolova, A. J. Verbiscer, D. W. Mackowski, E. C. S. Joseph, (2017), Coherent backscattering effect in spectra of icy satellites and its modeling using multi-sphere

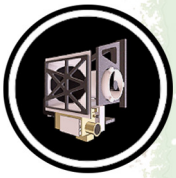

T-matrix (MSTM) code for layers of particles, Planetary and Space Science, 149, 23–31, doi: 10.1016/j.pss.2017.08.005.

Pitman, K. M., B. J. Buratti, J. A. Mosher, (2010), Disk-integrated bolometric Bond albedos and rotational light curves of saturnian satellites from Cassini Visual and Infrared Mapping Spectrometer, Icarus, 206, 2, 537–560, doi: 10.1016/j.icarus.2009.12.001.

Pitman, K. M., B. J. Buratti, J. A. Mosher, J. M. Bauer, T. W. Momary, R. H. Brown, P. D. Nicholson, M. M. Hedman, (2008), First high solar phase angle observations of rhea using Cassini VIMS: Upper limits on water vapor and geologic activity, The Astrophysical Journal, 680, L65–L68, doi: 10.1086/589745.

Porco, C., D. Dinino, F. Nimmo, (2014), How the geysers, tidal stresses, and thermal emission across the south polar terrain of Enceladus are related, The Astronomical Journal, 148, 3, doi: 10.1088/0004-6256/148/3/45.

Radebaugh, J., (2013), Dunes on Saturn’s moon Titan as revealed by the Cassini Mission, Aeolian Research, 11, 23–41, doi: 10.1016/j.aeolia.2013.07.001.

Radebaugh, J., R. D. Lorenz, S. D. Wall, R. L. Kirk, C. A. Wood, J. I. Lunine, E. R. Stofan, et al., (2011), Regional geomorphology and history of Titan’s Xanadu province, Icarus, 211, 1, 672–685, doi: 10.1016/j.icarus.2010.07.022.

Rannou, P., B. Seignovert, S. Le Mouélic, L. Maltagliati, M. Rey, C. Sotin, (2018), Transparency of 2 μm window of Titan's atmosphere, Planetary and Space Science, doi: 10.1016/j.pss.2017.11.015.

Rannou, P., D. Toledo, P. Lavvas, E. D’Aversa, M. L. Moriconi, A. Adriani, S. Le Mouélic, C. Sotin, R. Brown, (2016), Titan’s surface spectra at the Huygens landing site and Shangri-La, Icarus, 270, 291–306, doi: 10.1016/j.icarus.2015.09.016.

Rannou, P., S. Le Mouélic, C. Sotin, R. H. Brown, (2012), Cloud and haze in the winter polar region of titan observed with visual and infrared mapping spectrometer on board Cassini, The Astrophysical Journal, 748, 1, doi: 10.1088/0004-637X/748/1/4.

Rannou, P., T. Cours, S. Le Mouélic, S. Rodriguez, C. Sotin, P. Drossart, R. Brown, (2010), Titan haze distribution and optical properties retrieved from recent observations, Icarus, 208, 2, 850–867, doi: 10.1016/j.icarus.2010.03.016.

Reininger, F. M., M. Dami, R. Paolinetti, S. Pieri, S. Falugiani, (1994), Visible Infrared Mapping Spectrometer--visible channel (VIMS-V), In Instrumentation in Astronomy VIII, Symposium on Astronomical Telescopes and Instrumentation for the 21st Century, Kailua, Kona, HI, vol. 2198, pp. 239–250, doi: 10.1117/12.176753.

Rey, M., A. V. Nikitin, B. Bézard, P. Rannou, A. Coustenis, V. G. Tyuterev, (2018), New accurate theoretical line lists of $^{12}CH_4$ and $^{13}CH_4$ in the 0–13400 cm range: Application to the modeling of methane absorption in Titan’s atmosphere, Icarus, 303, 114–130, doi: 10.1016/j.icarus.2017.12.045.

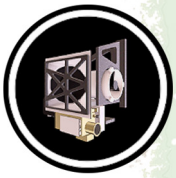

Rivera-Valentin, E. G., D. G. Blackburn, R. Ulrich, (2011), Revisiting the thermal inertia of Iapetus: Clues to the thickness of the dark material, Icarus, 216, 1, 347–358, doi: 10.1016/j.icarus.2011.09.006.

Roatsch, T., R. Jaumann, K. Stephan, P. C. Thomas, (2009), Cartographic mapping of the icy satellites using ISS and VIMS data, in Saturn from Cassini-Huygens, pp. 763–781, doi: 10.1007/978-1-4020-9217-6_24.

Robinson, T. D., L. Maltagliati, M. S. Marley, J. J. Fortney, (2014), Titan solar occultation observations reveal transit spectra of a hazy world, Proceedings of the National Academy of Science, 111, 9042–9047, doi: 10.1073/pnas.1403473111.

Rodriguez, S., S. Le Mouélic, J. W. Barnes, J. F. Kok, S. C. R. Rafkin, R. D. Lorenz, B. Charnay, et al., (2018), Observational evidence for active dust storms on Titan at equinox, Nature Geoscience, 11, 10, 727–732, doi:10.1038/s41561-018-0233-2.

Rodriguez, S., A. Garcia, A. Lucas, T. Appéré, Alice Le Gall, E. Reffet, L. Le Corre, et al., (2014), Global mapping and characterization of Titan's dune fields with Cassini: Correlation between RADAR and VIMS observations, Icarus, 230, 168–179, doi: 10.1016/j.icarus.2013.11.017.

Rodriguez, S., S. Le Mouélic, P. Rannou, C. Sotin, R. H. Brown, J. W. Barnes, C. A. Griffith, et al., (2011), Titan's cloud seasonal activity from winter to spring with Cassini/VIMS, Icarus, 216, 1, 89–110, doi: 10.1016/j.icarus.2011.07.031.

Rodriguez, S., S. Le Mouélic, P. Rannou, G. Tobie, K. H. Baines, J. W. Barnes, C. A. Griffith, et al., (2009), Global circulation as the main source of cloud activity on Titan, Nature, 459, 678, doi: 10.1038/nature08014.

Rodriguez, S., S. Le Mouélic, C. Sotin, H. Clénet, R. N. Clark, B. Buratti, R. H. Brown, T. B. McCord, P. D. Nicholson, K. H. Baines, (2006), Cassini/VIMS hyperspectral observations of the HUYGENS landing site on Titan, Planetary and Space Science, 54, 15, 1510–1523, doi: 10.1016/j.pss.2006.06.016

Sayanagi, K. M., K. H. Baines, U. Dyudina, L. N. Fletcher, A. Sánchez-Lavega, R. A. West, (2018), Saturn’s polar atmosphere, Chapter 12, In Saturn in the 21st Century, (eds.), F. M. Flasar, K. H. Baines, N. Krupp, T. Stallard, Cambridge University Press, pp. 337–376, doi: 10.1017/9781316227220.012.

Sayanagi, K. M., R. Morales-Juberías, A. P. Ingersoll, (2010), Saturn's northern hemisphere ribbon: Simulations and comparison with the meandering Gulf Stream, Journal of the Atmospheric Sciences, 67, 8, 2658–2678, doi: 10.1175/2010JAS3315.1.

Schenk, P. M., B. J. Buratti, P. K. Byrne, W. B. McKinnon, F. Nimmo, F. Scipioni, (2015), Blood stains on Tethys: evidence of recent activity, European Planetary Science Congress (EPSC), vol. 10, abstract EPSC2015-893.

Schenk, P., D. P. Hamilton, R. E. Johnson, W. B. McKinnon, C. Paranicas, J. Schmidt, M. R. Showalter, (2011), Plasma, plumes and rings: Saturn system dynamics as recorded in global color patterns on its midsize icy satellites, Icarus, 211, no. 1, 740–757.

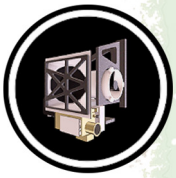

Schurmeier, L. R. and A. J. Dombard, (2018), Crater relaxation on Titan aided by low thermal conductivity sand infill, Icarus, doi: 10.1016/j.icarus.2017.10.034.

Sciamma-O'Brien, E., K. T. Upton, F. Salama, (2017), The Titan Haze Simulation (THS) experiment on COSmIC, Part II, Ex-situ analysis of aerosols produced at low temperature, Icarus, 289, 214–226, doi: 10.1016/j.icarus.2017.02.004.

Sciamma-O'Brien, E., P. R. Dahoo, E. Hadamcik, N. Carrasco, E. Quirico, C. Szopa, G. Cernogora, (2012), Optical constants from 370 nm to 900 nm of Titan tholins produced in a low pressure RF plasma discharge, Icarus, 218, 1, 356–363, doi: 10.1016/j.icarus.2011.12.014.

Scipioni, F., P. Schenk, F. Tosi, E. D'Aversa, R. Clark, J. P. Combe, C. M. D. Ore, (2017), Deciphering sub-micron ice particles on Enceladus surface, Icarus, 290, 183–200, doi: 10.1016/j.icarus.2017.02.012.

Scipioni, F., F. Tosi, K. Stephan, G. Filacchione, M. Ciarniello, F. Capaccioni, P. Cerroni, (2014), Spectroscopic classification of icy satellites of Saturn II: Identification of terrain units on Rhea, Icarus, 234, 1–16, doi: 10.1016/j.icarus.2014.02.010.

Scipioni, F., F. Tosi, K. Stephan, G. Filacchione, M. Ciarniello, F. Capaccioni, P. Cerroni, (2013), Spectroscopic classification of icy satellites of Saturn I: Identification of terrain units on Dione, Icarus, 226, 2, 1331–1349, doi: 10.1016/j.icarus.2013.08.008.

Scipioni, F., A. Coradini, F. Tosi, F. Capaccioni, P. Cerroni, G. Filacchione, C. Federico, (2012), Spectroscopic investigation of Dione' surface using Cassini VIMS images, Memorie della Societa Astronomica Italiana Supplementi, vol. 20, p. 114.

Sim, C. K., S. J. Kim, R. Courtin, M. Sohn, D.-H. Lee, (2013), The two-micron spectral characteristics of the Titanian haze derived from Cassini/VIMS solar occultation spectra, Planetary and Space Science, 88, 93–99, doi: 10.1016/j.pss.2013.10.003.

Simon, S., J. Saur, F. M. Neubauer, A. Wennmacher, M. K. Dougherty, (2011), Magnetic signatures of a tenuous atmosphere at Dione, Geophysical Research Letters 38, no. 15, doi: 10.1029/2011GL048454.

Simonelli, D. P. and B. J. Buratti, (2004), Europa's opposition surge in the near-infrared: Interpreting disk-integrated observations by Cassini VIMS, Icarus, 172, 149–162, doi: 10.1016/j.icarus.2004.06.004.

Sinclair, J. A., P. G. J. Irwin, L. N. Fletcher, J. I. Moses, T. K. Greathouse, A. J. Friedson, B. Hesman, J. Hurley, C. Merlet, (2013), Seasonal variations of temperature, acetylene and ethane in Saturn's atmosphere from 2005 to 2010, as observed by Cassini-CIRS, Icarus, 225, 1, 257–271, doi: 10.1016/j.icarus.2013.03.011.

Singh, G., S. Singh, A. Wagner, V. F. Chevrier, J. P. Combe, M. Gainor, (2017a), Experimental reflectance study of methane and ethane ice at Titan's surface conditions, Astrophysics and Space Science, 362, 10, doi: 10.1007/s10509-017-3166-0.

Singh, S., J. P. Combe, D. Cordier, A. Wagner, V. F. Chevrier, Z. McMahon, (2017b), Experimental determination of acetylene and ethylene solubility in liquid methane and ethane:

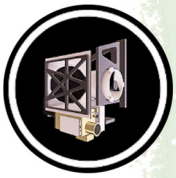

Implications to Titan's surface, Geochimica et Cosmochimica Acta, 208, 86–101, doi: 10.1016/j.gca.2017.03.007.

Singh, S., T. Cornet, V. F. Chevrier, J. P. Combe, T. B. McCord, L. A. Roe, S. Le Mouélic, E. Le Menn, F. C. Wasiak, (2016), Near-infrared spectra of liquid/solid acetylene under Titan relevant conditions and implications for Cassini/VIMS detections, Icarus, 270, 429–434, doi: 10.1016/j.icarus.2015.11.002.

Soderblom, J. M., J. W. Barnes, L. A. Soderblom, R. H. Brown, C. A. Griffith, P. D. Nicholson, K. Stephan, et al., (2012), Modeling specular reflections from hydrocarbon lakes on Titan, Icarus, 220, 2, 744–751, doi: 10.1016/j.icarus.2012.05.030.

Soderblom, J. M., R. H. Brown, L. A. Soderblom, J. W. Barnes, R. Jaumann, S. Le Mouélic, C. Sotin, et al., (2010a), Geology of the Selk crater region on Titan from Cassini VIMS observations, Icarus, 208, 2, 905–912, doi: 10.1016/j.icarus.2010.03.001.

Soderblom, L. A., J. W. Barnes, R. H. Brown, R. N. Clark, M. A. Janssen, T. B. McCord, H. B. Niemann, M. G. Tomasko, (2010b), Composition of titan's surface, in Titan from Cassini-Huygens, pp. 141–175, doi:10.1007/978-1-4020-9215-2_6.

Soderblom, L. A., R. H. Brown, J. M. Soderblom, J. W. Barnes, R. L. Kirk, C. Sotin, R. Jaumann, et al., (2009), The geology of Hotei Regio, Titan: Correlation of Cassini VIMS and RADAR, Icarus, 204, 2, 610–618, doi: 10.1016/j.icarus.2009.07.033.

Soderblom, L. A., R. L. Kirk, J. I. Lunine, J. A. Anderson, K. H. Baines, J. W. Barnes, J. M. Barrett, et al., (2007a), Correlations between Cassini VIMS spectra and RADAR SAR images: Implications for Titan's surface composition and the character of the Huygens Probe Landing Site, Planetary and Space Science, 55, 13, 2025–2036, doi: 10.1016/j.pss.2007.04.014.

Soderblom, L. A., M. G. Tomasko, B. A. Archinal, T. L. Becker, M. W. Bushroe, D. A. Cook, L. R. Doose, et al., (2007b), Topography and geomorphology of the Huygens landing site on Titan, Planetary and Space Science, 55, 13, 2015–2024, doi: 10.1016/j.pss.2007.04.015.

Solomonidou, A., A. Coustenis, M. Hirtzig, S. Rodriguez, K. Stephan, R. M. C. Lopes, P. Drossart, et al., (2016), Temporal variations of Titan's surface with Cassini/VIMS, Icarus, 270, 85–99, doi: 10.1016/j.icarus.2015.05.003.

Solomonidou, A., G. Bampasidis, M. Hirtzig, A. Coustenis, K. Kyriakopoulos, K. St. Seymour, E. Bratsolis, X. Moussas, (2013), Morphotectonic features on Titan and their possible origin, Planetary and Space Science, 77, 104–117, doi: 10.1016/j.pss.2012.05.003.

Sotin, C., J. W. Barnes, K. J. Lawrence, J. M. Soderblom, E. Audi, R. Hamilton Brown, S. Le Mouelic, et al, (2015), Tidal Currents between Titan's Seas Detected by Solar Glints, In American Geophysical Union (AGU) Fall Meeting, abstract.

Sotin, C., K. J. Lawrence, B. Reinhardt, J. W. Barnes, Robert H. Brown, A. G. Hayes, S. Le Mouélic, et al., (2012), Observations of Titan's Northern lakes at 5μm: Implications for the organic cycle and geology, Icarus, 221, 2, 768–786, doi: 10.1016/j.icarus.2012.08.017.

Sotin, C., R. Jaumann, B. J. Buratti, Robert H. Brown, R. N. Clark, L. A. Soderblom, K. H. Baines, et al., (2005), Release of volatiles from a possible cryovolcano from near-infrared imaging of Titan, Nature, 435, 7043, 786–789, doi:10.1038/nature03596.

Sromovsky, L. A., K. H. Baines, P. M. Fry, (2018), Models of bright storm clouds and related dark ovals in Saturn's Storm Alley as constrained by 2008 Cassini/VIMS spectra, Icarus, 302, 360–385, doi: 10.1016/j.icarus.2017.11.027.

Sromovsky, L. A., K. H. Baines, P. M. Fry, R. W. Carlson, (2017), A possibly universal red chromophore for modeling color variations on Jupiter, Icarus, 291, 232–244, doi: 10.1016/j.icarus.2016.12.014.

Sromovsky, L. A., K. H. Baines, P. M. Fry, T. W. Momary, (2016), Cloud clearing in the wake of Saturn’s Great Storm of 2010–2011 and suggested new constraints on Saturn’s He/H_2 ratio, Icarus, 276, 141–162, doi: 10.1016/j.icarus.2016.04.031.

Sromovsky, L. A., K. H. Baines, P. M. Fry, (2013), Saturn's Great Storm of 2010–2011: Evidence for ammonia and water ices from analysis of VIMS spectra, Icarus, 226, 1, 402–418, doi: 10.1016/j.icarus.2013.05.043.

Sromovsky, L. A. and P. M. Fry, (2010), The source of widespread 3-μm absorption in Jupiter's clouds: Constraints from 2000 Cassini VIMS observations, Icarus, 210, 1, 230–257, doi: 10.1016/j.icarus.2010.06.039.

Stallard, T. S., H. Melin, S. Miller, S. V. Badman, K. H. Baines, R. H. Brown, J. S. D. Blake, J. O’Donoghue, R. E. Johnson, B. Bools, N. M. Pilkington, O. T. L. East, M. Fletcher, (2015), Cassini VIMS observations of H_3^+ emission on the nightside of Jupiter, Journal of Geophysical Research, 120, 6948–6973, doi: 10.1002/2015JA021097.

Stallard, T. S., H. Melin, S. Miller, S. V. Badman, R. H. Brown, K. H. Baines, (2012a), Peak emission altitude of Saturn's H_3^+ aurora, Geophysical Research Letters, 39, 15, doi: 10.1029/2012GL052806.

Stallard, T. S., H. Melin, S. Miller, J. O'Donoghue, S. W. Cowley, S. V. Badman, A. Adriani, R. H. Brown, K. H. Baines, (2012b), Temperature changes and energy inputs in giant planet atmospheres: what we are learning from H_3^+, Philosophical Transactions of the Royal Society of London Series A 370, 370, 1978, 5213–5224, doi: 10.1098/rsta.2012.0028.

Stallard et al. 2012

Stallard, T., S. Miller, M. Lystrup, N. Achilleos, E. J. Bunce., C. S. Arridge, M. K. Dougherty, S. W. H. Cowley, S. V. Badman, D. L. Talboys, R. H. Brown, K. H. Baines, B. J. Buratti, R. N. Clark, C. Sotin, P. D. Nicholson, P. Drossart, (2008), Complex structure within Saturn’s infrared aurora, Nature, 456, 214–217, doi:10.1038/nature07440.

Stephan, K., R. Wagner, R. Jaumann, R. N. Clark, D. P. Cruikshank, R. H. Brown, B. Giese, et al., (2016), Cassini's geological and compositional view of Tethys, Icarus, 274, 1–22, doi: 10.1016/j.icarus.2016.03.002.

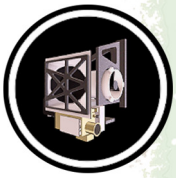

Stephan, K., R. Jaumann, R. Wagner, R. N. Clark, D. P. Cruikshank, B. Giese, C. A. Hibbitts, et al., (2012), The Saturnian satellite Rhea as seen by Cassini VIMS, Planetary and Space Science, 61, 1, 142–160, doi: 10.1016/j.pss.2011.07.019.

Stephan, K., R. Jaumann, R. H. Brown, J. M. Soderblom, L. A. Soderblom, J. W. Barnes, C. Sotin, et al., (2010a), Specular reflection on Titan: Liquids in Kraken Mare, Geophysical Research Letters, 37, L07104, doi: 10.1029/2009GL042312.

Stephan, K., R. Jaumann, E. Karkoschka, R. L. Kirk, J. W. Barnes, M. G. Tomasko, E. P. Turtle, et al., (2010b), Mapping products of titan's surface, Chapter 19, In Titan from Cassini-Huygens, (eds.) R. H. Brown, J. P. Lebreton, J. H. Waite, Springer Dordrecht, pp. 489–510, doi: 10.1007/978-1-4020-9215-2_19.

Stephan, K., R. Jaumann, R. Wagner, R. N. Clark, D. P. Cruikshank, C. A. Hibbitts, T. Roatsch, et al., (2010c), Dione's spectral and geological properties, Icarus, 206, 2, 631–652, doi: 10.1016/j.icarus.2009.07.036.

Stephan, K., R. Jaumann, R. H. Brown, J. M. Soderblom, L. A. Soderblom, J. W. Barnes, C. Sotin, et al., (2010d), Detection of a specular reflection on Titan by Cassini-VIMS, In Lunar and Planetary Science Conference, vol. 41, p. 1692.

Stewart, P. N., P. G. Tuthill, J. D. Monnier, M. J. Ireland, M. M. Hedman, P. D. Nicholson, S. Lacour, (2016a), The weather report from IRC+10216: evolving irregular clouds envelop carbon star, Monthly Notices of the Royal Astronomical Society, 455, 3102–3109, doi: 10.1093/mnras/stv2454.

Stewart, P. N., P. G. Tuthill, P. D. Nicholson, M. M. Hedman, (2016b), High-angular-resolution stellar imaging with occultations from the Cassini spacecraft - III. Mira, Monthly Notices of the Royal Astronomical Society, 457, 1410–1418, doi: 10.1093/mnras/stw045.

Stewart, P. N., P. G. Tuthill, P. D. Nicholson, M. M. Hedman, J. P. Lloyd, (2015a), High angular resolution stellar imaging with occultations from the Cassini spacecraft - II. Kronocyclic tomography, Monthly Notices of the Royal Astronomical Society, 449, 1760–1766, doi: 10.1093/mnras/stv446.

Stewart, P. N., P. G. Tuthill, P. D. Nicholson, G. C. Sloan, M. M. Hedman, (2015b), An Atlas of Bright Star Spectra in the Near-infrared from Cassini-VIMS, The Astrophysical Journal Supplement Series, 221, 2, doi: 10.1088/0067-0049/221/2/30.

Stewart, P. N., P. G. Tuthill, P. D. Nicholson, M. M. Hedman, J. P. Lloyd, (2014), Advances in stellar imaging with occultations from the Cassini spacecraft, Space Telescopes and Instrumentation 2014: Optical, Infrared, and Millimeter Wave, SPIE Astronomical Telescopes + Instrumentation, 2014, Montréal, Quebec, Canada, vol. 9143, p. 91431G, doi: 10.1117/12.2055631.

Stewart, P. N., P. G. Tuthill, M. M. Hedman, P. D. Nicholson, J. P. Lloyd, (2013), High-angular-resolution stellar imaging with occultations from the Cassini spacecraft - I. Observational technique, Monthly Notices of the Royal Astronomical Society, 433, 2286–2293, doi: 10.1093/mnras/stt894.

Studwell, A., L. Li, X. Jiang, K. H. Baines, P. M. Fry, T. W. Momary, U. A. Dyudina, (2018), Saturn's global zonal winds explored by Cassini/VIMS 5-μm Images, Geophysical Research Letters, 45, 14, 6823–6831, doi:10.1029/2018GL078139.

Taffin, C., O. Grasset, E. Le Menn, O. Bollengier, M. Giraud, S. Le Mouélic, (2012), Temperature and grain size dependence of near-IR spectral signature of crystalline water ice: From lab experiments to Enceladus' south pole, Planetary and Space Science, 61, 1, 124–134, doi: 10.1016/j.pss.2011.08.015.

Tajeddine, R., P. D. Nicholson, P. Y. Longaretti, M. E. Moutamid, J. A. Burns, (2017a), What Confines the Rings of Saturn?, The Astrophysical Journal Supplement Series, 232, 2, doi: 10.3847/1538-4365/aa8c09.

Tajeddine, R., P. D. Nicholson, M. S. Tiscareno, M. M. Hedman, J. A. Burns, M. E. Moutamid, (2017b), Dynamical phenomena at the inner edge of the Keeler gap, Icarus, 289, 80–93, doi: 10.1016/j.icarus.2017.02.002.

Tao, C., S. V. Badman, T. Uno, M. Fujimoto, (2012), On the feasibility of characterizing Jovian auroral electrons via infrared line-emission analysis, Icarus, 221, 1, 236–247, doi: 10.1016/j.icarus.2012.07.015.

Throop, H. B., C. C. Porco, R. A. West, J. A. Burns, M. R. Showalter, P. D. Nicholson, (2004), The Jovian rings: New results derived from Cassini, Galileo, Voyager, and Earth-based observations, Icarus, 172, 59–77, doi: 10.1016/j.icarus.2003.12.020.

Tiscareno, M. S., M. M. Hedman, J. A. Burns, J. W. Weiss, C. C. Porco, (2013), Probing the inner boundaries of Saturn’s A-ring with the Iapetus −1:0 nodal bending wave, Icarus, 224, 1, 201–208, doi: 10.1016/j.icarus.2013.02.026.

Tobie, G., N. A. Teanby, A. Coustenis, R. Jaumann, F. Raulin, J. Schmidt, N. Carrasco, et al., (2014), Science goals and mission concept for the future exploration of Titan and Enceladus, Planetary and Space Science, 104, 59–77, doi: 10.1016/j.pss.2014.10.002.

Tokar, R. L., R. E. Johnson, M. F. Thomsen, E. C. Sittler, A. J. Coates, R. J. Wilson, F. J. Crary, D. T. Young, G. H. Jones, (2012), Detection of exospheric O_2^+ at Saturn's moon Dione, Geophysical Research Letters, 39, no. 3, doi: 10.1029/2011GL050452.

Tosi, F., R. Orosei, R. Seu, A. Coradini, J. I. Lunine, G. Filacchione, A. I. Gavrishin, et al., (2010a), Correlations between VIMS and RADAR data over the surface of Titan: Implications for Titan's surface properties, Icarus, 208, 1, 366–384, doi: 10.1016/j.icarus.2010.02.003.

Tosi, F., D. Turrini, A. Coradini, G. Filacchione, (2010b), Probing the origin of the dark material on Iapetus, Monthly Notices of the Royal Astronomical Society, 403, 3, 1113–1130, doi: 10.1111/j.1365-2966.2010.16044.x.

Tosi, F., A. Coradini, A. Adriani, F. Capaccioni, P. Cerroni, G. Filacchione, A. I. Gavrishin, R. H. Brown, (2006), G-mode classification of spectroscopic data, Earth, Moon and Planets, 96, 3–4, 165–197, doi: 10.1007/s11038-005-9061-7.

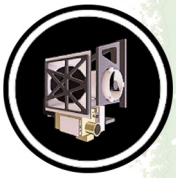

Turtle, E. P., J. E. Perry, J. M. Barbara, A. D. Del Genio, S. Rodriguez, S. Le Mouélic, C. Sotin, et al., (2018), Titan's Meteorology Over the Cassini Mission: Evidence for Extensive Subsurface Methane Reservoirs, Geophysical Research Letters, 45, 1, 5320–5328, doi: 10.1029/2018GL078170.

Vahidinia, S., J. N. Cuzzi, M. Hedman, B. Draine, R. N. Clark, T. Roush, G. Filacchione, et al., (2011), Saturn's F ring grains: Aggregates made of crystalline water ice, Icarus, 215, 2, 682–694, doi: 10.1016/j.icarus.2011.04.011.

Veeder, G. J., A. G. Davies, D. L. Matson, T. V. Johnson, D. A. Williams, J. Radebaugh, (2012), Io: Volcanic thermal sources and global heat flow, Icarus, 219, 2, 701–722, doi: 10.1016/j.icarus.2012.04.004.

Verbiscer, A. J., D. E. Peterson, M. F. Skrutskie, M. Cushing, P. Helfenstein, M. J. Nelson, J. D. Smith, J. C. Wilson, (2006), Near-infrared spectra of the leading and trailing hemispheres of Enceladus, Icarus, 182, 1, 211–223, doi: 10.1016/j.icarus.2005.12.008.

Vilas, F., S. M. Lederer, S. L. Gill, K. S. Jarvis, J. E. Thomas-Osip, (2006), Aqueous alteration affecting the irregular outer planets satellites: Evidence from spectral reflectance, Icarus, 180, 2, 453–463, doi: 10.1016/j.icarus.2005.10.004.

Vincendon, M. and Y. Langevin, (2010), A spherical Monte-Carlo model of aerosols: Validation and first applications to Mars and Titan, Icarus, 207, 2, 923–931, doi: 10.1016/j.icarus.2009.12.018.

Vixie, G., J. W. Barnes, B. Jackson, S. Rodriguez, S. Le Mouélic, C. Sotin, S. MacKenzie, P. Wilson, (2015), Possible temperate lakes on Titan, Icarus, 257, 313–323, doi: 10.1016/j.icarus.2015.05.009.

Vixie, G., J. W. Barnes, J. Bow, S. Le Mouélic, S. Rodriguez, R. H. Brown, P. Cerroni, et al., (2012), Mapping Titan's surface features within the visible spectrum via Cassini VIMS, Planetary and Space Science, 60, 1, 52–61, doi: 10.1016/j.pss.2011.03.021.

Vuitton, V., R. V. Yelle, S. J. Klippenstein, S. M. Hörst, P. Lavvas, (2018), Simulating the density of organic species in the atmosphere of Titan with a coupled ion-neutral photochemical model, Icarus, 324, 120–197, doi: 10.1016/j.icarus.2018.06.013.

Waite, J. H., J. Bell, R. Lorenz, R. Achterberg, F. M. Flasar, (2013), A model of variability in Titan's atmospheric structure, Planetary and Space Science, 86, 45–56, doi: 10.1016/j.pss.2013.05.018.

Walch, M., D. W. Juergens, S. Anthony, P. D. Nicholson, (1993), Stellar occultation experiment with the Cassini VIMS instrument, Infrared Technology XVIII, International Society for Optics and Photonics, San Diego, CA, vol. 1762, pp. 483–494, doi: 10.1117/12.138989.

Waldmann, I. P. and C. A. Griffith, (2019), Mapping Saturn using deep learning, Nature Astronomy, doi: 10.1038/s41550-019-0753-8.

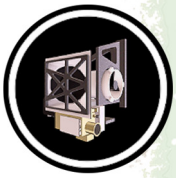

Werynski, A., C. D. Neish, A. L. Gall, M. A. Janssen, R. T. The Cassini, (2019), Compositional variations of Titan's impact craters indicates active surface erosion, Icarus, 321, 508–521, doi: 10.1016/j.icarus.2018.12.007.

West, R. A., K. H. Baines, E. Karkoschka, A. Sánchez-Lavega, (2009), Clouds and aerosols in Saturn’s atmosphere, Chapter 7, In Saturn from Cassini-Huygens, (eds.) M. Dougherty, L. Esposito, S. Krimigis, Springer Dordrecht, pp. 161–179, doi: 10.1007/978-1-4020-9217-6_7.